

Homogenization Relations for Elastic Properties Based on Two-Point Statistical Functions

A Dissertation
Presented to
The Academic Faculty

by

Ghazal Peydaye Saheli

In Partial Fulfillment
of the Requirements for the Degree
Doctor of Philosophy in the
School of Materials Science and Engineering

Georgia Institute of Technology
May 2006

HOMOGENIZATION RELATIONS FOR ELASTIC PROPERTIES
BASED ON TWO-POINT STATISTICAL FUNCTIONS

Approved by:

Dr. Hamid Garmestani, Advisor
School of Materials Science and
Engineering
Georgia Institute of Technology

Dr. David McDowell
School of Mechanical Engineering
Georgia Institute of Technology

Dr. Arun Gokhale, Co-Advisor
School of Materials Science and
Engineering
Georgia Institute of Technology

Dr. Naresh Thadhani
School of Materials Science and
Engineering
Georgia Institute of Technology

Dr. W. Steven Johnson
School of Materials Science and
Engineering
Georgia Institute of Technology

Date Approved: 03/30/2006

To
My parents
(Farmarz and Manijeh)

My grandma
(Khadijeh)

and
My husband
(Kaveh)

ACKNOWLEDGEMENT

First and foremost, I would like to thank my thesis advisor professor Hamid Garmestani for his continuous support, guidance and supervision throughout my PhD work. I have learned invaluable lessons from his insight not only in my professional work but also in my personal life and I am extremely grateful for his patience and support in every step of my research.

I would also like to express my acknowledgement to my co-advisor, professor Arun Gokhale for his guidance and valuable advices during my work. I am also gratefully thankful to my reading committee members including professors Steven Johnson, David McDowell, and Naresh Thadhani for their time to attend my thesis defense meeting and to read my thesis in spite of their busy schedules. Their useful suggestion on my thesis is greatly appreciated. I would also like to thank LMM group especially Dr. Dongsheng Li for his useful discussions and Houman Saheli for his constant assistance. I am also very thankful to my uncle and aunt (Drs Babak and Judy Etemadi) whom provided the opportunity for me to continue my education toward PhD degree.

Finally I like to gratefully thank my parents and my grandma for their continuous and never-ending love, support and encouragement in every step of my education. They are always there for me to help me to reach my goals and dreams and at last I would like to thank my kind and caring husband who has been always very supportive in the last steps of my work.

TABLE OF CONTENTS

ACKNOWLEDGEMENT	IV
LIST OF TABLES	VII
LIST OF FIGURES	VIII
SUMMARY	XI
CHAPTER 1 INTRODUCTION	1
PART I: BACKGROUND AND LITERATURE REVIEW	6
CHAPTER 2 MICROMECHANICAL MODELS FOR ELASTIC PROPERTIES.....	7
2.1 RIGOROUS BOUNDS: VARIATIONAL METHOD	7
2.1.1 Voigt model (upper bound)	14
2.1.2 Reuss Model (lower bound)	15
2.2 DEGRADED BOUNDS FOR ELASTIC COEFFICIENTS BASED ON MINIMUM-ENERGY THEORY.....	16
2.3 HASHIN-SHTRIKMAN VARIATIONAL METHOD	22
2.4 APPROXIMATION METHODS	26
2.4.1 Maxwell approximation method	27
2.4.2 Self-Consistent approximation method	32
CHAPTER 3 STATISTICAL MECHANICS MODELING	36
3.1 STATISTICAL CONTINUUM MECHANICS THEORY.....	37
3.1.1 Distribution functions and density functions.....	37
3.1.2 Important average quantities.....	38
3.2 STATISTICAL DESCRIPTIONS OF MICROSTRUCTURE.....	39
3.2.1 One-point probability functions.....	40
3.2.2 Two-point probability functions	40
3.2.3 Mathematical configuration of two-point statistical functions.....	42
3.3 THE BASIC ASSUMPTIONS OF STATISTICAL CONTINUUM MECHANICS	45
3.4 HOMOGENIZATION RELATIONS FOR ELASTIC PROPERTIES	46
PART II: EXTENSION OF HOMOGENIZATION RELATIONS TO ANISOTROPIC DISTRIBUTION.....	53

CHAPTER 4	ANISOTROPIC HOMOGENIZATION RELATIONS.....	54
4.1	TWO-POINT PROBABILITY FUNCTIONS FOR COMPOSITES.....	54
4.2	MODIFIED CORSON’S PROBABILITY FUNCTION	55
4.3	TWO-POINT PROBABILITY FUNCTION FOR POLYCRYSTALLINE MATERIALS	56
4.4	ANALYTICAL ANALYSIS OF HOMOGENIZATION RELATIONS	58
CHAPTER 5	HOMOGENIZATION RELATIONS IN COMPOSITES.....	67
5.1	SIMULATION OF AL-Pb COMPOSITE- PROPERTY ENCLOSURE	67
5.1.1	Isotropic distribution	68
5.1.2	Anisotropic distribution.....	72
5.1.4	Numerical analysis	78
5.2	SAMPLES OF AL-SiC COMPOSITE.....	80
5.2.1	Ultrasounds technique	86
5.2.2	Results	88
CHAPTER 6	HOMOGENIZATION RELATIONS IN POLYCRYSTALLINE MATERIALS... ..	94
6.1	STATISTICAL MECHANICS MODELING FOR POLYCRYSTALLINE MICROSTRUCTURES	94
6.2	ALUMINUM ALLOY POLYCRYSTALLINE MICROSTRUCTURES	97
6.3	NEAR- α TITANIUM POLYCRYSTALLINE MICROSTRUCTURES.....	103
CHAPTER 7	CONCLUSIONS AND RECOMMENDATIONS.....	111
7.1	CONCLUSIONS.....	111
7.2	CONTRIBUTIONS.....	113
7.3	FUTURE WORKS	114
APPENDIX	116
A.1	GREEN’S FUNCTION DEFINITION.....	116
A.2	FIRST AND THE SECOND DERIVATIVES OF GREEN’S FUNCTION	117
A.3	EMPIRICAL COEFFICIENTS IN CORSON’S EQUATION	118
A.4	IMPLEMENTATION OF THE HOMOGENIZATIONS RELATIONS IN C++ PROGRAMMING	119
REFERENCES	150

LIST OF TABLES

Table 3.1 Empirical coefficients in Corson's equation for a two-phase composite	42
Table 5.1 Calculation of Degree of Anisotropy (A) in modified Corson's equation.....	73
Table 5.2 Contribution of one-point and two-point statistics in effective elastic stiffness	76
Table 5.3 Nonzero terms of elastic stiffness tensor for Al-SiC PSR: 2:1 to represent the contribution of one-point and two-point statistical information.....	88
Table 5.4 Measured and calculated values of transverse elastic shear modulus (G_{12}) for two samples of Al-SiC composite.....	90
Table 6.1 Comparison of contribution of one-point and two-point statistics in elastic stiffness calculation for different samples of simulated polycrystalline Aluminum with different textures.....	103
Table 6.2 Elastic stiffness tensor calculated for 60% cold rolled Cp-Ti samples.....	108
Table 6.3 Elastic modulus of two samples of Titanium in different directions- Statistical and Ultrasounds measurement.....	109
Table 6.4 Elastic shear modulus of two samples in transverse plane- Statistical and Ultrasounds measurement.....	110

LIST OF FIGURES

Figure 1.1 A schematically representation of mechanical design parameters	1
Figure 2.1 Voigt model: Uniform strain field in both phases	14
Figure 2.2 Reuss model: Uniform stress field in both phases.....	15
Figure 2.3 A Schematic diagram to show the single spherical inclusion in an infinite matrix	27
Figure 2.4 Effective properties of a composite with spherical inclusion - Maxwell approximation	31
Figure 2.5 A portion of an RVE containing spherical micro-inclusion, Self-Consistent approximation	33
Figure 3.1 OIM representation of the microstructure	40
Figure 3.2 Schematic representations of one-point statistics measurement in a two-phase composite microstructure.....	41
Figure 3.3 Schematic representations of two-point statistics measurment in a two-phase composite microstructure.....	41
Figure 3.4 Comparison of different proposed formulas for probability functions (Corson and Torquato equation)	44
Figure 4.1 Schematic representation of two-point probabilities measurements in an anisotropic microstructure	56
Figure 4.2 Schematic representation of orientation coherence function for polycrystalline microstructures.....	58
Figure 4.3 Schematic representation of two-point probabilities measurements in an anisotropic microstructures.....	66

Figure 5.1 Effective elastic modulus of Al-Pb composite (isotropic)	69
Figure 5.2 Effective elastic shear modulus of Al-Pb (isotropic)	70
Figure 5.3 Digital representation of the anisotropic composite	71
Figure 5.4 Modified Corson's equation fitted to measured values of P_{11}	74
Figure 5.5 Variation of anisotropy in the microstructure for different values of A.....	74
Figure 5.6 A property enclosure for anisotropic composite Al-Pb (anisotropy)	75
Figure 5.7 Composite Design- Minimizing the longitudinal/transverse properties of anisotropic Al-Pb composite.....	78
Figure 5.8 Schematic diagrams of probability functions	79
Figure 5.9 Micrographs of two samples of Al-SiC.....	82
Figure 5.10 Representation of symmetry in samples of Al-SiC	83
Figure 5.11 Measurement of two-point statistics in vertical section for two samples.....	84
Figure 5.12 Curves fitted to the measured values of P_{11} for sample of Al-SiC with PSR: 2:1	85
Figure 5.13 Measured P_{11} for two samples of Al-SiC composite	85
Figure 5.14 Range of frequency in ultrasound.....	87
Figure 5.15 Comparing the slope of the elastic region of stress-strain curves with the simulation results and other bounds.....	91
Figure 5.16 Comparison of longitudinal elastic modulus (E_3) vs transverse elastic modulus (E_1) for two samples of Al-SiC composite.....	93
Figure 6.1 Representation of Euler's angles.....	96
Figure 6.2 Elastic stiffness of Al polycrystalline microstructures in (123) directions for different percentages of texture in $\langle 0\ 0\ 1 \rangle$ direction.....	100

Figure 6.3 Elastic shear stiffness of Al Polycrystalline microstructures for different degree of texture in $\langle 001 \rangle$ direction.....	101
Figure 6.4 Elastic shear stiffness of Al Polycrystalline microstructures for different degree of texture in $\langle 001 \rangle$ direction.....	102
Figure 6.5 Representation of the cross section of the microstructure to measure OIM and two-point statistics	104
Figure 6.6 Microstructures of Cp-Ti and their OIM representations	105
Figure 6.7 Pole figures for two samples of Cp-Ti (As received and 60% cold rolled)	107

SUMMARY

In this research, the homogenization relations for elastic properties of isotropic and anisotropic materials including composites and polycrystalline materials are studied by applying two-point statistical mechanics theory. The validity of the results is investigated by direct comparison with experimental results.

In today's technology, where advanced processing methods can provide materials with a variety of morphologies and features in different scales, a methodology to link properties to microstructure is necessary to develop a framework for material design. The link between structure of materials in any length scale (from nano to macro) and their properties whether they are mechanical, electrical, magnetic, or optical is critical in every engineering discipline. For this purpose, this research is focused on the homogenization relationships based on two-point statistical information to correlate the microstructure of the materials to their mechanical properties. Statistical distribution functions are commonly used for the representation of microstructures and also for homogenization of materials properties. The use of two-point statistics allows the materials designer to include the morphology and distribution in addition to the properties of the individual phases and components. Statistical mechanics modeling not only enables us to correlate the morphology of the microstructures to properties, it can also predict the microstructures from the properties. The latter issue which is called inverse structure-property problem has received a lot of attention in materials community in recent years.

Microstructure design based on statistical mechanics facilitates and optimizes choosing the microstructures of materials for specific design with desired properties. Therefore studying the statistical mechanics theory in different length scale becomes very important.

In this research, the main focus was to study the effect of one-point and two-point statistics on homogenization relationship for elastic properties of materials. Applying the homogenization relations to the microstructure of simulated isotropic and anisotropic composites, the mathematical representation of two-point probability functions was modified in anisotropic composites and the contribution of one-point and two-point statistics in the calculation of elastic properties was studied. Then, this methodology was applied to two samples of Al-SiC composites which were fabricated by extrusion (PSR: 2:1 and PSR: 8:1). Finally, the technique was extended to completely random and textured polycrystalline materials and the effect of cold rolling on the annealing texture of near- α Titanium alloy was presented.

It was shown analytically and numerically that the two-point statistics measurement does not contribute to the calculation of elastic properties in isotropic composites and random polycrystalline materials; however, its contribution is significant in anisotropic composites and textured polycrystalline materials (70% more than the contribution of one-point statistics). Furthermore, the results show that the two-point statistics can represent the effect of clustering in properties in two anisotropic samples of Al-SiC composite. Although the volume fraction of the two samples was the same, two-point statistics was able to capture the morphology of both microstructures and predict the differences in their elastic modulus and shear modulus. In addition, it was shown that the

contribution of two-point statistics in calculation of elastic properties of textured polycrystalline is much smaller than its contribution for anisotropic composite materials. All the final results were compared to several micromechanics models. Comparing the computational results to experimental results shows that this methodology is a good tool for structure-property relationships, and can lead to the design new materials with optimized properties as a fundamental backbone to microstructure design.

CHAPTER 1

INTRODUCTION

Structure, properties, and processing are the three significant elements in materials design. In today's technology, where advanced processing methods can provide materials with a variety of size and scales, the need for tools to properly select advanced materials such as composites and nano materials with desired properties is recognized. Further, a methodology to predict properties from any microstructure, and microstructure from properties is definitely required in a unified methodology for material design.

Statistical representation of the microstructure and applying the statistical mechanics modeling enable us to correlate properties, microstructure and processing in a unified methodology (Figure 1.1)

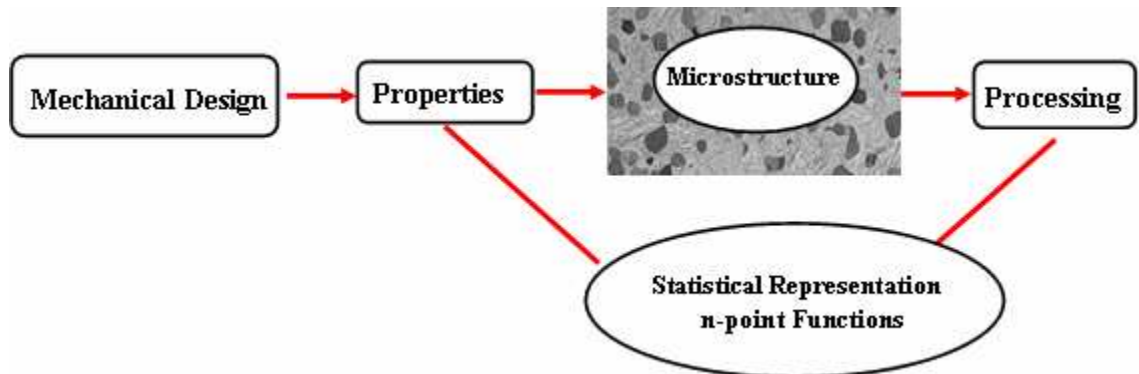


Figure 1.1 A schematically representation of mechanical design parameters

Statistical distribution functions are commonly used to represent microstructures in digital forms. Two-point statistical functions can be used as a first order correction to the average (volume fraction) representation. Two-point correlation functions provide information about near neighbor and far field effects and allow the defect sensitive properties to be incorporated in the analysis.

Statistical continuum mechanics provides a direct link between microstructure and properties (elastic and plastic) in terms of these two-point statistical functions. The prediction of mechanical properties from the details of the microstructure such as phase, crystalline grain orientation distribution and morphology has received a special attention in the mechanics and materials community (Torquato, 1982; Adams, 1987). In polycrystalline microstructures, internal structure refers to the size and shape of crystallites (grain), the distribution of their crystallographic orientations (texture), and the spatial correlations between these geometrical and crystallographic features. However, in composites, internal structure refers to spatial correlations between geometrical features of the two phases. The mathematical description of heterogeneity has received some breakthroughs in the last few decades with the works of Kröner (1972, 1977) and Beran (1968). More progress has been achieved to calculate the effective properties by making simple assumptions about the microstructure distribution (random, isotropic, and periodic microstructures) or the shape of the second phase (spherical, ellipsoidal...). These studies have relied primarily on the one-point probability functions (number or volume fractions of individual states within the microstructure), which ignored shape and geometric characteristics of the microstructure(Beran (1965), Beran and Molynex (1966), and Hashin (1962)). (Some of these models will be reviewed in chapter 2.) It

was realized that in order to use the measured materials heterogeneity it is necessary to incorporate two and higher order probability functions. However progress was hindered due to lack of experimental techniques to obtain two and three-point correlation functions. These techniques are now available which makes it possible to measure individual crystalline orientations in polycrystalline materials. Extension of this effort to non-random microstructures requires proper definition of n th degree statistical correlation functions.

Microstructure can be represented by a set of two-point correlation functions for a variety of states. In a polycrystalline material, each orientation is considered a different state and an n -dimensional space is then formulated for the homogenization relation (Garmestani, 2001; Adams, 2002). For instance, Orientation Distribution Function (ODF) is a one-point statistical distribution function that only considers volume fractions (or number fractions) of crystallites with the same orientation. However recent improvements in electron microscopy and image analysis have led to new techniques for analyzing the structure of polycrystalline materials at the scale of the crystalline grains. Orientation Imaging Microscopy (OIM) provides information on the spatial arrangement of lattice orientations in polycrystalline structures and is based on Kikuchi diffractometry (Garmestani, 1998). A two-phase composite consists of only two phases and the n -dimensional space is reduced to a two-dimensional state assuming that the anisotropic properties within each phase are ignored. In composites, if the orientation of each phase is ignored, the correlation functions can be measured using imaging techniques (optical, SEM,..). The use of OIM for the measurement of orientation for a multiphase composite can introduce a large amount of detail and complexity. Therefore,

higher order statistical formulations will be needed to incorporate such information for each phase and also the interaction of the two phases.

This research is focused on studying the effect of anisotropy on the homogenization relations based on two-point statistics. An analytical solution will be derived for the contribution of two-point statistics in homogenization relations for elastic properties of composites and polycrystalline materials. The importance of contribution of one-point and two-point statistical information will be investigated in calculation of elastic properties of composite and polycrystalline materials. In addition, an explanation will be provided why the effect of two-point statistical information was not observed in previous works. (Adam 1995, Garmestani 2000)

Several micromechanics models based on one-point probability information will be reviewed in chapter two and an overview on statistical continuum mechanics theory will be studied in chapter three. Two-point distribution functions will be then used to characterize and represent heterogeneity in two-phase composites in chapter four and five. An empirical form of the two-point statistical function is used which allows the construction of a composite enclosure (property enclosure is defined as a universe of all variation in inter relation among several properties for the same microstructure). Two different composites (isotropic and anisotropic) are considered and the effect of one-point and two-point statistics for the prediction of the elastic properties is discussed.

For this purpose, first, the elastic properties for an isotropic and anisotropic Al-Pb composite with quantified microstructures are computed in chapter five. In this simulation a mathematical form for the two-point correlation function is considered in isotropic composites. In addition, the mathematical formulation for probability

functions is extended for anisotropic composites. A new design variable will be defined to introduce anisotropy in the microstructures. The simulated values are compared with some micromechanics models including Voigt (upper) and Reuss (lower) bounds, and Hashin-Shtrikman bounds. Then, two-point probabilities are measured for Al-SiC composite with two different PSR (Particle Size Ratio) and the elastic properties are estimated for this composite directly from the measured two-point statistics of the microstructure. Finally, the simulation results will be compared with experimental results from mechanical testing and ultrasounds.

In chapter six, the structure-property relations will be developed for random and consequently for textured polycrystalline materials. In polycrystalline microstructures, two-point statistics are measured by considering the orientations of different grains and their coordinates. Therefore, first the methodology is applied to a simulated polycrystalline aluminum microstructure with completely random orientation of crystallites and also including different percentage of texture in one direction, then the methodology will be applied to two samples of near- α Titanium alloy (as received and 60% cold rolled) where the crystal structure is HCP. One and two-point statistics of lattice orientation distributions are measured using the OIM file and the effect of statistical measurement will be studied in calculation of elastic properties. The simulation results will be compared with Taylor upper and lower bounds and the effect of texture on properties of two samples will be studied. In addition the elastic properties of two samples will be measured by ultrasound techniques to verify the simulation results.

PART I:
BACKGROUND AND LITERATURE REVIEW

CHAPTER 2

MICROMECHANICAL MODELS FOR ELASTIC PROPERTIES

In this section, several theories to predict the elastic properties of heterogeneous materials which consist of several phases of the same phase in different states will be reviewed.

For heterogeneous materials with arbitrary microstructures, it is not possible to find a general analytical solution form elastic properties. Therefore there are two ways to approximate the elastic properties of the materials: rigorous bounds and approximation solutions. Both these evaluations are called micromechanics models to calculate elastic properties of a heterogeneous material. In other words these models are the primary tools for homogenization of materials' elastic properties. All of these models use one-point probability distribution functions (number or volume fractions of individual states within the microstructure) or use an assumption for the distribution and morphology of the second phase(s) in the matrix.

2.1 Rigorous Bounds: Variational Method

As it was mentioned before, bounding theories are among the methodologies to homogenize the effective properties of materials based on some microstructural information. Bounds can be shown as limiting values (upper and lower bounds) for properties for any computational work (Torquato 2000). Therefore knowing the properties of each phase and their volume fraction, there are several rigorous bounding

relationships to calculate the elastic properties of heterogeneous materials. All of these models assume a mathematical representation for the microstructure for the calculation of the effective properties. All of these bounds get close when more microstructural information is used in the approximation.

To calculate a variational bound, the effective properties can be expressed with a functional that has to be optimized. This kind of variational analysis for elastic properties of random heterogeneous media dates back to the work of Beran (1965) and Beran and Molyneux (1966). To derive a rigorous bound on elastic properties, the strain elastic energy in the system needs to be defined, and then this function has to be minimized so that the system reaches a stable state. In this section, upper and lower bounds will be determined based on the minimum potential energy principle.

Effective stiffness and compliance of the representative volume can be represented by:

$$\begin{aligned} C_{ijkl} &= \langle c_{ijkl} \rangle \\ S_{ijkl}^{-1} &= \langle s_{ijkl}^{-1} \rangle \end{aligned} \quad (2-1)$$

Where c and s are local variables and $\langle h \rangle$ is the ensemble average of variable h and can be defined by the following equation (Kroner, 1972):

$$\langle h \rangle = \langle h(x) \rangle = \frac{1}{V} \int_V h(x) dV = \frac{1}{N} \sum_{i=1}^N h_i(x) \quad (2-2)$$

A composite is composed of M anisotropic phases. Therefore the elasticity tensor can be shown by the following equation: (Torquato, 2001)

$$C(x) = \sum_{i=1}^M c_i I^{(i)}(x), \quad (2-3)$$

where $I^{(i)}(x)$ is the indicator that is equal to 1 in phase i and 0 if it is not in phase i . This function is defined as:

$$I^{(i)}(x) = \begin{cases} 1 & x \in i \\ 0 & x \notin i \end{cases} \quad (2-4)$$

Here, a brief overview of homogenization relations in elastic domain will be shown (more details for homogenization relationship based on two-point statistics will be presented in later chapters). The equilibrium equation and the constitutive equation for static state can be shown by:

$$\begin{aligned} \nabla \cdot \boldsymbol{\sigma}(x) &= 0 \\ \boldsymbol{\sigma}(x) &= c(x)\boldsymbol{\varepsilon}(x) \end{aligned} \quad , \quad (2-5)$$

where, $\boldsymbol{\sigma}(x)$, $c(x)$, and $\boldsymbol{\varepsilon}(x)$ are local variables. Also assuming the material as a homogenous media, the effective elastic stiffness can be defined by:

$$\langle \boldsymbol{\sigma} \rangle = C \langle \boldsymbol{\varepsilon} \rangle \quad (2-6)$$

Local elastic stiffness and stress can be defined by: (Beran (1965))

$$\begin{aligned} \boldsymbol{\varepsilon} &= \langle \boldsymbol{\varepsilon} \rangle + \tilde{\boldsymbol{\varepsilon}} \\ \boldsymbol{\sigma} &= \langle \boldsymbol{\sigma} \rangle + \tilde{\boldsymbol{\sigma}} \end{aligned} \quad , \quad (2-7)$$

where $\tilde{\boldsymbol{\sigma}}$ and $\tilde{\boldsymbol{\varepsilon}}$ are deviation or fluctuation fields. The local energy stored in a homogenous linearly elastic material is equal to $\frac{1}{2}\boldsymbol{\varepsilon}(x)C(x)\boldsymbol{\varepsilon}(x)$, and the macroscopic values of the strain energy can be defined by (Sokolnikoff, 1956):

$$\begin{aligned} W(\boldsymbol{\varepsilon}) &= \langle w_{\boldsymbol{\varepsilon}}(x) \rangle = \frac{1}{2} \langle \boldsymbol{\varepsilon}(x)C(x)\boldsymbol{\varepsilon}(x) \rangle \\ W(\boldsymbol{\sigma}) &= \langle w_{\boldsymbol{\sigma}}(x) \rangle = \frac{1}{2} \langle \boldsymbol{\sigma}(x)C^{-1}(x)\boldsymbol{\sigma}(x) \rangle \end{aligned} \quad (2-8)$$

There are two general theorems applied on energy configuration:

Theorem 1. For ergodic macroscopically anisotropic multiphase composites, the elastic strain energy is equal to the ensemble average of the local strain energy.

$$\begin{aligned}\frac{1}{2}\langle \boldsymbol{\varepsilon} \rangle : \mathbf{C} : \langle \boldsymbol{\varepsilon} \rangle &= \frac{1}{2}\langle \boldsymbol{\varepsilon} : \mathbf{c} : \boldsymbol{\varepsilon} \rangle \\ \frac{1}{2}\langle \boldsymbol{\sigma} \rangle : \mathbf{C}^{-1} : \langle \boldsymbol{\sigma} \rangle &= \frac{1}{2}\langle \boldsymbol{\sigma} : \mathbf{c}^{-1} : \boldsymbol{\sigma} \rangle\end{aligned}\quad (2-9)$$

Theorem 2. The effective stiffness tensor is symmetric and positive definite.

Recall: Suppose B is a second order matrix, then B is semi-positive if for any vector \vec{a} :

$$a_i B_{ij} a_j \geq 0$$

If only the inequality applies for $\vec{a} \neq 0$, then B is called positive definite.

For the general equilibrium equation in elasticity, there are two types of boundary conditions that can be applied (Brush, 1975):

Type I: Displacement boundary condition: displacement $u(x)$ is prescribed on the boundary (∂V or S). In other words; strain has been defined for the domain:

$$\boldsymbol{\varepsilon}_{ij} = \frac{1}{2} \left(\frac{\partial u_i}{\partial x_j} + \frac{\partial u_j}{\partial x_i} \right) \quad (\text{is defined for all } x \in V) \quad (2-10)$$

Type II: Traction boundary condition: surface traction $t^n(x)$ is prescribed on the boundary for all $x \in S$.

Assuming the first type of boundary condition $u(x)$ is the true displacement field and fluctuation $\tilde{u}(x)$ is the new displacement field where $\tilde{u}(x) = 0$ when $x \in S$.

Therefore the strain field can be defined by:

$$\boldsymbol{\varepsilon}_{ij} + \tilde{\boldsymbol{\varepsilon}}_{ij} = \frac{1}{2} \left(\frac{\partial u_i}{\partial x_j} + \frac{\partial u_j}{\partial x_i} \right) + \frac{1}{2} \left(\frac{\partial \tilde{u}_i}{\partial x_j} + \frac{\partial \tilde{u}_j}{\partial x_i} \right) \quad (2-11)$$

Hence the strain energy in the system can be defined by:

$$\begin{aligned}
w + \tilde{w} &= \frac{1}{2} c_{ijkl} (\boldsymbol{\varepsilon}_{ij} + \tilde{\boldsymbol{\varepsilon}}_{ij}) (\boldsymbol{\varepsilon}_{kl} + \tilde{\boldsymbol{\varepsilon}}_{kl}) \\
&= w + \frac{1}{2} c_{ijkl} (\boldsymbol{\varepsilon}_{ij} \tilde{\boldsymbol{\varepsilon}}_{kl} + \tilde{\boldsymbol{\varepsilon}}_{ij} \boldsymbol{\varepsilon}_{kl} + \tilde{\boldsymbol{\varepsilon}}_{ij} \tilde{\boldsymbol{\varepsilon}}_{kl}) \\
&= w + c_{ijkl} (\boldsymbol{\varepsilon}_{ij} \tilde{\boldsymbol{\varepsilon}}_{kl}) + \underbrace{\frac{1}{2} c_{ijkl} \tilde{\boldsymbol{\varepsilon}}_{ij} \tilde{\boldsymbol{\varepsilon}}_{kl}}_{\geq 0} \quad (\text{by symmetry})
\end{aligned} \tag{2-12}$$

Since C is a positive definite matrix ($\frac{1}{2} c_{ijkl} \tilde{\boldsymbol{\varepsilon}}_{ij} \tilde{\boldsymbol{\varepsilon}}_{kl} \geq 0$), therefore the other term can be calculated by:

$$\begin{aligned}
c_{ijkl} (\boldsymbol{\varepsilon}_{ij} \tilde{\boldsymbol{\varepsilon}}_{kl}) &= \sigma_{kl} \tilde{\boldsymbol{\varepsilon}}_{kl} = \frac{1}{2} \sigma_{kl} \left(\frac{\partial \tilde{u}_k}{\partial x_l} + \frac{\partial \tilde{u}_l}{\partial x_k} \right) \\
&= \sigma_{kl} \frac{\partial \tilde{u}_k}{\partial x_l} \quad (\text{since } \sigma_{kl} = \sigma_{lk}) \\
&= \frac{\partial}{\partial x_l} (\sigma_{kl} \tilde{u}_k) - \left(\frac{\partial \sigma_{kl}}{\partial x_l} \right) \tilde{u}_k \\
&= \frac{\partial}{\partial x_l} (\sigma_{kl} \tilde{u}_k) \quad (\text{since } \left(\frac{\partial \sigma_{kl}}{\partial x_l} \right) = 0) \\
&= (\sigma_{kl} \tilde{u}_k)_{,l} \quad (\text{shorthand notation})
\end{aligned} \tag{2-13}$$

The total macroscopic strain energy can be calculated by:

$$W = \langle w \rangle = \iiint_V w dV \tag{2-14}$$

The increase in elastic energy due to the fluctuation field is:

$$\Delta W = \underbrace{\iiint_V \frac{1}{2} c_{ijkl} \tilde{\boldsymbol{\varepsilon}}_{ij} \tilde{\boldsymbol{\varepsilon}}_{kl} dV}_{\geq 0} + \iiint_V c_{ijkl} \boldsymbol{\varepsilon}_{ij} \tilde{\boldsymbol{\varepsilon}}_{kl} dV \tag{2-15}$$

The first term on the right hand side is positive, since C is positive definite (theorem 2). The second integral can be converted into a surface integral by applying Divergence theorem:

$$\begin{aligned}
\iiint_V c_{ijkl} \boldsymbol{\varepsilon}_{ij} \tilde{\boldsymbol{\varepsilon}}_{kl} dV &= \iiint_V (\sigma_{kl} \tilde{u}_k)_{,l} dV \\
&= \iint_S \sigma_{kl} \tilde{u}_k n_l dS = \iint_S t_k^{(\hat{n})} \tilde{u}_k dS = 0 \quad (\text{since } \tilde{u}_k = 0 \text{ on } S)
\end{aligned} \tag{2-16}$$

Note that the second term in eq. (2-15) becomes zero when the displacement satisfies the boundary conditions. Therefore, the displacement field that satisfies the equilibrium equation and the displacement boundary conditions everywhere will result in an increase in the strain energy of the system or:

$$\Delta W \geq 0 \quad (2-17)$$

So the principle of Minimum Energy can be stated as follows:

“Of all displacement fields satisfying the prescribed displacement boundary conditions (type I), that field which satisfies stress equilibrium and is symmetric minimizes the stored elastic energy of the system, W .” (Hirt and Lothar, 1968)

The same steps can be applied to boundary condition type II. In that case the minimum complementary potential energy can be stated as follows:

“Among all those stress fields that satisfy the prescribed stress boundary condition, the field that satisfies the stress equilibrium and are in equilibrium with the external loads acting on the body, true stress, minimizes the strain energy distribution.” (Hirt and Lothar, 1968)

This theory has an application in finding the boundary relationships for elastic properties of composites and polycrystalline materials, which will be shown here:

Assuming uniform strain in both phases:

$$\boldsymbol{\varepsilon}(r) = \langle \boldsymbol{\varepsilon} \rangle = \bar{\boldsymbol{\varepsilon}} \quad (2-18)$$

Average elastic energy density in a representative volume is related to the effective or macroscopic stiffness C and is equal to the average of the microscopic strain energy:

$$\langle w \rangle = \left\langle \frac{1}{2} \boldsymbol{\varepsilon}_{ij} C_{ijkl} \boldsymbol{\varepsilon}_{kl} \right\rangle \equiv \frac{1}{2} \langle \boldsymbol{\varepsilon}_{ij} \rangle C_{ijkl} \langle \boldsymbol{\varepsilon}_{kl} \rangle \quad (2-19)$$

Assuming $\varepsilon^*(x)$ as a strain field that satisfies boundary conditions of type I (prescribed displacement field at ∂R) but $\varepsilon^* \neq \langle \varepsilon \rangle$, The principle of minimum energy can be implied as follows (Beran, 1996):

$$\langle \frac{1}{2} \varepsilon_{ij} c_{ijkl} \varepsilon_{kl} \rangle \equiv \frac{1}{2} \langle \varepsilon_{ij} \rangle C_{ijkl} \langle \varepsilon_{kl} \rangle \leq \langle \frac{1}{2} \varepsilon_{ij}^* c_{ijkl} \varepsilon_{kl}^* \rangle \quad (2-20)$$

Now assuming $\varepsilon^* = \langle \varepsilon \rangle$

$$\frac{1}{2} \langle \varepsilon_{ij} \rangle C_{ijkl} \langle \varepsilon_{kl} \rangle \leq \frac{1}{2} \langle \langle \varepsilon_{ij} \rangle c_{ijkl} \langle \varepsilon_{kl} \rangle \rangle \equiv \frac{1}{2} \langle \varepsilon_{ij} \rangle \langle c_{ijkl} \rangle \langle \varepsilon_{kl} \rangle \quad (2-21)$$

Therefore:

$$C_{ijkl} \leq \langle c_{ijkl} \rangle \quad (2-22)$$

This is called Voight upper bound which will be discussed in later sections in more detail.

Alternatively the elastic strain energy in the system can be represented with an expression in terms of the compliance tensor

$$\langle w \rangle = \langle \frac{1}{2} \sigma_{ij} S_{ijkl} \sigma_{kl} \rangle \equiv \frac{1}{2} \langle \sigma_{ij} \rangle S_{ijkl} \langle \sigma_{kl} \rangle$$

Choosing $\sigma^* = \langle \sigma \rangle$:

$$\frac{1}{2} \langle \sigma_{ij} \rangle S_{ijkl} \langle \sigma_{kl} \rangle \leq \langle \frac{1}{2} \langle \sigma_{ij} \rangle s_{ijkl} \langle \sigma_{kl} \rangle \rangle \equiv \frac{1}{2} \langle \sigma_{ij} \rangle \langle s_{ijkl} \rangle \langle \sigma_{kl} \rangle \quad (2-23)$$

Therefore:

$$S_{ijkl} \leq \langle s_{ijkl} \rangle \quad (2-24)$$

This is called Reuss upper bound on elastic compliance.

Inverting the above equations (eq. (2-21) and eq. (2-23)) and combining them, the bounds for effective elastic constants can be calculated by (Beran 1996):

$$\begin{aligned} \langle \varepsilon_{ij} \rangle \langle s_{ijkl}^{-1} \rangle \langle \varepsilon_{kl} \rangle &\leq \langle \varepsilon_{ij} \rangle C_{ijkl} \langle \varepsilon_{kl} \rangle \leq \langle \varepsilon_{ij} \rangle \langle c_{ijkl} \rangle \langle \varepsilon_{kl} \rangle \\ \langle \sigma_{ij} \rangle \langle c_{ijkl}^{-1} \rangle \langle \sigma_{kl} \rangle &\leq \langle \sigma_{ij} \rangle S_{ijkl} \langle \sigma_{kl} \rangle \leq \langle \sigma_{ij} \rangle \langle s_{ijkl} \rangle \langle \sigma_{kl} \rangle \end{aligned} \quad (2-25)$$

or:

$$\begin{aligned}\bar{\epsilon}_{ij} \bar{S}_{ijkl}^{-1} \bar{\epsilon}_{ij} &\leq \bar{\epsilon}_{ij} C_{ijkl} \bar{\epsilon}_{ij} \leq \bar{\epsilon}_{ij} \bar{C}_{ijkl} \bar{\epsilon}_{ij} \\ \bar{\epsilon}_{ij} \bar{C}_{ijkl}^{-1} \bar{\epsilon}_{ij} &\leq \bar{\epsilon}_{ij} S_{ijkl} \bar{\epsilon}_{ij} \leq \bar{\epsilon}_{ij} \bar{S}_{ijkl} \bar{\epsilon}_{ij}\end{aligned}\quad (2-26)$$

These are bounding relationship that can be used to calculate upper and lower bounds. It is very important to consider that these bounds are on the energy of the representative volume. Therefore $\langle \epsilon \rangle = \bar{\epsilon}$ or $\langle \sigma \rangle = \bar{\sigma}$ can not be omitted from the two sides unless the applied strain or stress would result in such. To make more clarification on the use of these bounding relationships, more details will be discussed in next section.

2.1.1 Voigt model (upper bound)

Voigt model assumes a uniform strain in throughout the phases in the composite. (Voigt, 1889)

$$\epsilon(r) = \langle \epsilon \rangle = \bar{\epsilon} \quad (2-27)$$

Effective elastic properties through the material is defined by:

$$\bar{\sigma} = C \bar{\epsilon}, \quad (2-28)$$

therefore:

$$\langle c \epsilon \rangle = C \bar{\epsilon} = \langle c \bar{\epsilon} \rangle = \langle c \rangle \bar{\epsilon} \Rightarrow C = \langle c \rangle \quad (2-29)$$



Figure 2.1 Voigt model: Uniform strain field in both phases

Therefore the effective elastic stiffness which can be calculated as $\langle c \rangle$ represents the upper bound. The average ensemble of stiffness can be calculated by the rule of mixture. Assuming v_1 and v_2 as the volume fractions of two phases, the total force in the media can be calculated by:

$$F = F_1 + F_2 = \bar{\sigma}_1 A_1 + \bar{\sigma}_2 A_2 = (C^1 A_1 + C^2 A_2) \bar{\epsilon} \quad (2-30)$$

The average stress in the media can be calculated by:

$$\bar{\sigma} = C \bar{\epsilon} = \frac{F}{A} = \frac{(C^1 A_1 + C^2 A_2) \bar{\epsilon}}{A} = (C^1 v_1 + C^2 v_2) \bar{\epsilon} \quad (2-31)$$

Therefore elastic stiffness is:

$$C = \sum_{i=1}^M v_i c^i = \bar{C} \quad (2-32)$$

This is called Voigt upper bound. (Voigt, 1889)

2.1.2 Reuss Model (lower bound)

Reuss model assumes a uniform stress throughout the phases (Reuss, 1929):

$$\sigma(r) = \langle \sigma \rangle = \bar{\sigma}, \quad (2-33)$$

the average strain can be defined by:

$$\bar{\epsilon} = \langle \epsilon \rangle = \langle s \sigma \rangle \quad (2-34)$$

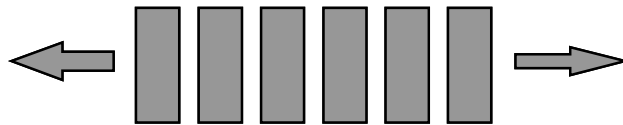


Figure 2.2 Reuss model: Uniform stress field in both phases

By applying eq. (2-33) the above equation can be reformulated as:

$$\bar{\varepsilon} = \langle s\sigma \rangle = \langle s\bar{\sigma} \rangle = \bar{\sigma} \langle s \rangle = \bar{\sigma} S, \quad (2-35)$$

therefore:

$$S = \langle s \rangle \Rightarrow C = \langle s \rangle^{-1} \quad (2-36)$$

The effective elastic compliance in this case is equal to the average of compliances which can be obtained by rule of mixture. This value represents the upper bound for compliance (S) or lower bound for stiffness. Assuming v_1 and v_2 as the volume fractions, the total increase in length of the media is estimated as follows:

$$\Delta l = \Delta l_1 + \Delta l_2 = \varepsilon_1 l_1 + \varepsilon_2 l_2 \quad (2-37)$$

Dividing both sides by total length (l), the average strain is estimated by:

$$\bar{\varepsilon} = \frac{\Delta l}{l} = \frac{\varepsilon_1 l_1 + \varepsilon_2 l_2}{l} = S^1 \bar{\sigma}_1 v_1 + S^2 \bar{\sigma}_2 v_2 = (v_1 S^1 + v_2 S^2) \bar{\sigma} \quad (2-38)$$

Using eq. (2-35), it follows:

$$S = v_1 S^1 + v_2 S^2 \quad (2-39)$$

Or:

$$S = C^{-1} = \sum_{i=1}^M v_i S^i = \bar{S} \quad (2-40)$$

2.2 Degraded bounds for elastic coefficients based on minimum-energy theory

The elastic strain energy functional was derived for a force-free homogenous medium in the previous section and the upper and lower bounds were developed in general by minimizing the energy. Here the bounds for each component of the elastic stiffness

tensor will be derived. For this purpose, first an overview of different symmetry operations applicable to crystalline materials and corresponding elastic stiffness tensors will be presented. (Lai, 1993)

For a general case of a homogenous medium, implying the symmetric properties of stress and strain and the positive definite properties of strain energy, there are 21 independent terms in the stiffness matrix. Therefore the general form of stress-strain relationship of a general case can be shown as (Lai, 1993):

$$\begin{bmatrix} \bar{\sigma}_{11} \\ \bar{\sigma}_{22} \\ \bar{\sigma}_{33} \\ \bar{\sigma}_{23} \\ \bar{\sigma}_{31} \\ \bar{\sigma}_{12} \end{bmatrix} = \begin{bmatrix} C_{1111} & C_{1122} & C_{1133} & C_{1123} & C_{1113} & C_{1112} \\ C_{1122} & C_{2222} & C_{2233} & C_{2223} & C_{2213} & C_{1222} \\ C_{1133} & C_{2233} & C_{3333} & C_{2333} & C_{1333} & C_{1233} \\ C_{1123} & C_{2223} & C_{2333} & C_{2323} & C_{2313} & C_{1223} \\ C_{1113} & C_{2213} & C_{1343} & C_{2313} & C_{1313} & C_{1213} \\ C_{1112} & C_{1222} & C_{1233} & C_{1223} & C_{1213} & C_{1212} \end{bmatrix} \begin{bmatrix} \bar{\epsilon}_{11} \\ \bar{\epsilon}_{22} \\ \bar{\epsilon}_{33} \\ 2\bar{\epsilon}_{23} \\ 2\bar{\epsilon}_{31} \\ 2\bar{\epsilon}_{12} \end{bmatrix} \quad (2-41)$$

Monoclinic anisotropic linearly elastic solid is defined in such a way that the linearly elastic solid has one plane of symmetry. Therefore there are 13 independent elastic coefficients, and the resulting tensor can be written as follows (Lai, 1993):

$$\begin{bmatrix} \bar{\sigma}_{11} \\ \bar{\sigma}_{22} \\ \bar{\sigma}_{33} \\ \bar{\sigma}_{23} \\ \bar{\sigma}_{31} \\ \bar{\sigma}_{12} \end{bmatrix} = \begin{bmatrix} C_{1111} & C_{1122} & C_{1133} & C_{1123} & 0 & 0 \\ C_{1122} & C_{2222} & C_{2233} & C_{2223} & 0 & 0 \\ C_{1133} & C_{2233} & C_{3333} & C_{2333} & 0 & 0 \\ C_{1123} & C_{2223} & C_{2333} & C_{2323} & 0 & 0 \\ 0 & 0 & 0 & 0 & C_{1313} & C_{1213} \\ 0 & 0 & 0 & 0 & C_{1213} & C_{1212} \end{bmatrix} \begin{bmatrix} \epsilon_{11} \\ \epsilon_{22} \\ \epsilon_{33} \\ 2\epsilon_{23} \\ 2\epsilon_{31} \\ 2\epsilon_{12} \end{bmatrix} \quad (2-42)$$

If the elastic body has two mutually perpendicular planes of symmetry, then the material is called orthotropic and there are only 9 independent coefficients (Lai, 1993).

$$\begin{bmatrix} \bar{\sigma}_{11} \\ \bar{\sigma}_{22} \\ \bar{\sigma}_{33} \\ \bar{\sigma}_{23} \\ \bar{\sigma}_{31} \\ \bar{\sigma}_{12} \end{bmatrix} = \begin{bmatrix} C_{1111} & C_{1122} & C_{1133} & 0 & 0 & 0 \\ C_{1122} & C_{2222} & C_{2233} & 0 & 0 & 0 \\ C_{1133} & C_{2233} & C_{3333} & 0 & 0 & 0 \\ 0 & 0 & 0 & C_{2323} & 0 & 0 \\ 0 & 0 & 0 & 0 & C_{1313} & 0 \\ 0 & 0 & 0 & 0 & 0 & C_{1212} \end{bmatrix} \begin{bmatrix} \varepsilon_{11} \\ \varepsilon_{22} \\ \varepsilon_{33} \\ 2\varepsilon_{23} \\ 2\varepsilon_{31} \\ 2\varepsilon_{12} \end{bmatrix} \quad (2-43)$$

Whereas for a transverse-isotropic media, there are just 6 nonzero coefficients where only five of them are independent (Lai, 1993):

$$C_{1111} = C_{2222}; C_{3333}; C_{1133} = C_{2233}; C_{1122}; C_{1313} = C_{2323}; C_{1212} = \frac{C_{1111} - C_{1122}}{2} \quad (2-44)$$

In addition if the media is isotropic, there will be two independent stiffness coefficients:

$$C_{1111}; C_{1122}; C_{1212} = \frac{C_{1111} - C_{1122}}{2}$$

In next subsection, bounds will be derived for an orthotropic media which has 9 independent elastic stiffness coefficients.

2.2.1 Bounds for diagonal terms of the matrix

Recalling the bounding relationship in eq. (2-25), the bounds will be derived here for diagonal terms of the elastic stiffness matrix. Assuming the uniaxial tensile test the only nonzero component of the induced strain will be $\bar{\varepsilon}_{11} \neq 0$, (Kroner, 1977)

$$\varepsilon = \begin{bmatrix} \bar{\varepsilon}_{11} & 0 & 0 \\ 0 & 0 & 0 \\ 0 & 0 & 0 \end{bmatrix} \quad (2-45)$$

Therefore the strain bounding relations for strain will be summarized by:

$$\bar{\varepsilon}_{11} \bar{S}_{1111}^{-1} \bar{\varepsilon}_{11} \leq \bar{\varepsilon}_{11} C_{1111} \bar{\varepsilon}_{11} \leq \bar{\varepsilon}_{11} \bar{C}_{1111} \bar{\varepsilon}_{11} \quad (2-46)$$

and therefore:

$$\bar{S}_{1111}^{-1} \leq C_{1111} \leq \bar{C}_{1111}$$

In general, these bounding relations can be represented as follows:

$$\bar{S}_{iii}^{-1} \leq C_{iii} \leq \bar{C}_{iii} \quad (2-47)$$

Note that there is no summation on the indices. The same philosophy can be assumed for other diagonal terms (C_{2222}, C_{3333}).

On the other hand, assuming pure torsion test for the sample results in nonzero component of shear strain as in the following (Kroner, 1977):

$$\boldsymbol{\varepsilon} = \begin{bmatrix} 0 & \bar{\varepsilon}_{12} & 0 \\ \bar{\varepsilon}_{12} & 0 & 0 \\ 0 & 0 & 0 \end{bmatrix} \quad (2-48)$$

Substituting in the bounding relationship (2-25), the following inequality will be achieved:

$$4\bar{\varepsilon}_{12}\bar{S}_{1212}^{-1}\bar{\varepsilon}_{12} \leq 4\bar{\varepsilon}_{12}C_{1212}\bar{\varepsilon}_{12} \leq 4\bar{\varepsilon}_{12}\bar{C}_{1212}\bar{\varepsilon}_{12} \quad (2-49)$$

or:

$$\bar{S}_{1212}^{-1} \leq C_{1212} \leq \bar{C}_{1212}$$

So in general, it follows:

$$\bar{S}_{ijj}^{-1} \leq C_{ijj} \leq \bar{C}_{ijj} \quad (2-50)$$

Note that i and j are free indices and vary between 1 and 3.

2.2.2 Bounds for off-diagonal terms

Now that the bounds are known for the diagonal terms, the effect of bounding relationships will be studied for other coefficients. Expanding the right hand side of the

eq. (2-25) or (2-26), $(\bar{\varepsilon}_{ij}C_{ijkl}\bar{\varepsilon}_{kl} \leq \bar{\varepsilon}_{kl}\bar{C}_{ijkl}\bar{\varepsilon}_{kl})$ results in the following equation (Kroner, 1977):

$$\bar{\varepsilon}_{11}C_{1111}\bar{\varepsilon}_{11} + 2\bar{\varepsilon}_{11}C_{1122}\bar{\varepsilon}_{22} + \bar{\varepsilon}_{22}C_{2222}\bar{\varepsilon}_{22} \leq \bar{\varepsilon}_{11}\bar{C}_{1111}\bar{\varepsilon}_{11} + 2\bar{\varepsilon}_{11}\bar{C}_{1122}\bar{\varepsilon}_{22} + \bar{\varepsilon}_{22}\bar{C}_{2222}\bar{\varepsilon}_{22} \quad (2-51)$$

Assuming $\varepsilon_{11} \neq 0$ and $\varepsilon_{22} \neq 0$ and other components as zero, then the above equation can be rewritten as:

$$2\bar{\varepsilon}_{11}C_{1122}\bar{\varepsilon}_{22} \leq 2\bar{\varepsilon}_{11}\bar{C}_{1122}\bar{\varepsilon}_{22} + \bar{\varepsilon}_{11}^2(\bar{C}_{1111} - C_{1111}) + \bar{\varepsilon}_{22}^2(\bar{C}_{2222} - C_{2222}) \quad (2-52)$$

Assuming $\frac{\bar{\varepsilon}_{22}}{\bar{\varepsilon}_{11}} = \zeta$, it follows:

$$2\zeta(C_{1122} - \bar{C}_{1122}) \leq (\bar{C}_{1111} - C_{1111}) + \zeta^2(\bar{C}_{2222} - C_{2222}) \quad (2-53)$$

Both sides of the equations can be divided by 2ζ . Therefore there are two cases that can be considered:

CASE 1: Positive ζ :

Since the bounds have been calculated for C_{1111} and C_{2222} in eq. (2-47),

$$C_{1122} \leq \bar{C}_{1122} + \underbrace{\frac{1}{2\rho}\bar{\varepsilon}_{11}^2(\bar{C}_{1111} - S_{1111}^{-1}) + \frac{\zeta}{2}(\bar{C}_{2222} - S_{2222}^{-1})}_{\phi(\zeta)} \quad (2-54)$$

(a)-CALCULATION OF ζ AND UPPER BOUND:

Minimizing function ϕ results in:

$$\frac{d\phi}{d\rho} = 0 \Rightarrow \zeta = \sqrt{\frac{\bar{C}_{1111} - \bar{S}_{1111}^{-1}}{\bar{C}_{2222} - \bar{S}_{2222}^{-1}}} \quad (2-55)$$

The upper bound would be (Proust, 2005):

$$C_{1212} \leq \bar{C}_{1212} + \sqrt{(\bar{C}_{1111} - \bar{S}_{1111}^{-1})(\bar{C}_{2222} - \bar{S}_{2222}^{-1})} \quad (2-56)$$

CASE 2: Negative ρ :

$$C_{1122} \geq \bar{C}_{1122} + \underbrace{\frac{1}{2\zeta} \bar{\epsilon}_{11}^2 (\bar{C}_{1111} - S_{1111}^{-1}) + \frac{\zeta}{2} (\bar{C}_{2222} - S_{2222}^{-1})}_{\phi(\zeta)} \quad (2-57)$$

(b)-CALCULATION OF ρ AND LOWR BOUND:

$$\frac{d\phi}{d\zeta} = 0 \Rightarrow \zeta = \sqrt{\frac{\bar{C}_{1111} - \bar{S}_{1111}^{-1}}{\bar{C}_{2222} - \bar{S}_{2222}^{-1}}} \quad (2-58)$$

The lower bound can be calculated:

$$C_{1212} \geq \bar{C}_{1212} - \sqrt{(\bar{C}_{1111} - \bar{S}_{1111}^{-1})(\bar{C}_{2222} - \bar{S}_{2222}^{-1})} \quad (2-59)$$

The following equation is obtained by combining relations (2-56) and (2-59) (Proust, 2005):

$$\bar{C}_{1212} - \sqrt{(\bar{C}_{1111} - \bar{S}_{1111}^{-1})(\bar{C}_{2222} - \bar{S}_{2222}^{-1})} \leq C_{1212} \leq \bar{C}_{1212} + \sqrt{(\bar{C}_{1111} - \bar{S}_{1111}^{-1})(\bar{C}_{2222} - \bar{S}_{2222}^{-1})} \quad (2-60)$$

Now by considering the left hand side of the eq. (2-25),

$$\bar{\epsilon}_{ij} S_{ijkl}^{-1} \bar{\epsilon}_{kl} \leq \bar{\epsilon}_{ij} C_{ijkl} \bar{\epsilon}_{kl} \leq \bar{\epsilon}_{ij} C_{ijkl} \bar{\epsilon}_{kl},$$

Another set of upper bound and lower bound will be calculated for C_{1122} as follows:

$$\bar{S}_{1212}^{-1} - \sqrt{(\bar{C}_{1111} - \bar{S}_{1111}^{-1})(\bar{C}_{2222} - \bar{S}_{2222}^{-1})} \leq C_{1212} \leq \bar{S}_{1212}^{-1} + \sqrt{(\bar{C}_{1111} - \bar{S}_{1111}^{-1})(\bar{C}_{2222} - \bar{S}_{2222}^{-1})} \quad (2-61)$$

Comparing (2-59) and (2-60) the final relationship for the degraded bounds will be (Proust, 2005):

$$\begin{aligned} & \text{MAX}(\bar{S}_{1212}^{-1}, \bar{C}_{1212}) - \sqrt{(\bar{C}_{1111} - \bar{S}_{1111}^{-1})(\bar{C}_{2222} - \bar{S}_{2222}^{-1})} \\ & \leq C_{1212} \leq \text{MIN}(\bar{C}_{1212}, \bar{S}_{1212}^{-1}) + \sqrt{(\bar{C}_{1111} - \bar{S}_{1111}^{-1})(\bar{C}_{2222} - \bar{S}_{2222}^{-1})} \end{aligned} \quad (2-62)$$

2.3 Hashin-Shtrikman Variational Method

In this section a brief review on the bounds of Hashin-Shtrikman (1962, 1963) for elasticity will be presented. In this variational method, the upper and lower bounds on elastic properties will be derived based on strain energy variation of a quasi-isotropic and quasi-homogenous media. The microstructure of the media has been assumed arbitrary which includes a number of isotropic and homogenous elastic phases.

As it was mentioned before, the effective elastic properties of the media (composite) can be calculated by the average of microscopic strain energy of the system that has been subjected to a surface displacement or traction. Since it is not possible to calculate the local stress and strain at each point, therefore the variational principle is a good tool to bound the strain energy and consequently the effective elastic properties of the media.

Hashin and Shtrikman have worked on variational methods for isotropic case in (1961) and for the general anisotropic case in (1962). In this section the variational method for nonhomogenous and isotropic elasticity will be reviewed for a multiphase media.

Hook's law is given by:

$$\sigma^0 = C_0 \varepsilon^0 = \lambda_0 \varepsilon_{kk}^0 \delta_{ij} + 2G_0 \varepsilon_{ij}^0, \quad (2-63)$$

where, σ_{ij}^0 and ε_{ij}^0 are the stress and strain tensor fields in a deformed elastic body of volume V and surface S (the case of no body force). Now the body changes to a material with different microstructures and properties. ($C\varepsilon_{ij} = \lambda\varepsilon_{kk} \delta_{ij} + 2G\varepsilon_{ij}$)

The stress polarization tensor is defined by:

$$\sigma_{ij} = C^0 \varepsilon_{ij} + \tilde{\sigma}_{ij} \quad (2-64)$$

It follows:

$$\sigma_{ij} = C \varepsilon_{ij} - C^0 \varepsilon_{ij} = (C - C^0) \varepsilon_{ij} \quad (2-65)$$

Define the deviation of strain as:

$$\tilde{\varepsilon}_{ij} = \varepsilon_{ij} - \varepsilon_{ij}^0 \quad (2-66)$$

Now define the strain energy as a general form:

$$W = \frac{1}{2} \int \sigma_{ij} \varepsilon_{ij} dV$$

This equation can be reduced to the following form:

$$W = \frac{1}{2} \int \sigma_{ij}^0 \varepsilon_{ij}^0 dV + \frac{1}{2} \int \tilde{\sigma}_{ij} \varepsilon_{ij}^0 dV = W_0 - \frac{1}{2} \int [\tilde{\sigma}_{ij} (C - C^0)^{-1} - \tilde{\sigma}_{ij} \varepsilon'_{ij} - 2\tilde{\sigma}_{ij} \varepsilon_{ij}^0] dV \quad (2-67)$$

Equilibrium equation on the other hand can be reduced to:

$$\sigma_{ij,j} = 0 \Rightarrow C^0 (\tilde{\varepsilon}_{ij})_{,j} + \tilde{\sigma}_{ij,j} = 0 \Rightarrow (\lambda_0 + G_0) \tilde{u}_{j,ji} + G_0 \tilde{u}_{i,jj} + \tilde{\sigma}_{ij,j} = 0;$$

Finally the following PDE and the boundary condition has to be solved:

$$\begin{aligned} (\lambda_0 + G_0) \tilde{u}_{j,ji} + G_0 \tilde{u}_{i,jj} + \tilde{\sigma}_{ij,j} &= 0 \\ \tilde{u}(x) &= 0, \quad x \in S \end{aligned} \quad (2-68)$$

Eq. (2-65), eq. (2-66) and eq. (2.68) are showing the second boundary problem of the theory of elasticity (Sokolnikoff, 1956). Therefore the stationary value of W is an absolute maximum when (Shtrikman, 1962)

$$\lambda > \lambda_0, G > G_0 \quad (2-69)$$

And an absolute minimum when:

$$\lambda < \lambda_0, G < G_0 \quad (2-70)$$

For a composite body of M different phases, a reference cube with a unit volume in composite will be considered. The reference cube has to be chosen large enough compared to the size of inhomogeneity and small enough compared to the whole medium size. Therefore the average strain within each cube will be assumed as ε_{ij}^0 .

The elastic strain energy in the media is shown by (Shtrikman, 1962):

$$W = \frac{1}{2} (9K\varepsilon_0^2 + 2Ge_0^2), \quad (2-71)$$

where ε_0 and e_0 are the isotropic and deviatoric parts of the strain matrix ($\varepsilon_{ij}^0 = \varepsilon_0 \delta_{ij} + e_{ij}^0$; and $\varepsilon_0 = \frac{1}{3} \varepsilon_{kk}$) and K and G are the effective bulk and shear modulus.

Applying the variational method and assuming the volume fraction of each phase is v_i , it will be found that the following upper and lower bounds for elastic properties are satisfied:

$$K^*_1 < K < K^*_2, \quad (2-72)$$

where K^*_1 and K^*_2 are the upper and lower bounds on Bulk modulus and are estimated as follows (Hashin and Shtrikman, 1962):

$$\begin{aligned} K^*_1 &= K_1 + \frac{A_1}{1 + \alpha_1 A_1} \\ K^*_2 &= K_2 + \frac{A_n}{1 + \alpha_n A_n} \end{aligned} \quad (2-73)$$

Where:

$$\alpha_1 = -\frac{3}{3K_1 + 4G_1} \quad \text{where} \quad A_1 = \sum_{i=2}^n \frac{v_i}{\frac{1}{K_i - K_1} - \alpha_1} \quad (2-74)$$

$$\alpha_n = -\frac{3}{3K_n + 4G_n} \quad A_n = \sum_{i=1}^{n-1} \frac{v_i}{\frac{1}{K_i - K_n} - \alpha_n}$$

The upper and lower bounds for shear modulus can be calculated as in the following:

$$G^*_{1} < G < G^*_{2} \quad (2-75)$$

Where:

$$G^*_{1} = G_1 + \frac{\beta_1}{1 + \beta_1 B_1}, \quad (2-76)$$

$$G^*_{2} = G_2 + \frac{B_n}{1 + \beta_n B_n}$$

Where:

$$\beta_1 = -\frac{3(K_1 + 2G_1)}{5G_1(3K_1 + 4G_1)} \quad \text{and} \quad B_1 = \sum_{i=2}^n \frac{v_i}{\frac{1}{2(K_i - K_1)} - \beta_1} \quad (2-77)$$

$$\beta_n = -\frac{3(K_n + 2G_n)}{5G_n(3K_n + 4G_n)} \quad B_n = \sum_{i=1}^{n-1} \frac{v_i}{\frac{1}{2(G_i - G_n)} - \beta_n}$$

Note that K_1 , G_1 and K_n , G_n are respectively the smallest and the largest elastic moduli among all the phases.

For a two-phase composite material these formulation will reduce to:

$$K^*_{1} = K_1 + \frac{v_2}{\frac{1}{K_2 - K_1} + \frac{3v_1}{3K_1 + 4G_1}} \quad (2-78)$$

$$K^*_{2} = K_2 + \frac{v_1}{\frac{1}{K_1 - K_2} + \frac{3v_2}{3K_2 + 4G_2}}$$

$$G^*_1 = G_1 + \frac{v_2}{\frac{1}{G_2 - G_1} + \frac{6(K_1 + 2G_1)v_1}{5G_1(3K_1 + 4G_1)}} \quad (2-79)$$

$$G^*_2 = G_2 + \frac{v_1}{\frac{1}{G_1 - G_2} + \frac{6(K_2 + 2G_2)v_2}{5G_2(3K_2 + 4G_2)}}$$

Here $K_2 > K_1$ and $G_2 > G_1$. This variational method has been extended to anisotropic and non-homogenous forms (Hashin and Shtrikman, 1962), which are not discussed here.

2.4 Approximation Methods

As it was mentioned before, an exact solution for effective properties of materials might not be attainable. In the last section it was mentioned how rigorous bounds can provide a rigorous statement for elastic properties of composites. (This can be applied for polycrystalline materials as well). On the other hand, assuming some microstructural information, the effective elastic properties can be approximated. These methods are applicable when some simple microstructural information such as volume fractions and properties of each of the phases are known. Volume fractions here are assumed as one-point probabilities. Having more information about the microstructures and using higher order probabilities are the solutions to get a closer approximation to the real values of elastic properties. This will be discussed in later chapters. In this section, it will be shown that in many case, the calculation of the effective properties of heterogeneous materials, requires the solution to a boundary value problem for a single inclusion. As a result some form of averaging method has to be applied to homogenize the properties of a heterogeneous medium.

2.4.1 Maxwell approximation method

Here the Maxwell approximation method to calculate the effective properties (elastic) will be reviewed in detail (Maxwell, 1873). This approximation relies on the knowledge of the value of the effective elastic properties of single inclusion under a strain field ϵ_{APP} at infinity (Torquato, 2001).

Therefore here, a problem of single inclusion with radius R and Lamé constants λ_2 , and G_2 which is embedded in an infinite matrix with Lamé constants λ_1 , and G_1 is considered.

The Navier's equation has to be solved for a single inclusion: (Torquato, 2001)

$$\begin{aligned} (\lambda_1 + G_1)\nabla \cdot (\nabla u) + G_1 \Delta u &= 0, & r \geq R \\ (\lambda_2 + G_2)\nabla \cdot (\nabla u) + G_2 \Delta u &= 0, & r \leq R \end{aligned} \quad (2-80)$$

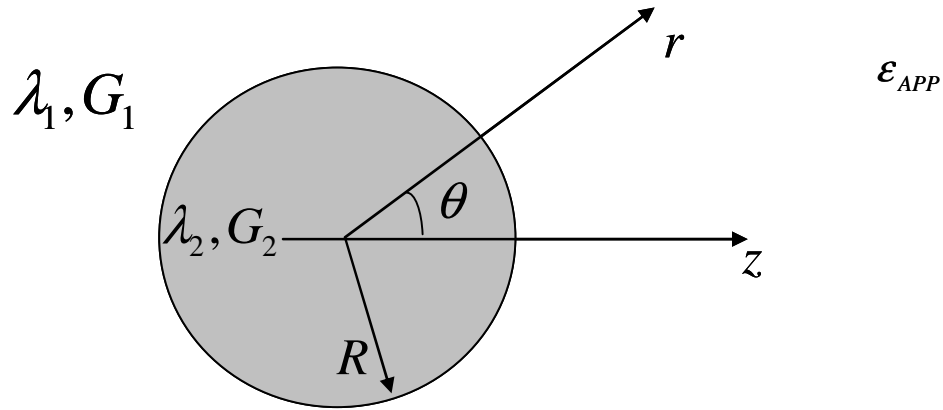


Figure 2.3 A Schematic diagram to show the single spherical inclusion in an infinite matrix

and the following boundary conditions has to be satisfied, (because of the continuity of the fields) :

$$\begin{aligned}
u_+ &= u_-, & r &= R \\
n.\tau_+ &= n.\tau_-, & r &= R \\
u &= \mathcal{E}_{APP}.r, & r &\rightarrow \infty
\end{aligned} \tag{2-81}$$

To solve the above equations, first a hydrostatic field has been applied:

$$\mathcal{E}_{APP} = \frac{\mathcal{E}_{app}}{3} I \tag{2-82}$$

where I is the second order identity tensor ($I_{ijkl} = \frac{1}{2}(\delta_{ik}\delta_{jl} + \delta_{il}\delta_{jk})$) and \mathcal{E}_{app} is the applied scalar field.

Applying the boundary condition, eq. (2-80) can be solved for displacement u and then strain field can be obtained as follows (for details refer to Torquato, 2001)

$$\mathcal{E} = \begin{cases} \mathcal{E}_{APP} + \kappa_{21}R^3t(r).\mathcal{E}_{APP}, & r \geq R \\ \mathcal{E}_{APP} - \kappa_{21}\mathcal{E}_{APP}, & r \leq R \end{cases} \tag{2-83}$$

where $t(r)$ is the dipole tensor and is defined by:

$$t(r) = \nabla\nabla\left(\frac{1}{R}\right) = \frac{3nn - I}{r^3} \tag{2-84}$$

and κ_{21} is the bulk modulus polarizability:

$$\kappa_{21} = \frac{K_2 - K_1}{K_2 + \frac{4}{3}G_1} \tag{2-85}$$

Furthermore, the displacement field inside and outside the inclusion can be calculated as follows when the deviatoric strain has been applied at infinity ($tr(\mathcal{E}_{APP})=0$):

(Torquato, 2001)

$$\begin{aligned}
u &= \mathcal{E}_{APP}.r + B \mathcal{E}_{APP}.r & r &\leq R \\
u_i &= \left(1 - \frac{A}{r^3} + \frac{6B}{r^5} - \frac{2C}{r^3}\right)(\mathcal{E}_{APP})_{ij}r_j + 3\left(C - \frac{5B}{r^2}\right)\frac{r_i r_j r_k}{r^5}(\mathcal{E}_{APP})_{jk} & r &\geq R
\end{aligned} , \tag{2-86}$$

where A, B, and C can be estimated by applying the boundary conditions. Knowing the displacement field, the strain can be calculated in the inclusion; however the derivation is beyond the discussion here. (for more details refer to Torquato, 2001)

Combining the hydrostatic and deviatoric strain field, strain inside the inclusion will be calculated by:

$$\boldsymbol{\varepsilon} = T\boldsymbol{\varepsilon}_{APP} \quad r < R, \quad (2-87)$$

where, T is the fourth rank tensor:

$$T = \frac{1}{d} \delta_{ij} \delta_{kl} (1 - \kappa_{21}) + \left[(\delta_{ik} \delta_{jl} + \delta_{il} \delta_{jk}) - \frac{1}{d} \delta_{ij} \delta_{kl} \right] (1 - \mu_{21}), \quad (2-88)$$

where κ_{21} has been defined in eq. (2-85) and μ_{21} is the shear modulus polarizability and is defined by:

$$\mu_{21} = \frac{G_2 - G_1}{G_2 + H_1} \quad (2-89)$$

where:

$$H_1 = \frac{G_1 [3K_1/2 + 4G_1/3]}{K_1 + 2G_1}$$

Now that the strain field for each inclusion has been calculated, the approximated elastic properties can be calculated as follows:

Consider a large sphere of radius R_0 containing M smaller spheres with radius R and Lamé's constants λ_2 , and G_2 in a matrix with Lamé's constants λ_1 , and G_1 .

The volume fraction of each sphere is:

$$v_2 = M(R/R_0)^3 \quad (2-90)$$

It should be noted that the interactions between the spheres can be neglected since the volume fraction of the spheres is assumed to be very small.

Now suppose that the strain hydrostatic field ϵ_{APP} has been applied at infinity. The strain field at distance r can be evaluated by superposition of the fields of each small sphere:

$$\epsilon(r) = \epsilon_{APP} + \frac{v_2 R_0^3 \kappa_{21}}{r^3} [3nn - I] \epsilon_{APP} \quad (2-91)$$

where κ_{21} has been defined by equation(2-84)

On the other hand the large sphere which includes small spheres can be considered as a homogeneous sphere which has the effective bulk modulus as: K . Therefore the strain field that has been induced at distance r which is large compared to R_0 : (Torquato, 2001)

$$\epsilon(r) = \epsilon_{APP} + \frac{R_0^3 \kappa_{e1}}{r^3} [3nn - I] \epsilon_{APP}, \quad (2-92)$$

where polarizability is defined by:

$$\kappa_{e1} = \frac{K - K_1}{K + \frac{4}{3}G_1}, \quad (2-93)$$

Making eq. (2-91) and eq. (2-92) identical results in:

$$\kappa_{e1} = v_2 \kappa_{21}, \quad (2-94)$$

where this equation can be rewritten as:

$$\frac{K - K_1}{K + \frac{4}{3}G_1} = v_2 \frac{K_2 - K_1}{K_2 + \frac{4}{3}G_1} \quad (2-95)$$

Therefore knowing the bulk modulus of two phases and their volume fractions, the effective bulk modulus of the composite can be averaged.

The same procedure can be done for the shear modulus of the composite, whereas the applied field at infinity will be a uniform shear strain. The following equations are obtained for effective shear modulus (G) (Torquato, 2001):

$$\frac{G - G_1}{G + H_1} = v_2 \left[\frac{G_2 - G_1}{G_2 + H_1} \right] \quad (2-96)$$

where:

$$H_i \equiv \frac{G_i \left[\frac{3}{2} K_i + \frac{4}{3} G_i \right]}{K_i + 2G_i}$$

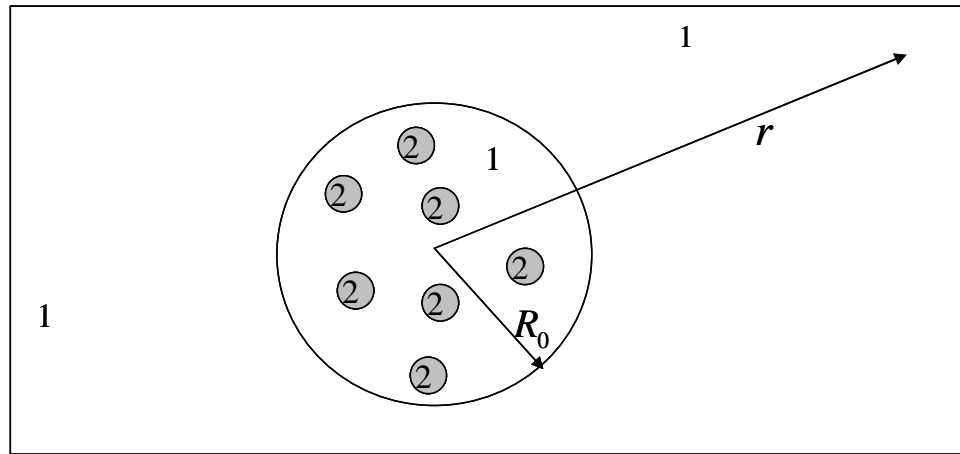


Figure 2.4 Effective properties of a composite with spherical inclusion - Maxwell approximation

Now assume there are M-1 different types of spheres (M>2) with volume fractions v_2, v_3, \dots, v_M and the properties of $K_2, G_2, K_3, G_3, \dots, K_M, G_M$, then the Maxwell's formula can be applied as (Maxwell, 1873):

$$\frac{K - K_1}{K + \frac{4}{3} G_1} = \sum_{j=1}^M v_j \left[\frac{K_j - K_1}{K_j + \frac{4}{3} G_1} \right], \quad (2-97)$$

$$\frac{K - G_1}{K + H_1} = \sum_{j=1}^M v_j \left[\frac{G_j - G_1}{G_j + H_1} \right]$$

When all the inclusions are stiffer than the matrix phase, this approximation is equal to Hashin-Shtrikman lower bound. The Maxwell approximation results in a good approximation when the spheres are separated from each other and they are non-dilute (Torquato, 2000)

2.4.2 Self-Consistent approximation method

This method is based on the solution to an auxiliary inclusion problem where a single ellipsoidal /spherical inclusion is embedded in an infinite medium which has the unknown effective elasticity and compliance tensor (Hill, 1965). The bond between inclusion and the infinite medium is assumed to be perfect, resulting in displacement and traction continuity across the interface between phases. In this method, uniform stresses or strains are applied at infinity with the objective of determining the stresses and strains in the inclusion. Eshelby (1975) has shown that in these types of problems, the stress and strain fields in the inclusion are uniform. The self-consistent method can be used to estimate the effective properties when the particles distribution is assumed random and the effect of interaction is considered.

2.4.2.1 Random distribution of spherical micro-inclusion

In this model all the microinclusions have been considered as spherical inclusions. Both the matrix and inclusions are elastic and isotropic with different elastic properties. Assume a macroscopically isotropic composite which includes M different types of spheres with volume fractions v_1, v_M , and bulk and shear moduli K_1, G_1, K_M, G_M . The effect of all the inclusions outside the inclusion j is to produce a homogenous medium with effective bulk modulus K where the value of this effective modulus has to be

calculated. For this purpose, first a dilute distribution of the inclusion is considered and an effective elasticity and compliance tensor of the RVE is calculated. Then, by applying self-consistent method the interaction of the inclusion will be considered in the calculation of the overall elasticity tensors. Assuming plane stress, the two independent elastic constant for the isotropic composite can be calculated by the following equation: (for further explanation refer to (Nemaat Naser, 1999))

$$\frac{K}{K_1} = 1 - v_2 \frac{K(K_1 - K_2)}{K_1(K - K_2)} \left(\frac{K}{K - K_2} - \bar{s}_1 \right)^{-1}$$

$$\frac{G}{G_1} = 1 - v_2 \frac{G(G_1 - G_2)}{G_1(G - G_2)} \left(\frac{G}{G - G_2} - \bar{s}_2 \right)^{-1}$$
(2-98)

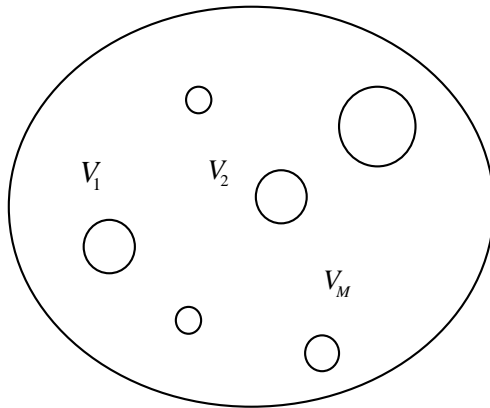


Figure 2.5 A portion of an RVE containing spherical micro-inclusion, Self-Consistent approximation

Where \bar{s}_1 and \bar{s}_2 are Eshelby tensors and are calculated in this case as follows:

$$\begin{aligned}\bar{s}_1 &= \frac{1 + \bar{\xi}}{3(1 - \bar{\xi})}; \\ \bar{s}_2 &= \frac{2(4 - 5\bar{\xi})}{15(1 - \bar{\xi})}\end{aligned}\tag{2-99}$$

Note that:

$$\bar{\xi} = \frac{(3K - 2G)}{2(3K + G)}\tag{2-100}$$

Therefore the equations for effective bulk modulus and shear modulus (K and G) are coupled and they can be solved by iteration method.

2.4.2.2 Effective moduli of an elastic plate containing aligned reinforcing fibers

In this section the composite has been assumed to have linearly elastic matrix and elastic aligned reinforcing fibers. The fibers can be assumed as long cylinders. Therefore the composite is considered transversely isotropic. Engineering elastic constants can be calculated by Nemaat Naser (1999):

$$\begin{aligned}\frac{K}{K_1} &= 1 - \nu_2 \frac{K(K_1 - K_2)}{K_1(K - K_2)} \left(\frac{K}{K - K_2} - \bar{s}_1 \right)^{-1} \\ \frac{G}{G_1} &= 1 - \nu_2 \frac{G(G_1 - G_2)}{G_1(G - G_2)} \left(\frac{G}{G - G_2} - \bar{s}_2 \right)^{-1}\end{aligned}\tag{2-101}$$

Where:

$$\begin{aligned}\bar{s}_1 &= \frac{2}{1 + \bar{\kappa}} \\ \bar{s}_2 &= \frac{\bar{\kappa}}{1 + \bar{\kappa}}\end{aligned}\tag{2-102}$$

and

$$\bar{k} = 3 - 8G \left(\frac{\nu}{E} + \frac{\nu^2}{E_3} \right) \quad (2-103)$$

CHAPTER 3

STATISTICAL MECHANICS MODELING

In the last chapter, several micromechanics models to estimate the elastic properties of multi-phase heterogeneous materials were studied. As it was shown all of those models were based on volume fractions which are one-point probability functions and involve some assumptions on the shape of the inclusions. It is clear that such a construction that uses volume fraction of the second phase can only present a limited description of the microstructure (composite/polycrystalline). Therefore in this research, two-point correlation functions are used as additional parameters for the description of a composite. They can incorporate not only the distribution and interaction of the two phases but also information on the shape and morphology of each individual phase.

As it was mentioned in the introduction, two-point statistics provide information about near neighbor and far neighbor at each point in the microstructure, and statistical information enables us to incorporate the spatial arrangement in the microstructure in addition to phase's properties.

In this section, first an overview on statistical representation of the microstructure and the measurement of one-point and two-point statistics will be shown. Then statistical continuum mechanics theory which correlates the microstructure and properties and the related assumptions will be studied and the homogenization formulation for materials based on two-point statistics will be established. Then in later

chapters the homogenization relations will be extended to anisotropic distribution and the effect of one-point and two-point statistics will be studied in details.

3.1 Statistical Continuum Mechanics Theory

Statistical continuum mechanics is used to solve problems in continuum mechanics based on statistical information. This theory can be used to predict the properties of materials when some structural information is known and has applications in polycrystalline aggregates, layered structures, multiphase mixtures, composites etc. Here are some statistical definitions which are used in this theory (Kroner 1972):

3.1.1 Distribution functions and density functions

a) Probability distribution functions

Assume u is an arbitrary outcome of an experiment and is a real number between $-\infty$ and $+\infty$. The probability of the outcome of the experiment that lies between $-\infty$ and u is shown by $F_1(u)$ and is called probability distribution function. It is obvious that (Kroner, 1972):

$$\lim_{u \rightarrow -\infty} F_1(u) = 0, \lim_{u \rightarrow +\infty} F_1(u) = 1 \quad (3-1)$$

and the probability that u lies between a and b is

$$P_1(a \leq u \leq b) = F_1(b) - F_1(a) \quad (3-2)$$

b) Probability density functions

When the difference between two points becomes infinitesimal, the probability density is defined by (Kroner, 1972):

$$P(a \leq u \leq a + da)_1 = F_1(a + da) - F_1(a) = dF_1(a)/da \quad (3-3)$$

Therefore the probability density for variable u can be evaluated by the following equation:

$$P_1(u) = dF_1(u)/du \quad (3-4)$$

This is the probability of an outcome in the range of $\langle u \dots u + du \rangle$, where:

$$\int_{-\infty}^{\infty} p_1(u) du = 1 \quad (3-5)$$

Higher dimensional probabilities are correspondingly defined as:

$$p_n(u_1, u_2, \dots, u_n) = \partial^n F_n(u_1, u_2, \dots, u_n) / \partial u_1 \partial u_2 \dots \partial u_n \quad (3-6)$$

3.1.2 Important average quantities

a) Expectations

The expectation of a random variable u is defined as the weighted mean of u:

$$E(u) \equiv \bar{u} \equiv \int_{-\infty}^{+\infty} u P_1(u) du \quad (3-7)$$

If u is a discrete variable then the integral can be replaced by a sum. Furthermore, the expectation for a function f(u) is defined by (Kroner, 1972):

$$E(f(u)) \equiv \overline{f(u)} \equiv \int_{-\infty}^{+\infty} f(u) P_1(u) du \quad (3-8)$$

b) Moments of the form $\overline{u^n}$

The moments of a density function $P_1(u)$ are defined by (Kroner, 1972):

$$\overline{u^n} = E(u^n) = \int_{-\infty}^{+\infty} u^n P_1(u) du \quad (3-9)$$

where \bar{u} is the mean value of u and $\overline{u^2}$ is the moment.

c) Correlation functions

One-dimensional moment has been defined in section (b). Here the moment for a two-dimensional function is defined (Kroner, 1972):

$$\overline{u_1^j u_2^k} = E(u_1^j u_2^k) = \int_{-\infty}^{\infty} \int_{-\infty}^{\infty} u_1^j u_2^k p_2(u_1, u_2) du_1 du_2 \quad (3-10)$$

A moment of this kind is called two-point correlation function.

3.2 Statistical Descriptions of Microstructure

The statistical details of a microstructure can be represented by an n -point probability distribution function. The volume fractions, v_1 and v_2 define the one-point probability distribution function that can be used to give an estimate of the effective properties.

The details of the shape and morphology of the microstructure including the interaction of the second phase in composite and orientation distribution of crystallographic grains (texture) can only be realized by using higher order distribution functions (Torquato, 1982; Corson, 1976; Adams, 1999).

The generalized distribution of the microstructure can be defined by $M(x, c, \phi, g, \dots)$, where the variables x , c , and ϕ indicates composition, phase and lattice orientation respectively. One and two-point statistics can be measured for local states including x , c , or ϕ .



Figure 3.1 OIM representation of the microstructure

3.2.1 One-point probability functions

To measure a one-point probability function, a random number of points (N) have to be inserted in the microstructure. The number of points located in one phase with respect to the total number of points (N) indicates a one-point probability:

$$\begin{aligned} P(\phi_1) &= P_1 = \frac{n_1}{N} = v_1 \\ P(\phi_2) &= P_2 = \frac{n_2}{N} = v_2 \end{aligned} \quad (3-11)$$

where phase one and phase two have been considered as matrix and particles respectively, and the following normalization relationship is always satisfied:

$$P(\phi_1) + P(\phi_2) = 1 \quad (3-12)$$

3.2.2 Two-point probability functions

A two-point probability function can be defined as a conditional probability function when the statistics of a three-dimensional vector “ \mathbf{r} ” is investigated once attached to each set of the random points in a particular microstructure. A two-point statistics can

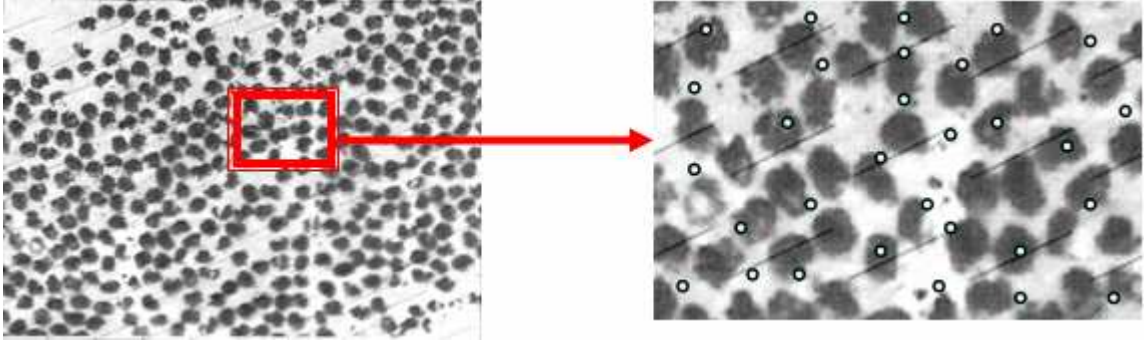


Figure 3.2 Schematic representations of one-point statistics measurement in a two-phase composite microstructure

be calculated by the probability of a specific phase at the head of the vector given the phase at the tail of the vector and can be shown by $P(r | \{1,2\}, \{1,2\})$. The following normalization relationship is valid for all the functions:

$$\begin{aligned}
 P_{11} + P_{12} &= v_1 \\
 P_{22} + P_{21} &= v_2 \\
 P_{11} + P_{12} + P_{21} + P_{22} &= 1
 \end{aligned}
 \tag{3-13}$$

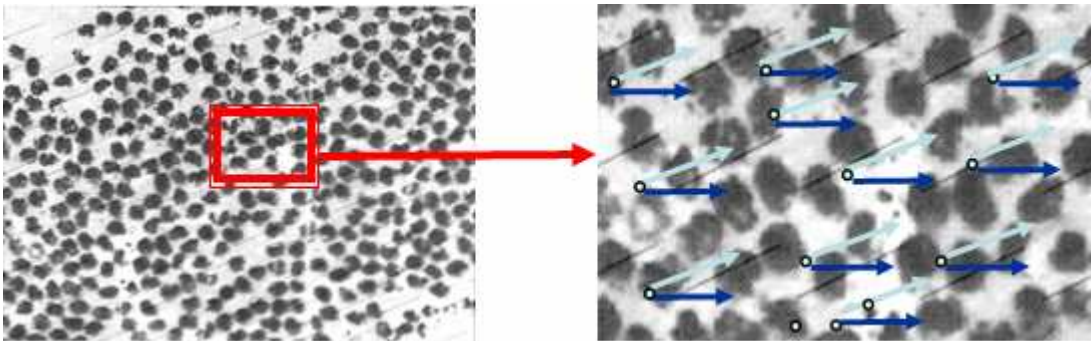


Figure 3.3 Schematic representations of two-point statistics measurement in a two-phase composite microstructure

As it is observed from the above normalization relationship, P_{11} is the only independent variable.

3.2.3 Mathematical configuration of two-point statistical functions

The exponential form of the distribution function as proposed by Corson (1976) has been shown to be appropriate for random microstructures. It is represented as,

$$P_{ij}(r) = A_{ij} + B_{ij} \exp(-c_{ij} r^{n_{ij}}), \quad (3-14)$$

where A_{ij} and B_{ij} are functions of v_i and v_j (volume fractions of phase i and j). For a two-phase composite, i and j correspond to phases 1 and 2, and for a polycrystalline material i and j can get values from 1 to M which is the total number of grains. For a two-phase composite, the components of A and B are shown in Table 3.1:

Table 3.1 Empirical coefficients in Corson's equation for a two-phase composite

	$i = 1; j = 1$	$i = 1; j = 2$	$i = 2; j = 1$	$i = 2; j = 2$
A_{ij}	$v_1 v_1$	$v_1 v_2$	$v_2 v_1$	$v_2 v_2$
B_{ij}	$v_1 v_2$	$-v_1 v_2$	$-v_2 v_1$	$v_1 v_2$

As it was shown before, the microstructure can be represented by $M(x, c, \phi, g, \dots)$, where phase (ϕ), and orientations (g) can be considered as state variables in composite and polycrystalline materials respectively.

The present form of eq. (3-14) is sufficient when the statistical information is uniform in one dimension for the composite. A three-dimensional form of the distribution can also be introduced. The three-dimensional form requires data from a

variety of sections through the sample. For composites, normality relations were defined by (3-13).

Since $P_{12} = P_{21}$ for a homogenous two-phase composite, it is observed that only P_{11} can be treated as an independent variable.

In addition, a closed form of probabilities is suggested by Torquato (1985) for random and homogenous system of impenetrable spheres

$$\begin{aligned} P_{11} &= 1 - \rho V(r) + \rho^2 M(r) \\ P_{12} &= P_{21} = v_1 - P_{11} \\ P_{22} &= v_2 - v_1 + P_{11} \end{aligned} \quad (3-15)$$

where ρ is the number density of spheres, v_1 and v_2 are the volume fractions, r is the distance between two points, and $V(r)$ and $M(r)$ are defined by :

$$\begin{aligned} V(r) &= \frac{4\pi}{3} \left[1 + \frac{3r}{4} - \frac{r^3}{16} \right] & r < 2 \\ V(r) &= \frac{8\pi}{3} & r > 2 \end{aligned} \quad (3-16)$$

$$\begin{aligned} M(r) &= \left[-\frac{16}{9} + \frac{r^3}{3} - \frac{r^4}{10} + \frac{r^6}{1260} \right] \pi^2 + \frac{16\pi^2}{9} & 0 \leq r < 2 \\ M(r) &= \left[\frac{256}{35r} - \frac{128}{9} + \frac{32r}{5} - \frac{5r^3}{9} + \frac{r^4}{10} - \frac{r^6}{1260} \right] \pi^2 + \frac{16\pi^2}{9} & 2 \leq r < 4 \\ M(r) &= \frac{16\pi^2}{9} & r \geq 4 \end{aligned} \quad (3-17)$$

In Figure 3.4 Corson's equation, Torquato equation, and real data of two-point statistics are shown. Corson's equation is a good approximation for real data.

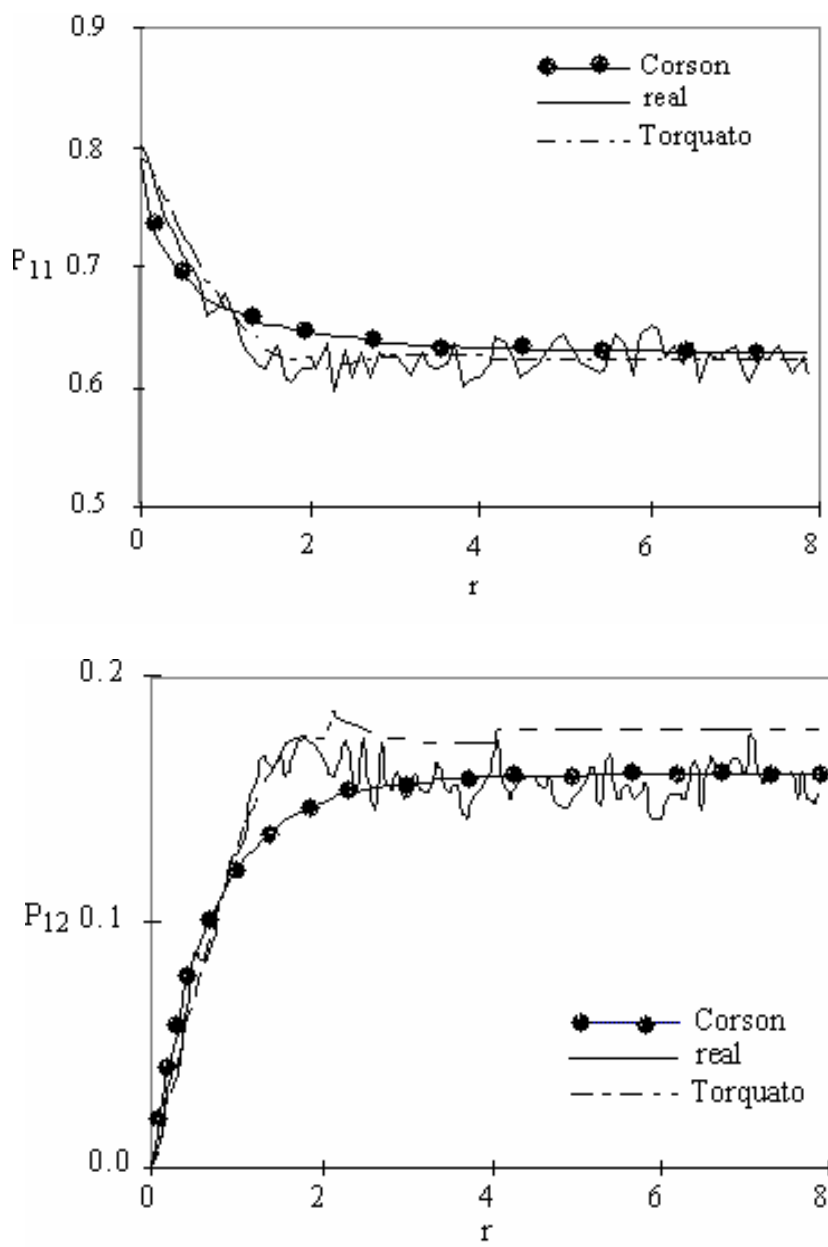


Figure 3.4 Comparison of different proposed formulas for probability functions (Corson and Torquato equation)

3.3 The Basic Assumptions of Statistical Continuum Mechanics

As it was mentioned before Statistical information of the microstructure can be used to predict the elastic properties. In this theory there are some assumption for the samples and the domains as follows:

- A. All the random variables of the media such as stress, strain, moduli and compliance have to obey the ergodic hypothesis. Therefore the ensemble average of each variable can be defined as (Kroner, 1972):

$$\langle c_{ijkl} \rangle = \langle c_{ijkl}(x) \rangle = \frac{1}{V} \int_V c_{ijkl}(x) dV = \sum c_{ijkl}(x) \quad (3-18)$$

- B. Distribution of the elastic and plastic moduli over the particles of the media is assumed statistically homogenous. This assumption doesn't prevent using the heterogeneous microstructures. Since the microstructure can be heterogeneous in each section however to calculate the overall elastic properties the microstructure is assumed to be statistically homogenous (Kroner, 1972).
- C. The linear elastic bodies which are infinite in extent are assumed to be in equilibrium condition at each point.
- D. Distribution of the elastic and plastic moduli over the particles of the media is assumed statistically homogenous. This assumption doesn't prevent using the heterogeneous microstructures. Since the microstructure can be heterogeneous in each section however to calculate the overall elastic properties the microstructure is assumed to be statistically homogenous.

E. The linear elastic bodies which are infinite in extent are assumed to be in equilibrium condition at each point.

3.4 Homogenization Relations for Elastic Properties

In the following section, the full homogenization relations for an elastic medium are derived for a representative volume element. The equilibrium equation is defined by:

$$\sigma_{ij,j} = 0, \quad (3-19)$$

where $\sigma_{ij}(x)$ is the local stress. The elastic constitutive relations are satisfied locally throughout the heterogeneous medium:

$$\sigma_{ij}(x) = c_{ijkl}(x)\varepsilon_{kl}(x) \quad (3-20)$$

$c_{ijkl}(x)$, $\sigma_{ij}(x)$, and $\varepsilon_{ij}(x)$ are local fields of stiffness, stress and strain respectively.

The strains are related to the displacement vectors u_i through:

$$\varepsilon_{ij} = (1/2)(\partial u_i / \partial x_j + \partial u_j / \partial x_i) \quad (3-21)$$

Let's define an effective elastic modulus C_{ijkl} such that

$$\langle \sigma_{ij} \rangle = C_{ijkl} \langle \varepsilon_{kl} \rangle, \quad (3-22)$$

where symbol $\langle h \rangle$ denotes the ensemble average over grains (phases. components...)

at state h. So $\langle c_{ijkl} \rangle$ is the average of the local stiffness defined as follows:

$$\langle c_{ijkl} \rangle = \langle c_{ijkl}(x) \rangle = \frac{1}{V} \int_V c_{ijkl}(x) dV \quad (3-23)$$

The same definition is applicable for stress, strain and compliance. The local moduli and compliance as well as the local stress and strain can be defined as a perturbation

from the average (mean) values $\langle \dots \rangle$ by defining a new parameter $\left(\tilde{\dots} \right)$ as in the

following equations(Adams 1995, Garmestani 2000):

$$\begin{aligned}
 c_{ijkl}(x) &= \langle c_{ijkl} \rangle + \tilde{c}_{ijkl}(x) \\
 s_{ijkl}(x) &= \langle s_{ijkl} \rangle + \tilde{s}_{ijkl}(x) \\
 \sigma_{ij}(x) &= \langle \sigma_{ij} \rangle + \tilde{\sigma}_{ij}(x) \\
 \varepsilon_{ij}(x) &= \langle \varepsilon_{ij} \rangle + \tilde{\varepsilon}_{ij}(x)
 \end{aligned} \tag{3-24}$$

where $\tilde{c}_{ijkl}(x)$, $\tilde{s}_{ijkl}(x)$, $\tilde{\sigma}_{ij}(x)$, and $\tilde{\varepsilon}_{ij}(x)$ are, respectively, the deviation field of stiffness, compliance, stress and strain at each point from the mean value. The following equations should always be satisfied for a statistically homogenous media:

$$\begin{aligned}
 \langle \tilde{c}_{ijkl}(x) \rangle &= 0, \langle \tilde{s}_{ijkl}(x) \rangle = 0 \\
 \langle \tilde{\sigma}_{ij}(x) \rangle &= 0, \langle \tilde{\varepsilon}_{ij}(x) \rangle = 0
 \end{aligned} \tag{3-25}$$

In the following, statistical continuum mechanics analysis is applied to a two-phase composite for the prediction of elastic properties. A theoretical framework has already been developed for isotropic distributions in composites by Garmestani, et. al. (1999, 2000) and for a textured polycrystalline material by Adams, et.al. (1995). Here, a detailed discussion is provided for the calculation of the effective elastic constants for isotropic distribution and will be extended in next chapter to anisotropic distributions.

Taking ensemble (average) from eq. (3-20):

$$\langle \sigma_{ij}(x) \rangle = \langle c_{ijkl}(x) \varepsilon_{kl}(x) \rangle \tag{3-26}$$

Substituting the local strain and stiffness from eqs. (3-24) into eq. (3-26):

$$\begin{aligned}
 \langle \sigma_{ij}(x) \rangle &= \left\langle \left(\langle c_{ijkl} \rangle + \tilde{c}_{ijkl}(x) \right) \left(\langle \varepsilon_{kl} \rangle + \tilde{\varepsilon}_{kl}(x) \right) \right\rangle \Rightarrow \\
 \langle \sigma_{ij}(x) \rangle &= \left\langle \left\langle c_{ijkl}(x) \right\rangle \langle \varepsilon_{kl}(x) \rangle + \langle c_{ijkl}(x) \rangle \tilde{\varepsilon}_{kl}(x) + \tilde{c}_{ijk} \langle \varepsilon_{kl}(x) \rangle + \tilde{c}_{ijkl}(x) \tilde{\varepsilon}_{kl}(x) \right\rangle
 \end{aligned} \tag{3-27}$$

The ensemble value of $\langle c_{ijkl}(x) \rangle$ and $\langle \varepsilon_{kl}(x) \rangle$ are independent of x , so that they can be taken out of the ensemble:

$$\langle \sigma_{ij}(x) \rangle = \langle c_{ijkl}(x) \rangle \langle \varepsilon_{kl}(x) \rangle + \langle c_{ijkl}(x) \rangle \overbrace{\langle \tilde{\varepsilon}_{kl}(x) \rangle}^0 + \overbrace{\langle \tilde{c}_{ijkl}(x) \rangle}^0 \langle \varepsilon_{kl}(x) \rangle + \langle \tilde{c}_{ijkl}(x) \tilde{\varepsilon}_{kl}(x) \rangle \quad (3-28)$$

Applying eq. (3-25) into eq. (3-28), the average stress is calculated by:

$$\langle \sigma_{ij}(x) \rangle = \langle c_{ijkl} \rangle \langle \varepsilon_{kl} \rangle + \langle \tilde{c}_{ijkl}(x) \tilde{\varepsilon}_{kl}(x) \rangle \quad (3-29)$$

A fourth rank tensor a_{mnkl} defined here in such a way to show the heterogeneity in strain field by the following relationship (Garmestani, 2000):

$$\tilde{\varepsilon}_{kl} = a_{mnkl} \langle \varepsilon_{kl} \rangle \quad (3-30)$$

Substituting the definition of effective elastic constant from eq. (3-22) into eq. (3-29) and using eq. (3-30), the effective elastic constants can be derived as:

$$C_{ijkl} = \langle c_{ijkl} \rangle + \langle \tilde{c}_{ijmn}(x) a_{mnkl}(x) \rangle \quad (3-31)$$

Therefore, in order to calculate effective elastic constants, the second term in eq. (3-31) needs to be calculated since the first term can be calculated easily by assuming an average value for elastic stiffness. For this purpose the equilibrium equation (eq. (3-19)) has to be solved in order to estimate a_{mnkl} . By substituting local stress and strain from eq. (3-20), into the equilibrium equations in eq. (3-19), an equation for displacement is obtained. Differentiating this equation and multiplying the result by c_{ijkl} , the second term in eq. (3-31) can be derived. The following is the details of the derivations:

Substituting the local moduli in the equilibrium equation,

$$\begin{aligned}
& \left(\langle c_{ijkl} \rangle + \tilde{c}_{ijkl}(x) \right) \mathcal{E}_{kl,j} = 0 \\
& \left(\langle c_{ijkl} \rangle + \tilde{c}_{ijkl}(x) \right)_{,j} \mathcal{E}_{kl}(x) + \left(\langle c_{ijkl} \rangle + \tilde{c}_{ijkl}(x) \right) \mathcal{E}_{kl,j}(x) = 0 \Rightarrow \\
& \tilde{c}_{ijkl,j}(x) \mathcal{E}_{kl}(x) + \langle c_{ijkl} \rangle \mathcal{E}_{kl,j}(x) + \tilde{c}_{ijkl}(x) \mathcal{E}_{kl,j}(x) = 0 \Rightarrow \\
& \left(\tilde{c}_{ijkl}(x) \mathcal{E}_{kl}(x) \right)_{,j} + \langle c_{ijkl} \rangle \mathcal{E}_{kl,j}(x) = 0 \tag{3-32}
\end{aligned}$$

Now, substituting local strain in eq. (3-32):

$$\left(\tilde{c}_{ijkl}(x) \mathcal{E}_{kl}(x) \right)_{,j} + \langle c_{ijkl} \rangle \left(\langle \mathcal{E}_{kl,j} \rangle + \tilde{\mathcal{E}}_{kl,j}(x) \right)_{,j} = 0 \Rightarrow \left(\tilde{c}_{ijkl}(x) \mathcal{E}_{kl}(x) \right)_{,j} + \langle c_{ijkl} \rangle \tilde{\mathcal{E}}_{kl,j}(x) = 0 \tag{3-33}$$

Substituting strain in terms of displacement from eq. (3-21) into eq. (3-33):

$$\left(\tilde{c}_{ijkl}(x) \mathcal{E}_{kl}(x) \right)_{,j} + \langle c_{ijkl}(x) \rangle \frac{\tilde{u}_{kl,j}}{2} + \langle c_{ijkl}(x) \rangle \frac{\tilde{u}_{lk,j}}{2} = 0 \tag{3-34}$$

The repeated indices (lk) in the last term in eq. (3-34) can be reversed, therefore:

$$\left(\tilde{c}_{ijkl}(x) \mathcal{E}_{kl}(x) \right)_{,j} + \langle c_{ijkl}(x) \rangle \frac{\tilde{u}_{kl,j}}{2} + \langle c_{ijlk}(x) \rangle \frac{\tilde{u}_{kl,j}}{2} = 0, \tag{3-35}$$

since $\langle c_{ijkl} \rangle = \langle c_{ijlk} \rangle$, eq. (3-35) can be rewritten as::

$$\begin{aligned}
& \left(\tilde{c}_{ijkl}(x) \mathcal{E}_{kl}(x) \right)_{,j} + \langle c_{ijkl}(x) \rangle \tilde{u}_{k,lj}(x) = 0 \Rightarrow \\
& \langle c_{ijkl} \rangle \partial^2 \tilde{u}_k / \partial x_j \partial x_l + \partial / \partial x_j \left[\tilde{c}_{ijkl}(x) \mathcal{E}_{kl}(x) \right] = 0 \tag{3-36}
\end{aligned}$$

The solution for this PDE can be written as an integral equation using the Green's function defined by the following PDE (Kroner, 1972):

$$\langle c_{ijkl} \rangle \partial^2 G_{kp}(x, x') / \partial x_j \partial x_l + \delta_{ip} \delta(x - x') = 0, \tag{3-37}$$

where x and x' are two different positions in the media, and $\delta(x - x')$ is the Dirac's delta function for the vector relating any two points in the microstructure, and the term

$\delta_{ip} \delta(x - x')$ represents the i th component of a unit force acting at and being parallel to the direction p for a fixed point, p (Zarka,1987).

Green's function in the case of isotropy can be defined by a closed form and for the case of anisotropy has to be calculated numerically. The details of the calculations of Green's functions for both cases are presented in Appendix A1 and A2 . (Bacon (1978), Adams et. Al. (1998), and Garmestani (2000)).

Therefore, the displacement from the above PDE can be solved by:

$$\tilde{u}_k(x) = \int_V G_{kp}(x, x') \partial [\tilde{c}_{plrs}(x') \epsilon_{rs}(x')] / \partial x'_l dX', \quad (3-38)$$

where dX' is the volume integral on the volume element around position x' ,

By differentiating the above equation $\tilde{\epsilon}_{ku}(x)$ is calculated:

$$\tilde{u}_{k,u}(x) = \int_V G_{kp,u}(x, x') \partial [\tilde{c}_{plrs}(x') \epsilon_{rs}(x')] / \partial x'_l dX' + \overbrace{\int_V G_{kp}(x, x') \partial [\tilde{c}_{plrs}(x') \epsilon_{rs}(x')] / \partial x'_l \partial x'_u dX'}^0 \quad (3-39)$$

It is observed that the second term is zero, since the term $[\tilde{c}_{plrs}(x') \epsilon_{rs}(x')]$ is just a function of x' whereas the derivative is with respect to x . Therefore, the strain can be calculated as:

$$\tilde{\epsilon}_{ku} = \int_V \frac{1}{2} [G_{kp,u}(x, x') + G_{up,k}(x, x')] \partial [\tilde{c}_{plrs}(x') \epsilon_{rs}(x')] / \partial x'_l dX' \quad (3-40)$$

Defining the first derivative of the Green's function as follow:

$$K_{kpu} = (G_{kp,u} + G_{up,k}) / 2 \quad (3-41)$$

and multiplying the strain in eq. (3-40) by the value of the local moduli $\tilde{c}_{ijk}(x)$ and

averaging with respect to x :

$$\langle \tilde{c}_{ijku}(x) \tilde{\epsilon}_{ku}(x) \rangle = \int_V \int_{V'} K_{kpu} \tilde{c}_{ijku}(x) \partial [\tilde{c}_{plrs}(x') \epsilon_{rs}(x')] / \partial x'_i dX' dX, \quad (3-42)$$

where dX is the volume integral on the volume element around position x . Applying the equation for local strain from eq. (3-24):

$$\begin{aligned} \langle \tilde{c}_{ijku}(x) \tilde{\epsilon}_{ku}(x) \rangle &= \int_V \int_{V'} K_{kpu} \partial [\tilde{c}_{ijku}(x) \tilde{c}_{plrs}(x')] / \partial x'_i dX' dX \langle \epsilon_{rs}(x) \rangle \\ &+ \int_V \int_{V'} K_{kpu} \partial [\tilde{c}_{ijku}(x) \tilde{c}_{plrs}(x') \tilde{\epsilon}_{rs}(x')] / \partial x'_i dX' dX \end{aligned}, \quad (3-43)$$

the integral over the variable x can be shown as the ensemble average:

$$\begin{aligned} \langle \tilde{c}_{ijku}(x) \tilde{\epsilon}_{ku}(x) \rangle &= \int_V K_{kpu} \partial \langle \tilde{c}_{ijku}(x) \tilde{c}_{plrs}(x') \rangle / \partial x'_i \langle \epsilon_{rs} \rangle dX' \\ &+ \int_V K_{kpu} \partial \langle \tilde{c}_{ijku}(x) \tilde{c}_{plrs}(x') \tilde{\epsilon}_{rs}(x') \rangle / \partial x'_i dX' \end{aligned} \quad (3-44)$$

In above equation $\langle \tilde{c}_{ijku}(x) \tilde{c}_{pmrs}(x') \rangle$ is called two-point correlation function and based on the definition of the correlation functions in chapter 3, this function for variables \tilde{c}_{ijku} and \tilde{c}_{pmrs} is defined through the following equation:

$$\langle \tilde{c}_{ijku}(x) \tilde{c}_{pmrs}(x') \rangle = \int \int \tilde{c}_{ijku}(x) \tilde{c}_{pmrs}(x') P_2(x | h, x' | h') dh dh', \quad (3-45)$$

where P_2 is a two-point probability function for two states of h and h' , and this function can be derived for composites by the following relationship:

It is observed that the second term is a three-point correlation function. At this time the calculation is truncated up to a two-point probability function. For this research the second term is neglected. Therefore to get the microstructural information and correlate them to properties, one needs to calculate the first integral in eq. (3-44). This term has been calculated numerically for isotropic composites by Adams and Garmestani in previous works. However, it will be shown analytically in next chapters that since the composite was assumed isotropic, their final results didn't include the morphological

information. It will be proved in next chapters that this term consists of two integrals where one of them is completely dependant on one-point probabilities which shows up in calculations of elastic properties of isotropic composite. Although this term appears in the form of two-point correlation functions in the formulations. In later chapters, analytical and numerical analysis of the results will illustrate that the contribution of two-point statistics is significant for anisotropic composites and therefore the homogenization relations will be extended to anisotropic composite and textured polycrystalline microstructures to observe the two-point statistical information contributions.

PART II:
EXTENSION OF HOMOGENIZATION RELATIONS TO
ANISOTROPIC DISTRIBUTION

CHAPTER 4

ANISOTROPIC HOMOGENIZATION RELATIONS

The effect of anisotropy was not investigated in full in previous works (Adams 1995 and Garmestani 2000) and no other work clearly show whether and how the one-point and two-point statistics contribute in different types of distributions. Therefore it is very important to extend homogenization relations to anisotropic distributions and study the effect of two-point statistics. In this chapter, the correlation function is studied in detail for composites and polycrystalline materials and an analytical form will be derived for its representation.

4.1 Two-Point Probability Functions for Composites

For two-phase composite structures, the application of two-point statistics requires two different sets of probability functions: the first set can be chosen to describe the probability distribution functions for the interaction of the two phases. This reduces the problem to a composite formulation ignoring the crystalline phase for each component. The two phases can then be taken as isotropic (or anisotropic) phases and the effect of textures can be incorporated in the anisotropy parameters in the constitutive relations. The second set can consist of the probability distribution functions for the individual crystalline phases. This means incorporating the effect of orientation for each phase. Based on the arguments presented earlier, the first approach will use the composite formulation and develop the property space for the two-phase structure. Recall eq. (3-

45) the correlation term can be calculated by the following equation when the Lamé's constants are known for the two isotropic phases.

$$\langle \tilde{c}_{ijkl}(x) \tilde{c}_{pmrs}(x') \rangle = \tilde{C}^1_{ijkl} \tilde{C}^1_{pmrs} P_{11} + \tilde{C}^1_{ijkl} \tilde{C}^2_{pmrs} P_{12} + \tilde{C}^2_{ijkl} \tilde{C}^1_{pmrs} P_{21} + \tilde{C}^2_{ijkl} \tilde{C}^2_{pmrs} P_{22} \quad (4-1)$$

where, \tilde{C}^1, \tilde{C}^2 are defined as the difference between properties of each phase and the average value:

$$\begin{aligned} \tilde{C}^1 &= C^1 - \langle c \rangle = C^1 - (v_1 C^1 + v_2 C^2) = (C^1 - C^2) v_2 \\ \tilde{C}^2 &= C^2 - \langle c \rangle = C^2 - (v_1 C^1 + v_2 C^2) = (C^2 - C^1) v_1 \end{aligned} \quad (4-2)$$

4.2 Modified Corson's Probability Function

As introduced in the previous chapter, Corson's probability function is appropriate for a random orientation. For a two-phase composite, i and j correspond to phases 1 and 2, and for a polycrystal i and j can take values from 1 to n which is the total number of grains.

This reduces the number of two-point functions to four, $P_{11}(r)$, $P_{12}(r)$, $P_{21}(r)$, and $P_{22}(r)$ in the case of composites. Whereas for a homogenous composite, there is just one independent probability function (P_{11}). The other constants c_{ij} and n_{ij} are also microstructure parameters: n_{ij} is equal to 1 for a random microstructure (Gokhale, 2003) and c_{ij} is a scaling parameter representing the correlation distance. Corson's equation works very well for distribution in random microstructures, however to capture the anisotropy the equation needs to be modified. These empirical coefficients can be reformulated into an anisotropic form,

$$c_{ij}(\theta, A) = c_{ij}^0 (A + (1 - A) \cos(\theta - \theta_0)), \quad (4-3)$$

where A is a material parameter that represents the degree of anisotropy in a microstructure such that $A = 1$ corresponds to an isotropic microstructure and $A = 0$ represents a complete anisotropic composite, and c_{ij}^0 and θ_0 are the reference empirical coefficients and can be calculated from the microstructural statistical information. By applying this formulation the anisotropy can be captured in all direction by throwing vectors in different angles. A schematic diagram is shown to represent the measurement of two-point statistics in anisotropic microstructures. This equation will be further studied in detail in the next chapter.

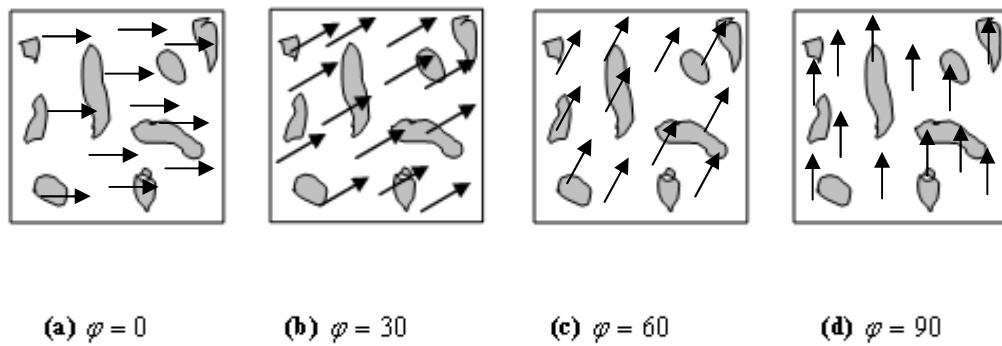


Figure 4.1 Schematic representation of two-point probabilities measurements in an anisotropic microstructure

4.3 Two-Point Probability Function for Polycrystalline Materials

If all the volume elements possessing a unique orientation are denoted by dV , and the total volume of the sample is denoted by V , then an orientation distribution function $f(g)$ can be defined by:

$$\frac{dV}{V} = f(g)dg, \quad (4-4)$$

if all orientations have been considered in the domain:

$$\int_V \frac{dV}{V} = \int_V f(g)dg = 1, \quad (4-5)$$

where $\frac{dV}{V}$ shows the volume fraction of a specific orientation, that is one-point statistics. By measuring the two-point statistics the estimation of properties can be related to the morphology.

The two-point correlation functions can be extended to polycrystalline cases by rewriting eq. (3-10) in the following way:

$$\langle \tilde{c}_{ijk_u}(x) \tilde{c}_{pmrs}(x') \rangle = \iint \tilde{c}_{ijk_u}(x) \tilde{c}_{pmrs}(x') P_2(x | g_i, x' | g_j) dg_i dg_j, \quad (4-6)$$

where i and j are the indicators for each crystal with specific orientation and they can vary from one to the total number of crystals (M); and P_2 is a two-point probability function that measures the correlation between different orientations in the polycrystalline microstructure. This can also be shown in the form of summation:

$$\langle \tilde{c}_{ijk_u}(x) \tilde{c}_{pmrs}(x') \rangle = \sum_{i=1}^N \sum_{j=1}^N \tilde{c}_{ijk_u}(x) \tilde{c}_{pmrs}(x') P_2^{ij}, \quad (4-7)$$

where P is defined for different orientations in the microstructure. A schematic representation for the measurement of two-point statistics is shown in Figure 4.2. To measure two-point probabilities, orientations for each of two crystals that are connected by a vector r_{ij} have to be known. More explanation will be given in chapter 6, where the statistical homogenization will be applied to polycrystalline microstructures.

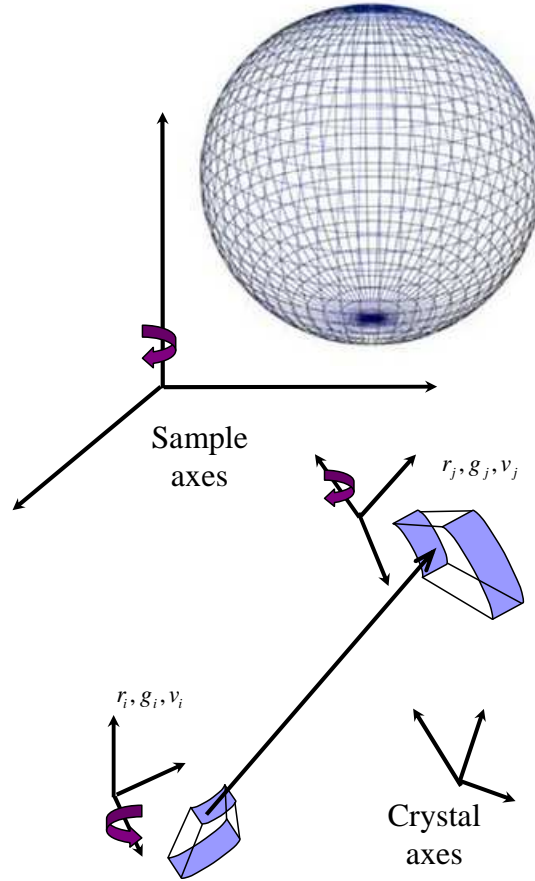


Figure 4.2 Schematic representation of orientation coherence function for polycrystalline microstructures

4.4 Analytical Analysis of Homogenization Relations

It was shown earlier that the effective modulus, C can be calculated through eq. (3-31), where the second term is defined by eq. (3-44). Recall eq.(3-44) and ignore the three-point statistical term:

$$\langle \tilde{c}_{ijku}(x) \tilde{\mathcal{E}}_{ku}(x) \rangle = \int_V K_{kpu} \partial \langle \tilde{c}_{ijku}(x) \tilde{c}_{plrs}(x') \rangle / \partial x_l \langle \epsilon_{rs} \rangle dX' \quad (4-8)$$

A fourth ran tensor $\langle a \rangle$ was introduced as the deviation in the strain field,

$$\langle \tilde{\epsilon}_{ku} \rangle = \langle a_{kurs} \rangle \langle \epsilon_{rs} \rangle, \quad (4-9)$$

Substituting the above equation in eq. (4-8) and omitting $\langle \epsilon_{ku} \rangle$ from two sides, reduces the equation to:

$$\langle \tilde{c}_{ijku}(x) a_{kurs} \rangle = \int_V K_{kpu} \partial \langle \tilde{c}_{ijku}(x) \tilde{c}_{plrs}(x') \rangle / \partial x'_l dX' \quad (4-10)$$

Applying integration by part to the above equation, it can be rewritten as follows:

$$\langle \tilde{c}_{ijku}(x) a_{kurs}(x) \rangle = \int_{V'} \partial [K_{kpu} \langle \tilde{c}_{ijku}(x) \tilde{c}_{plrs}(x') \rangle] / \partial x'_l dX' - \int_{V'} K_{kpul}(x, x') \langle \tilde{c}_{ijku}(x) \tilde{c}_{plrs}(x') \rangle dX', \quad (4-11)$$

where K_{kpul} is the second derivative of the Green's function:

$$K_{kpun} = (G_{kp,un} + G_{up,km}) / 2 \quad (4-12)$$

Let's rewrite the above equation as a summation of two integrals as in the following:

$$\langle \tilde{c}_{ijku}(x) a_{kurs}(x) \rangle = I^1_{ijrs} + I^2_{ijrs}, \quad (4-13)$$

where the two terms of I^1_{ijrs} , I^2_{ijrs} can be calculated by

$$I^1_{ijrs} = \int_{V'} \partial [K_{kpu}(x, x') \langle \tilde{c}_{ijku}(x) \tilde{c}_{pmrs}(x') \rangle] / \partial x'_m dX', \quad (4-14)$$

and

$$I^2_{ijrs} = - \int_{V'} K_{kpum}(x, x') \langle \tilde{c}_{ijku}(x) \tilde{c}_{pmrs}(x') \rangle dX' \quad (4-15)$$

In last sections, two-point probabilities were defined in composites and polycrystalline microstructures, now the integrals in equations (4-14) and (4-15) are calculated here:

The first integral is a volume integral which can be converted to a surface integral by applying Gauss' theorem. Gauss Theorem converts the volume integral in a sphere with infinite radius to a surface integral with the boundary of this sphere. The resulting surface integral requires evaluation on a surface at infinity and on a surface enclosing the singularity of K_{kpu} at $x=0$.

Choosing both surfaces as spheres and applying Gauss theorem:

$$I^1_{ijrs} = \left(\int_{x-x' \rightarrow 0} \langle \tilde{c}_{ijkl}(x) \tilde{c}_{pmrs}(x') \rangle K_{kpu} d\hat{A}_m \right) + \left(\int_{x-x' \rightarrow \infty} \langle \tilde{c}_{ijkl}(x) \tilde{c}_{pmrs}(x') \rangle K_{kpu} d\hat{A}_m \right) \quad (4-16)$$

To calculate the two surface integrals, the correlation term shown by $\langle \tilde{c}_{ijkl}(x) \tilde{c}_{pmrs}(x') \rangle$ has to be evaluated when $x-x' \rightarrow 0$ and $x-x' \rightarrow \infty$. When the distance between x and x' reaches zero, then the correlation will be independent of x (constant), and when the distance between x and x' reaches infinity, there will be no correlation between the two points (zero). This can be proved for the case of a two-phase composite by using eq. (3-14).

$$\text{When } x-x' \rightarrow 0 \text{ then: } \begin{cases} P_{11} \rightarrow v_1 \\ P_{12} \rightarrow 0 \\ P_{22} \rightarrow v_2 \end{cases}$$

Substituting these values in the definition of correlation term (eq. (4-1)):

$$\langle \tilde{c}_{ijkl}(x) \tilde{c}_{pmrs}(x') \rangle = \tilde{C}^1_{ijkl} \tilde{C}^1_{pmrs} v_1 + \tilde{C}^2_{ijkl} \tilde{C}^2_{pmrs} v_2 \equiv \text{Const} , \quad (4-17)$$

$$\text{and when } x-x' \rightarrow \infty , \text{ then: } \begin{cases} P_{11} \rightarrow v_1^2 \\ P_{12} \rightarrow v_1 v_2 \\ P_{22} \rightarrow v_2^2 \end{cases}$$

Substituting these values in the definition of correlation term in eq. (3-46) and applying the values of \tilde{C}^1 and \tilde{C}^2 into eq. (4-1):

$$\langle \tilde{c}_{ijk}(x) \tilde{c}_{pmrs}(x') \rangle = (C_1 - C_2)^2 v_2^2 v_1^2 - 2(C_1 - C_2)^2 v_1 v_2 v_1 v_2 + (C_2 - C_1)^2 v_1^2 v_2^2 \equiv 0 \quad (4-18)$$

Therefore, the second term in eq. (4-15) will be equal to zero and the components of the first integral (I^1_{ijrs}) can be calculated by:

$$I^1_{ijrs} = (\tilde{c}^1_{ijk} \tilde{c}^1_{pmrs} v_1 + \tilde{c}^2_{ijk} \tilde{c}^2_{pmrs} v_2) Kc_{kpum} \quad (4-19)$$

where:

$$Kc_{kpum} = \int K_{kpu} dA_m, \quad (4-20)$$

and is evaluated as follows:

$$\begin{aligned} Kc_{iii} &= -\frac{(16/15)\chi}{8\bar{G}} \\ Kc_{ijj} &= Kc_{jji} = \frac{(4/3 - 4/5)\chi}{8\bar{G}}, \\ Kc_{iji} &= Kc_{jij} = Kc_{ijj} = Kc_{jii} = -\frac{(2/3 + 2/15)\chi}{8\bar{G}} \end{aligned} \quad (4-21)$$

where χ is the average properties of two phases:

$$\chi = \frac{\bar{\lambda} + \bar{G}}{\bar{\lambda} + 2\bar{G}} \quad (4-22)$$

Note that i and j can vary from 1 to 3, but there is no summation on the indices in eq. (4-21). It is observed that I^1_{ijrs} is the contribution of one-point statistics since the only variable contributed in the calculations of eq. (4-20) is χ and this is the average value of elastic properties of the material. Therefore this term reduces to the volume fractions of two phases as the limiting values of two-point probabilities.

Recall the second term in eq. (4-13):

$$I^2_{ijrs} = -\int_V K_{kpum}(x, x') \langle \tilde{c}_{ijku}(x) \tilde{c}_{pmrs}(x') \rangle dX',$$

To calculate this integral, this integral has to be calculated over a sphere with infinite radius. The infinite sphere here is defined as a sphere where for bigger spheres the correlation term will be zero. Analytical analysis of this integral illustrates that when $r \rightarrow 0$ or $r \rightarrow \infty$ the correlation term will be a constant value and can be taken out of the integral. Evaluating $\int_V K_{kpum}(x, x') dX'$ and multiplying that by the correlation term, I^2_{ijrs} is calculated for two limiting values. It can be shown that this integral is zero (the proof is shown on the following pages).

Therefore, the second integral I^2_{ijrs} is now needed to be evaluated between two limits of r_0 and R_c . These values are defined as the limiting values for the radius of the sphere. R_c is large enough so that the correlation will disappear for larger values than that and r_0 is small enough so that the value of the volume integral (second integral) will not change by changing its value. The other important issue here is that r_0 has to be chosen small enough so that changing its value doesn't change the probabilities measured in the microstructure anymore.

Recall that there is just one independent probability function when the composite is isotropic (P_{11}) and also this is a function of r . Therefore, all other probability functions can be rewritten in terms of P_{11} as follows:

$$P_{12} = P_{21} = V_1 - P_{11}$$

and

$$P_{22} = 1 - 2V_1 + P_{11}$$

For the case of isotropic composites P_{11} is just a function of the value of vector r . Let's assume an exponential form for P_{11} , and then the correlation term can be rewritten as:

$$\langle \tilde{c}_{ijk} \tilde{c}_{pmrs} \rangle = \alpha_1 + \alpha_2 \exp(-cr^n) \quad (4-23)$$

Therefore, the second integral in eq. (4-13) can be rewritten as:

$$I^2_{ijrs} = - \int_V K_{kpum}(x, x') [\kappa_1 + \kappa_2 \text{Exp}(-cr^n)] dX' \quad (4-24)$$

By using the definition of isotropic Green's function, K_{kpum} is derived to be (details are shown in the appendix):

$$\begin{aligned} K_{kpum} = & 1/8\pi\bar{\mu} \left\{ [K\delta_{uk}\delta_{pm} + (K-1)(\delta_{pu}\delta_{km} + \delta_{um}\delta_{pk})] / |r|^3 \right. \\ & + [(3-3K)(r_m r_k \delta_{pu} + r_m r_u \delta_{kp})\delta_{uk}\delta_{pm} - 3K(r_m r_p \delta_{ku} + r_n r_p \delta_{km} + r_k r_p \delta_{um} + r_k r_n \delta_{pm})] / |r|^5 \\ & \left. + [15K(r_p r_m r_u r_k) / |r|^7] \right\} \end{aligned} \quad , (4-25)$$

Some components of the integral I^2_{ijrs} are evaluated here as an example:

$$\begin{aligned} \int_V K_{1111} dX' &= 1/8\pi\bar{\mu} \int_r \int_\theta \int_\phi [(3K-2)\sin\phi + (6-18K)\cos^2\theta\sin^3\phi + 15K\cos^4\theta\sin^5\phi] \\ & \quad [\kappa_1 + \kappa_2 \text{Exp}(-cr^n)] / r dr d\theta d\phi = 0 \\ \int_V K_{1212} dX' &= 1/8\pi\bar{\mu} \int_r \int_\theta \int_\phi [K\sin\phi - 3K\sin^3\phi + 15K\sin^2\theta\cos^2\theta\sin^5\phi] [\kappa_1 + \kappa_2 \text{Exp}(-cr^n)] \\ & \quad / r dr d\theta d\phi = 0 \\ \int_V K_{1122} dX' &= 1/8\pi\bar{\mu} \int_r \int_\theta \int_\phi [(K-1)\sin\phi + (3-3K)\sin^2\theta\sin^3\phi - 3K\cos^2\theta\sin^3\phi \\ & \quad + 15K\sin^2\theta\cos^2\theta\sin^5\phi] \cdot [\kappa_1 + \kappa_2 \text{Exp}(-cr^n)] / r dr d\theta d\phi = 0 \end{aligned} \quad (4-26)$$

It's observed that the terms that have to be integrated with respect to r are completely separated from the rest. Therefore, the two following integrals have to be calculated as:

$$\begin{aligned}
\int_{r_0}^{R_c} dr/r &= \lim_{r_0 \rightarrow 0} \left(\ln(r) \Big|_{r_0}^{R_c} \right)_{R_c \rightarrow \infty} = \ln(R_c/r_0) \\
\int_{r_0}^{R_c} \text{Exp}(-cr^n) dr/r &= -\frac{1}{n} \left\{ \ln(\ln(\text{Exp}(-cr^n))) + \ln(\text{Exp}(-cr^n)) + \frac{\ln^2(\text{Exp}(-cr^n))}{2.2!} + K \right\} \Big|_{r_0}^{R_c} \\
&= -\frac{1}{n} \left\{ \ln(\ln(\text{Exp}(-cR_c^n))/\ln(\text{Exp}(-cr_0^n))) \right. \\
&\quad + \ln(\text{Exp}(-cR_c^n)/\text{Exp}(-cr_0^n)) \\
&\quad \left. + \ln^2(\text{Exp}(-cR_c^n)/\text{Exp}(-cr_0^n))/2.2! + K \right\}
\end{aligned}$$

So, the integration with respect to r will give a finite value and the integration over θ and ϕ for the rest of the integrand will result in zero. So, the whole integration will result in zero.

In the same way, the general form of the integral can be shown as:

$$\begin{aligned}
\int_V K_{iii}(x, x') dX' &= 0 \\
\int_V K_{ijj}(x, x') dX' &= 0, \\
\int_V K_{ijj}(x, x') dX' &= 0
\end{aligned} \tag{4-27}$$

where i and j vary from 1 to 3 indicating three directions in the spherical coordinates.

Note that there is no summation on the indices in eq. (4-27).

Considering eq. (4-24) and eq. (4-27), I^2_{ijrs} will be shown to be zero for isotropic materials. This is in agreement with the numerical results of Adams et al. (Beran, 1996). In their work, as the Oxygen Free electronic (OFE) alloy 101 copper plates were nearly isotropic, it was observed numerically that the contribution of the second integral is almost zero in the calculation of elastic properties. So the effect of spatial arrangement of the crystals was not observed.

Also note that in the previous works by Garmestani (2000) only an isotropic composite was considered. Therefore, the effect of morphology and spatial arrangement in the microstructure on properties was not completely evident. This fact has been derived and proven in this chapter analytically. Furthermore it has been shown analytically that the contribution of the two-point statistics is not zero in anisotropic composites. In the following chapters, the effect of one-point and two-point statistics in the homogenization relationship for elastic properties of materials will be studied in detail and analyzed numerically for composites and polycrystalline materials.

4.4 Implementation of the Structure-Property Relations Based on Two-Point Statistics

Now that the homogenization relations has been extended to anisotropic distribution and the effect of one-point and two-point has been studied analytically, several programs will be written to implement the formulations. Therefore the numerical results will also show the contribution of one-point and two-point statistics in structure-property relationships. Figure 4.3 shows the flow chart of programs written based on the homogenization relations. The spatial information about the morphology of the microstructure (composite or polycrystalline), the properties of the constituent phases and the sample symmetry is assumed to be as input data. Implementing the established structure-property relationships the correlation between the microstructure and their properties will be observed and studied and microstructure optimization will be performed based on that.

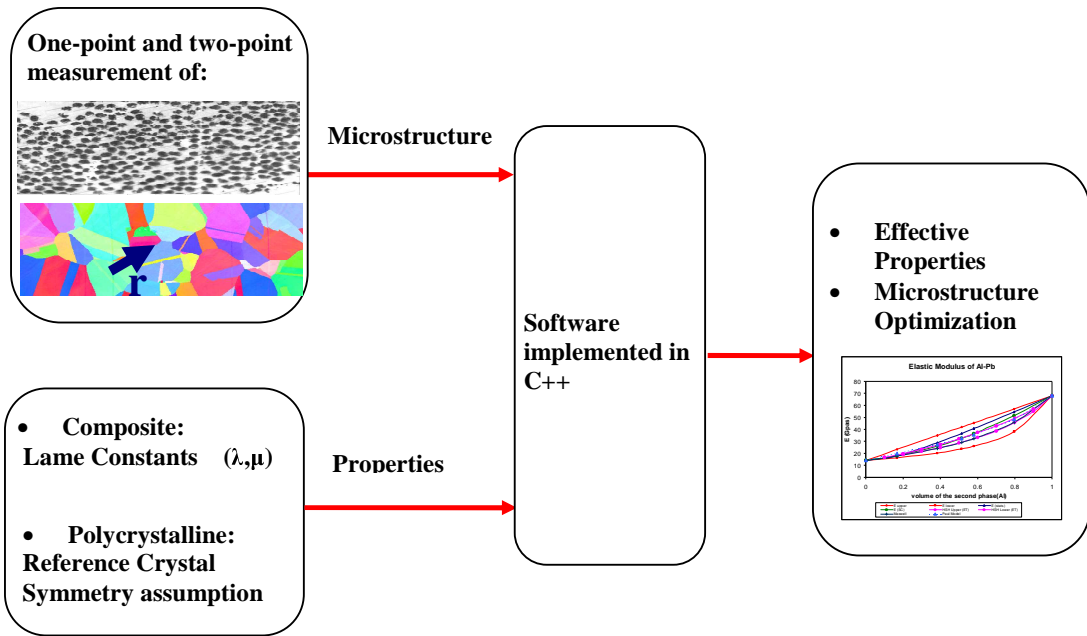


Figure 4.3 Schematic representation of two-point probabilities measurements in an anisotropic microstructures

CHAPTER 5

HOMOGENIZATION RELATIONS IN COMPOSITES

As it was discussed in last chapter, the two-point statistics has a significant role in calculating the elastic properties of anisotropic composites. This has been proven analytically in the last chapter. In this chapter, the homogenization relationships will be applied for several isotropic and anisotropic composites.

5.1 Simulation of Al-Pb Composite- Property Enclosure

In this section the homogenization relationship in previous sections are applied to two types of composites that are computer generated. First an isotropic composite with a randomly distributed second phase is considered. In such a composite, the probability distribution functions are isotropic and independent of orientation. In this case the probability functions in eq. (3-14) are sufficient to characterize the microstructure. Next, a special case of an anisotropic composite is considered such that the microstructure of any section perpendicular to a particular direction has the same statistics. The anisotropy is then considered in only two sections of the composite. In the simulation of this microstructure, the probability distribution function changes with orientation and magnitude of the vector “ \mathbf{r} ” for each section which was shown in Figure 4.1. The measurements of this composite on any section perpendicular to one particular direction provides the same statistical information within which the statistics maybe anisotropic.

5.1.1 Isotropic distribution

For a randomly distributed isotropic composite, the correlation functions are independent of orientation and are just function of the magnitude of “r”. Therefore, the volume integral in eq. (4-12) can be separated into two integrals in which one of them includes the variable r and the other one includes ϕ and θ . The integral has been shown to be zero in this case (eqs. (4-26)). This means that there is no contribution from the two-point statistics for an isotropic material and only the first integral or the one-point statistics (volume fractions) contributes to the effective elastic properties. This result is in good agreement with the experimental results of Adams et. al. on Oxygen Free electronic (OFE) alloy 101 copper plates (Beran, 1996). In their work experimental results showed that there is a negligible contribution from the second term as the material had a very small anisotropy.

In this work, the two reinforcing phases are Aluminum and Lead with Lamé's constants of ($\lambda = 64.286, G = 25$) and ($\lambda = 25.88, G = 4.926$), respectively. The effective elastic modulus for an isotropic distribution is plotted as a function of volume fraction in Figure 5.1 and Figure 5.2. Also, in these figures, Voigt upper bound and Reuss lower bound that are calculated by an imposed uniform strain and stress in both fibers and matrix are shown. (Voigt, 1889; Reuss, 1929). In addition the results based on Self-Consistent method, Hashin-Shtrikman bounds, and Maxwell approximations are shown for comparison. The simulation data has been also compared to Paul model (Johnson, 1991). This model assumes all the particles are cubic and an average value for

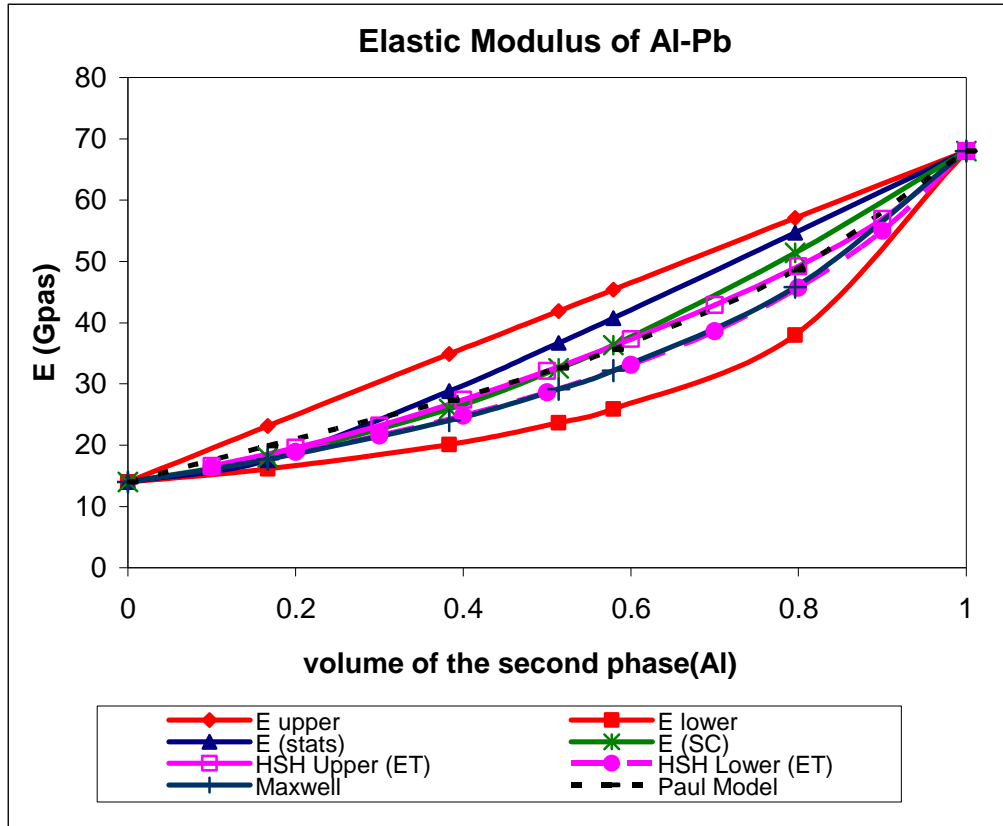


Figure 5.1 Effective elastic modulus of Al-Pb composite (isotropic)

elastic modulus is calculated. This model shows an intermediate value between upper and lower bounds. As it was mentioned before, the Maxwell approximation is equal to HS lower bound since the second phase is stiffer.

Figure 5.1 shows the variation of the elastic modulus for Al-Pb composite for different volume fractions of Aluminum. It illustrates that the statistical model provides a good estimate for the elastic properties. The predictions of the statistical model seem to be closer to the upper bound for larger volume fractions and closer to the lower bound for smaller volume fractions. The difference between the predictions and the upper bound decreases from 80% to 13% as the second phase volume fraction increases.

In addition, for smaller values of volume fractions most of the models are coincident whereas for large values of volume fraction they fall apart.

The statistical predictions for the shear modulus of the composite (commonly known as G) are shown in Figure 5.2. Three elastic coefficients (C_{1111} , C_{1122} , and C_{1212}) can be independently predicted for this simulation. The shear modulus, (G) can be predicted from C_{1111} and C_{1122} through the isotropic relation as:

$$G = (1/2)(C_{1111} - C_{1122}) \quad (5-1)$$

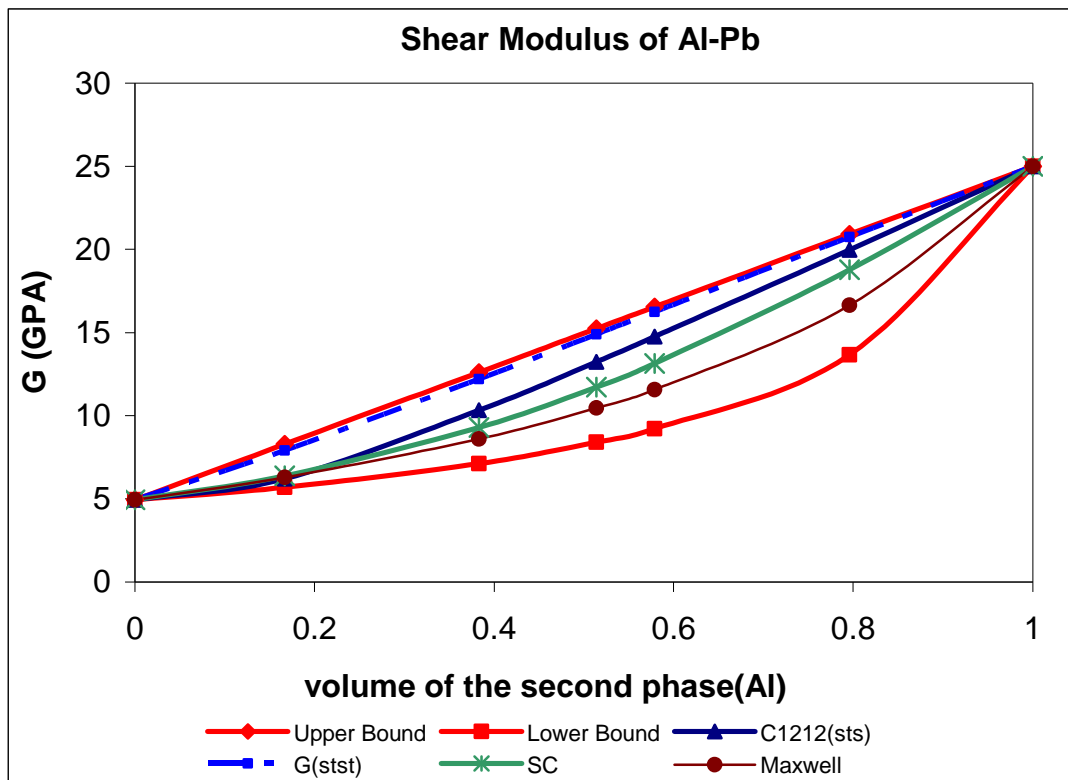


Figure 5.2 Effective elastic shear modulus of Al-Pb (isotropic)

The simulations show that the values obtained for C_{1212} are very close (identical) to the upper bound. The differences between these calculated values and the upper bound is less than 4%. Therefore, calculated value of C_{1212} from simulation doesn't provide any new information. However the values obtained from $(1/2)(C_{1111} - C_{1122})$ are good estimates for the shear modulus (G) of the composite. It is observed that the results of the simulation are very close to the upper bound for the larger volume fractions of aluminum, and closer to the lower bound for smaller values of volume fractions. The statistical simulation values have in addition compared with Hashin-Shtrikman bounds, Self-Consistent and Maxwell model. It is that the results are in good agreement especially for smaller values of volume fractions of the second phase.

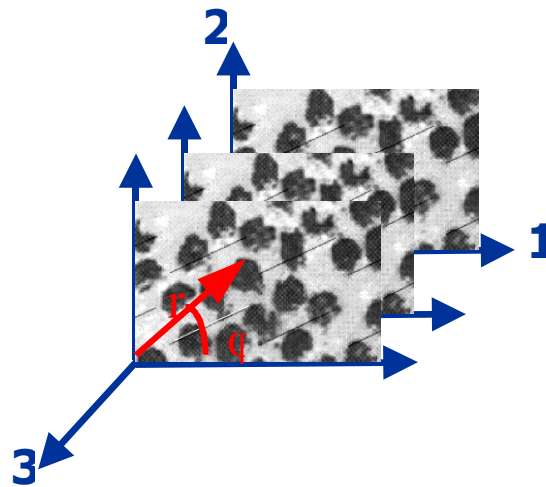


Figure 5.3 Digital representation of the anisotropic composite

5.1.2 Anisotropic distribution

The effect of anisotropy is examined here by considering a special type of a two-phase composite that gives the same anisotropic distribution in every plane perpendicular to a particular direction (Z-direction, Figure 5.3). This means that the three-dimensional distribution function can be measured to be identical from any plane normal to this direction. The two individual phases of the composite are considered to be isotropic and volume fractions (ν) and the degree of anisotropy (A), which was defined previously, are considered as two design parameters in this work. In this section the degree of anisotropy is calculated for three samples of Al-Pb composite by having the distribution of P_{11} . The volume fraction of Al in the samples is 20%, 30%, and 40% respectively. Recall eq. (4-3), at

$$\left. \begin{array}{l} \theta = \theta_0 \rightarrow [c_{ij}]_{\max} = c_{ij}^0 \\ \theta = \theta_0 + \frac{\pi}{2} \rightarrow [c_{ij}]_{\min} = c_{ij}^0 A \end{array} \right\} \rightarrow A = [c_{ij}]_{\min} / [c_{ij}]_{\max} \equiv 1/ASPECT \ RATIO \quad (5-3)$$

Therefore to calculate A, the lowest and largest value of “c” needs to be identified. In other words, θ^0 has to be known. As an example the measured values of m have been shown in Table 5.1. It is clear that the maximum value for m is 1.092 at $\theta = 90$ and its minimum value is 0.028 at $\theta = 0$. Therefore, the value of A has been calculated to be 0.0258 for the case of $\nu = 30\%$. The values of A for $\nu = 20\%$ and 40% have been calculated to be 0.01 and 0.048 respectively which are in agreement with the aspect ratio of corresponding microstructures.

Table 5.1 Calculation of Degree of Anisotropy (A) in modified Corson's equation

	c_{11} (measured)	c_{11} (calc)
0-5	0.028	0.121
5-15	0.151	0.213
15-25	0.364	0.392
25-35	0.591	0.56
35-45	0.753	0.71
45-55	0.89	0.84
55-65	0.987	0.95
65-75	1.027	1.028
75-85	1.067	1.076
85-90	1.092	1.092
K(aspect R)	30.87	
A	0.0258	

As an example the fitted curve through the modified Corson's equation for the case of 30% is shown in Figure 5.4. The fourth rank tensor of elastic constants is calculated for the three samples and the effect of the degree of anisotropy on properties is studied in transverse plane. In Figure 5.5 the variation of anisotropy is shown for different values of A for the case of vol2=30%. Note that as A gets closer to 1, C_{1111} gets closer to C_{2222} which corresponds to an isotropic distribution in transverse plane.

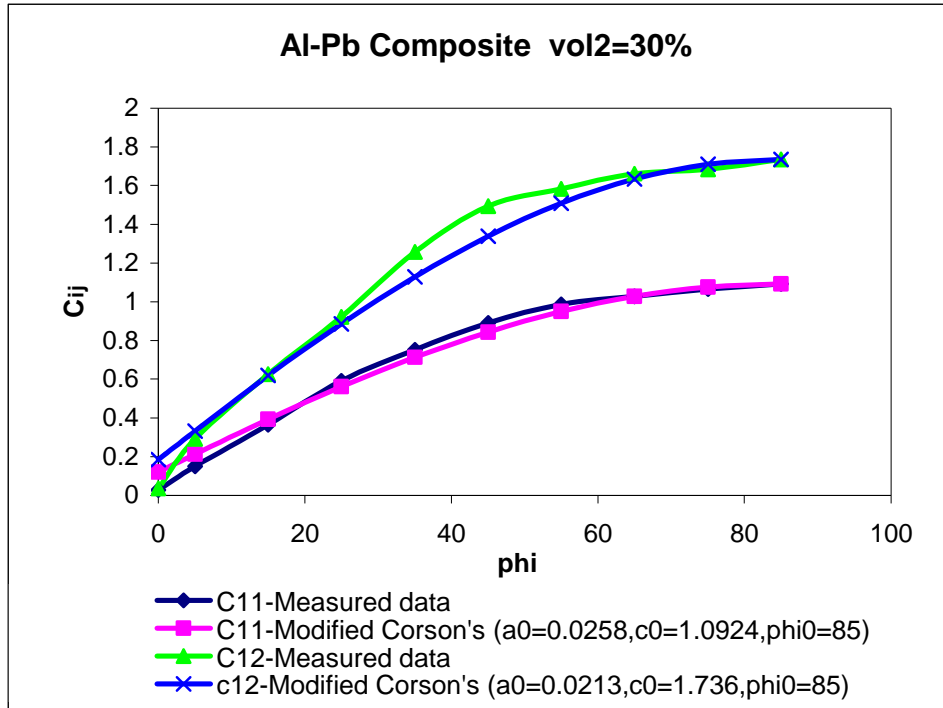


Figure 5.4 Modified Corson's equation fitted to measured values of P_{11}

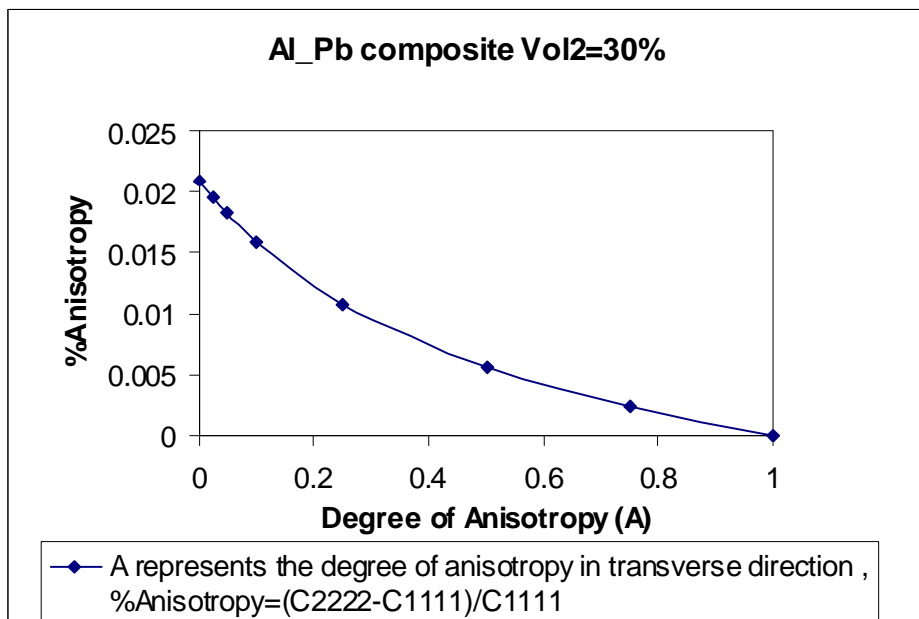


Figure 5.5 Variation of anisotropy in the microstructure for different values of A

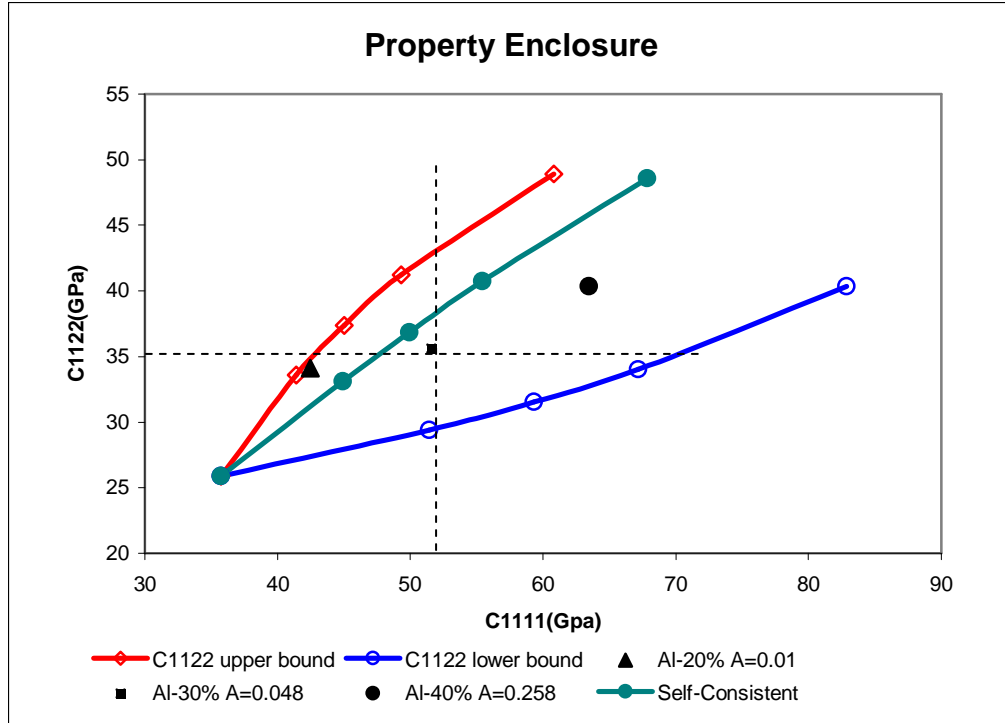


Figure 5.6 A property enclosure for anisotropic composite Al-Pb (anisotropy)

Figure 5.6 illustrates the property enclosure (the universe of all variation in inter relation among several properties for the same microstructure) of the composite Al-Pb. Each point in this enclosure represents a microstructure distribution with a specific volume fraction and specific anisotropy “A”. For example, if the axial elastic constant and shear elastic constant of 35 GPa and 53 GPa are needed respectively, the microstructure with vol (Pb) =30% and A (degree of anisotropy) of 0.0048 would be an answer.

In Table 5.2 the effective elastic coefficients C_{1111} and C_{3333} of the composite are also calculated for three samples. In this particular microstructure, Z-direction may be chosen such that the elastic properties in that direction, C_{3333} , are smaller than C_{1111} . It

is also evident that although the two phases are isotropic, the statistical model results in an anisotropic behavior for the elastic modulus.

The contribution of the different higher order statistical terms for the calculation of C_{1111} and C_{3333} is also shown in this Table. The 5th and 8th column show the contribution from the two-point statistical functions that are included in the second integral in eq. (4-11). This contribution is 15% to 27% in the calculation of C_{1111} . For the case of C_{3333} , the contribution of the second term is between 31% and 47%. As it was noted before, the second term does not contribute for the case of isotropy and is only observed in the anisotropic case.

Table 5.2 Contribution of one-point and two-point statistics in effective elastic stiffness

Al- vf	Upper Bound	C_{1111}	1-point Statistics	2-point Statistics	C_{3333}	1-point Statistics	2-point Statistics	Lower Bound
20%	51.45	42.47	-6.58	2.39	41.89	-6.58	2.97	41.43
30%	59.30	51.59	-6.49	1.20	46.99	-6.49	5.82	45.02
40%	67.15	59.129	-5.85	2.17	53.92	-5.85	7.37	49.28

5.1.3 Composite design

To illustrate the use of the present methodology in composite design, an example is given for a certain design project requiring knowledge of the variations in the ratio of the elastic moduli C_{3333}/C_{1111} . The composite system will be limited to the one discussed in the previous sections (Al-Pb). Let's consider a certain design in which the

ratio of the elastic moduli C_{3333}/C_{1111} needs to be minimized. The composite in this design project is quantified using the two-point statistical functions defined in equation (4-3). The design variables are now defined based on two parameters: volume fraction and degree of anisotropy as the representation of one and two-point functions. Let us consider the example above and for the purpose of illustration, the three microstructures above are considered. It is clear that these three microstructures can be extended to a large set of microstructures by varying A and the volume fraction of the second phase. The connection can be set up as an analytical tool for design using the homogenization relations explained above. Calculating the ratio of C_{3333}/C_{1111} for different values of volume fractions of (Al) and A (degree of Anisotropy), the statistical analysis above shows that for any given values of A , the composite has the lowest ratio of the longitudinal elastic properties with respect to transverse elastic properties at $\text{vol(Al)}=30\%$ (Figure 5.7). It means this methodology can be used to predict the microstructure in a specific design. The design constraints would lead us to a set of optimized properties as needed. The microstructure of the composite is predicted in terms of the statistical parameters (here as volume fractions and degree of anisotropy factor). However this microstructure is not unique. For instance for this case, having $\text{vol(Al)}=30\%$ and $A(\text{degree of anisotropy})=0.0258$, there are a variety of microstructures that ensure this specification. Meanwhile, knowing these two parameters limits the microstructure to a subset of microstructures with a specific volume fraction and degree of anisotropy. Therefore, two parameters defined in this section are adequate to represent the microstructure needed for design.

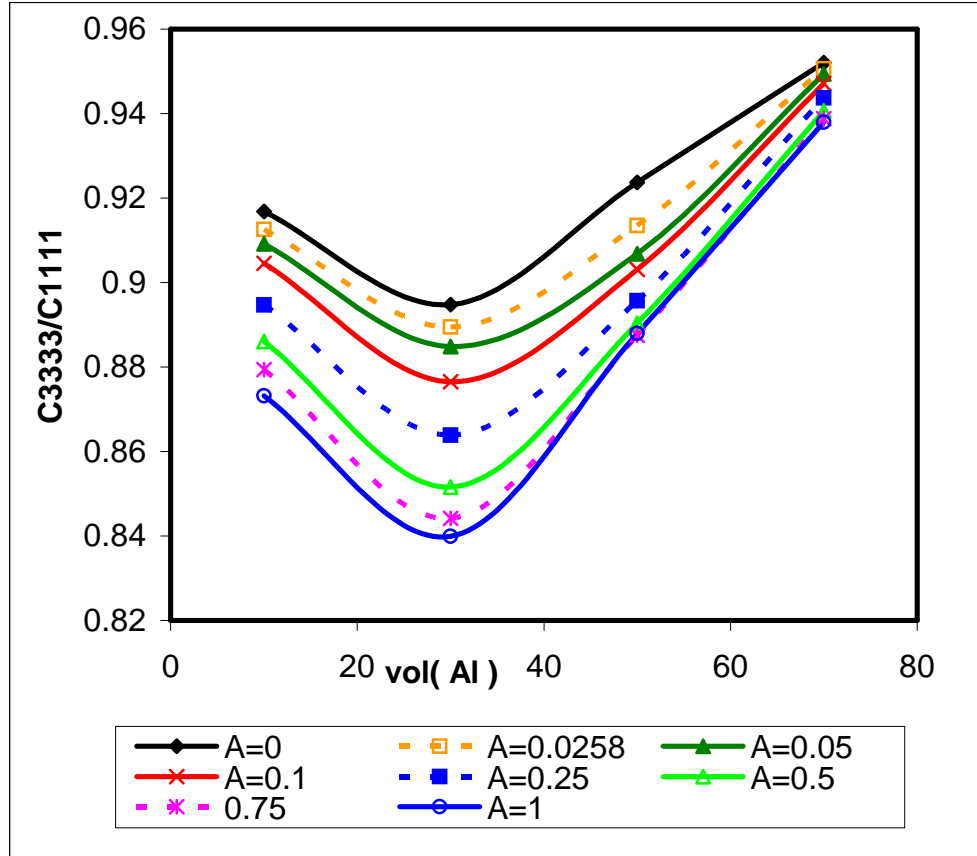


Figure 5. 7 Composite Design- Minimizing the longitudinal/transverse properties of anisotropic Al-Pb composite

5.1.4 Numerical analysis

To calculate I^2_{ijrs} , 1/3 Simpson integration method (the detail of the rule is demonstrated in the Appendix) has been used as an integration method. For this purpose, a sphere is divided into $n_r \times n_\theta \times n_\phi$ units. Where n_r is the number of sections for variable r (radius) and n_θ and n_ϕ are the number of sections for variables $0 < \theta < 2\pi$ and $0 < \phi < \pi$, respectively. The variable r also changes between 0 and ∞ . There

are two issues to be taken into account to perform the integration. One is the singularity of the Green's function at $r=0$ and the other is the definition of ∞ for r in the integration.

Empirical forms of the probability density functions were introduced earlier. It can be shown that for all physically realizable forms of the probability density functions in a random media, they merge to a constant value at large r . (as shown schematically in Figure 5.8)

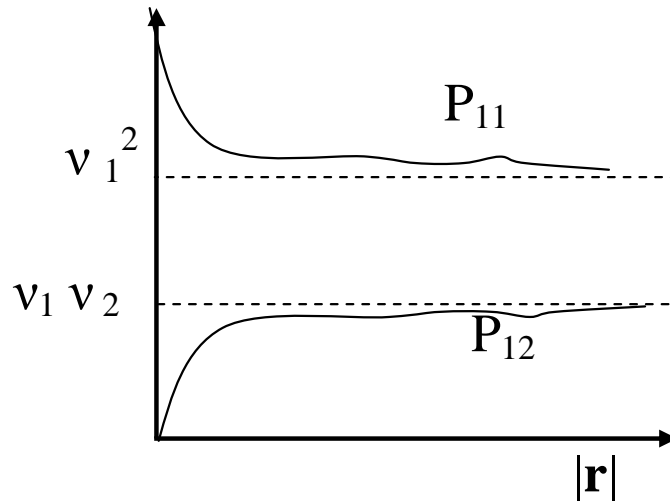


Figure 5.8 Schematic diagrams of probability functions

The correlation function defined in eq. (4-1) becomes zero when the probabilities P_{11} , P_{12} , P_{21} , and P_{22} reach their limits. Therefore, a Coherence Radius (R_C) will be defined as the limiting value of the probability functions. This value should be used as an upper limit (or ∞) for r in the triple integral. Since the Green's function is undefined at $r=0$ therefore r should be chosen a small nonzero value. For this purpose, a numerical procedure should be adopted that calculates a r_{\min} by reducing r until a saturation is reached for the value of the integral. On the other hand " r_0 " has to be chosen small

enough so that the measured probability functions don't change for smaller values. Time of operation is another aspect that has to be considered. For instance, in the case of Al-Pb composites (Garmestani, 2004); if $r_0=0.03$ micron and $\Delta r=0.1$ micron, it takes about 20 minutes for the codes to calculate one elastic constant in a Pentium IV machine, 2.4 MHZ. Thought, if r_0 is chosen the same and $\Delta r=0.01$ then it takes about 2 hours and 35 minutes to calculate one elastic constant. The difference between the two results is about 0.04 percent. Whereas for $r=0.003$, $\Delta r=0.01$ it takes about 20 hours where the differences in the calculation comparing to the first case is about 0.5 percent.

5.2 Samples of Al-SiC Composite

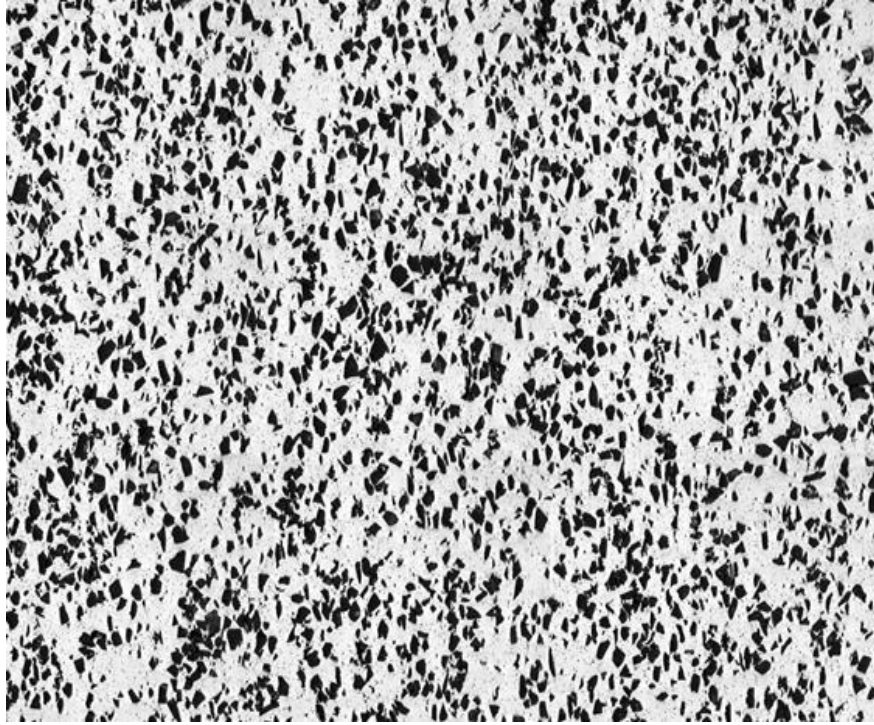
Elastic homogenization relations based on two-point statistics have been applied to a two-phase composite in previous chapters. It was shown analytically and numerically that two-point statistics doesn't contribute in the evaluation of elastic properties of isotropic composites; nonetheless it has a considerable effect in the case of anisotropy. The key to this approach is the correct representation of the microstructure. In previous chapters a simplified empirical form of the two-point probability function was used for the microstructure representation whereas in this section the statistical information will be measured directly from the microstructure.

For this purpose, elastic properties of two samples of Al-SiC composite are calculated by using the two-point statistical homogenization technique, and the contribution from the two-point statistics is discussed. The results of the simulation will be compared with experimental values to validate the applied homogenization observed technique. The composite was fabricated by extrusion with different distributions of the two different

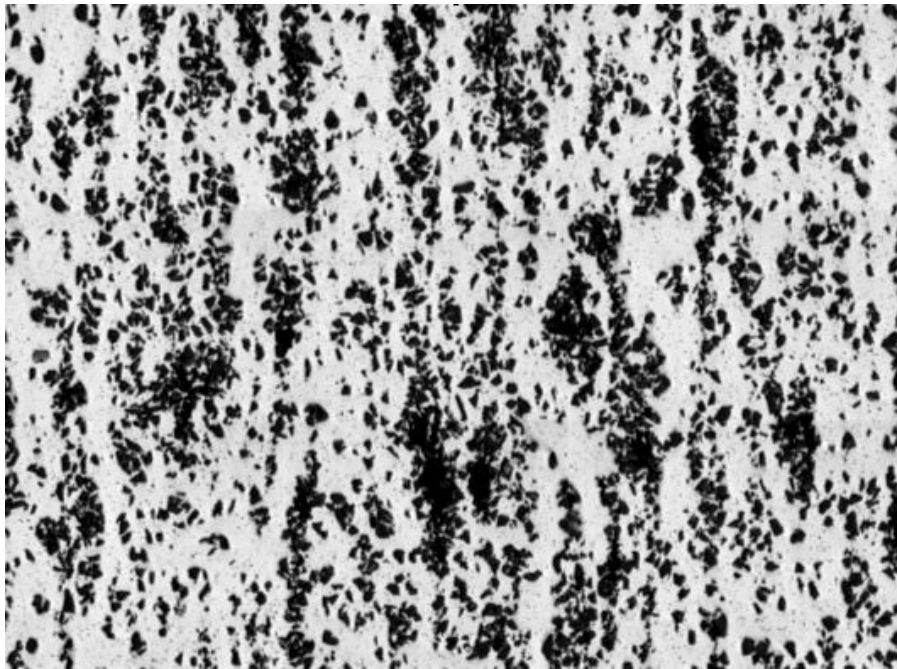
sizes of Al particles in SiC particles. So the difference in initial particle sizes of SiC reinforcement phases and Al-alloy matrix results in the heterogeneity of the microstructure. The micrographs of the two samples are shown in Figure 5.9. It is from the micrographs that the particles of SiC are clustered in the case of PSR: 8.1, therefore, they introduce more anisotropy in the microstructure in one direction compared to the microstructure with PSR: 2:1. The validation of this presumption will be studied by computing the elastic properties of the two samples. The distribution of the two-point correlation functions in these microstructures is symmetric with respect to the extrusion axis. Therefore, the extrusion axis is chosen as the vertical axis. The probability distribution function changes with orientation φ and magnitude of the vector “ \mathbf{r} ” on each section, Figure 5.10. The measurements of this composite on any section including the vertical axis (in direction 3) provides the same statistical information within which the statistics maybe anisotropic. Therefore, measurement of two-point correlations on just any section which includes the axis of symmetry is sufficient for simulation.

In this simulation, the two-point probability functions are measured directly from the microstructure and averaged as follows [Gokhale, 2003]:

$$\langle p_{ij}(r) \rangle = \frac{\int_0^{2\pi} [p_{ij}(r, \theta)]_v d\theta}{\int_0^{2\pi} d\theta} \quad (5-3)$$



(a) PSR: 2:1



(a) PSR: 8:1

Figure 5.9 Micrographs of two samples of Al-SiC

where

$$[p_{ij}(r, \theta)]_v = \int_0^{\pi/2} p_{ij}(r, \theta, \varphi) \sin \varphi d\varphi \quad (5-4)$$

θ , and φ are respectively the angles with respect to x-axis and z-axis in spherical coordinates.

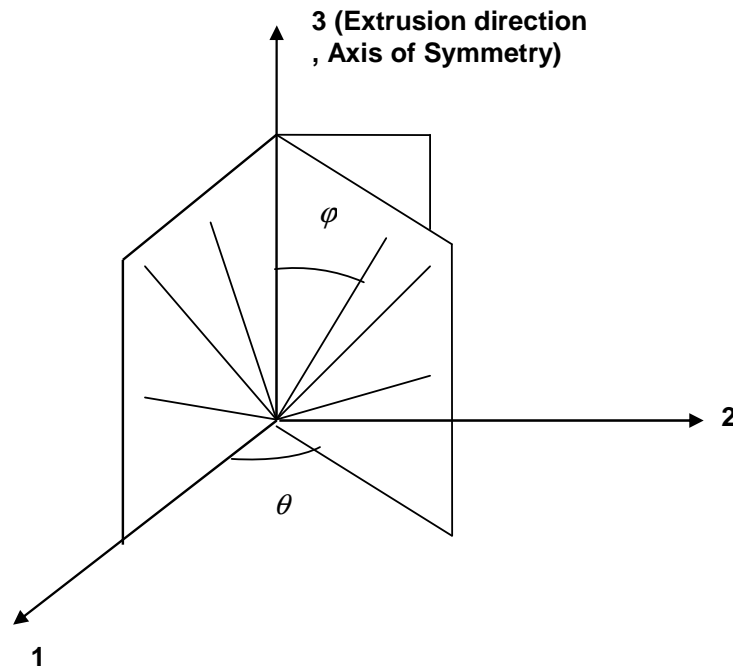


Figure 5.10 Representation of symmetry in samples of Al-SiC

As an example the measured values of p_{11} are shown in Figure 5.11 as a function of r and φ in each section containing extrusion axis. Also a Corson's equation is used to measure values of P_{11} in Figure 5.12. It is observed that the measured values show an exponential trend which is the same as Corson's eq. (3-14), and empirical factor "n"

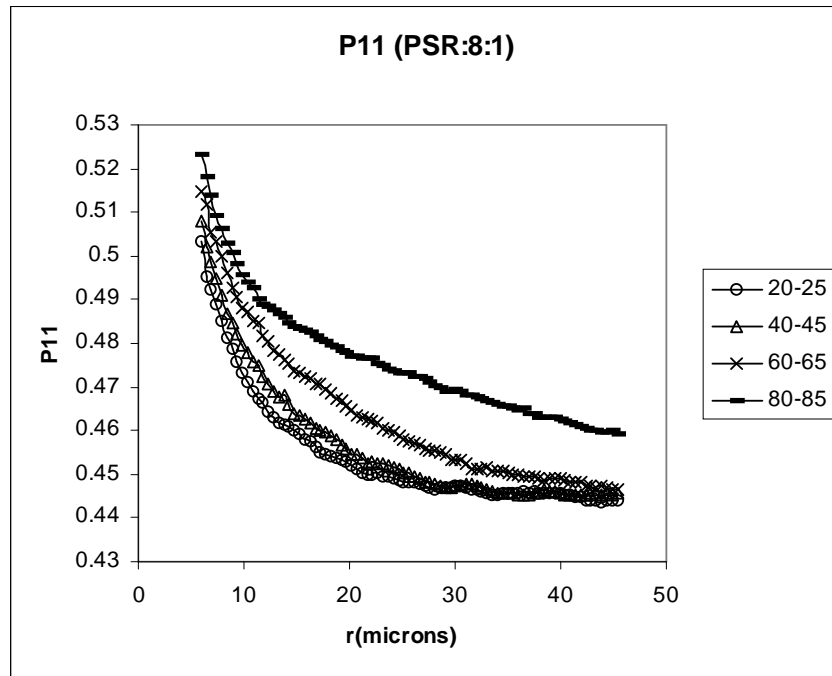
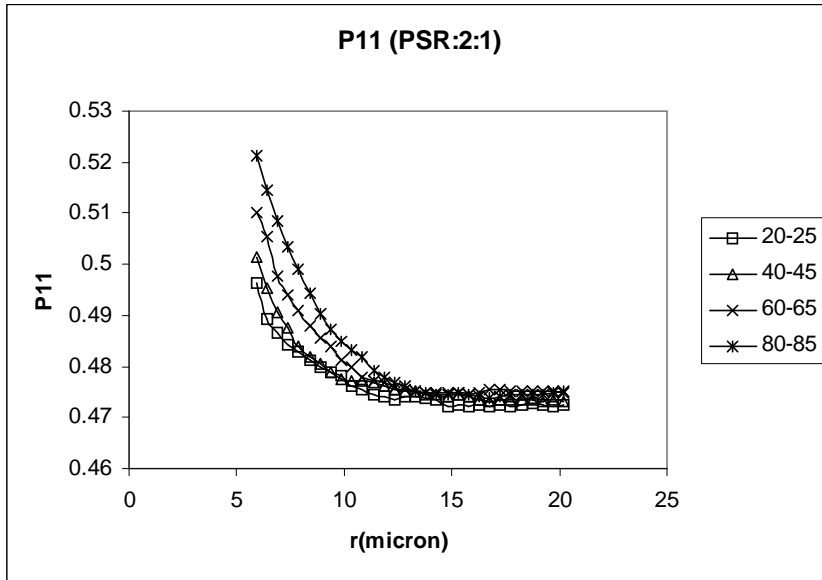


Figure 5.11 Measurement of two-point statistics in vertical section for two samples

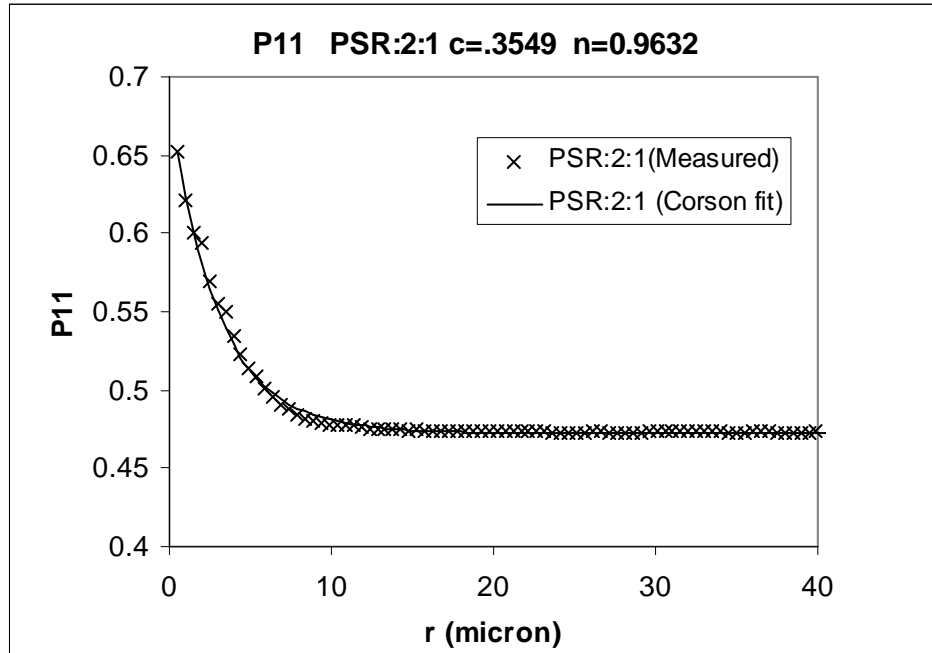


Figure 5.12 Curves fitted to the measured values of P_{11} for sample of Al-SiC with PSR: 2:1

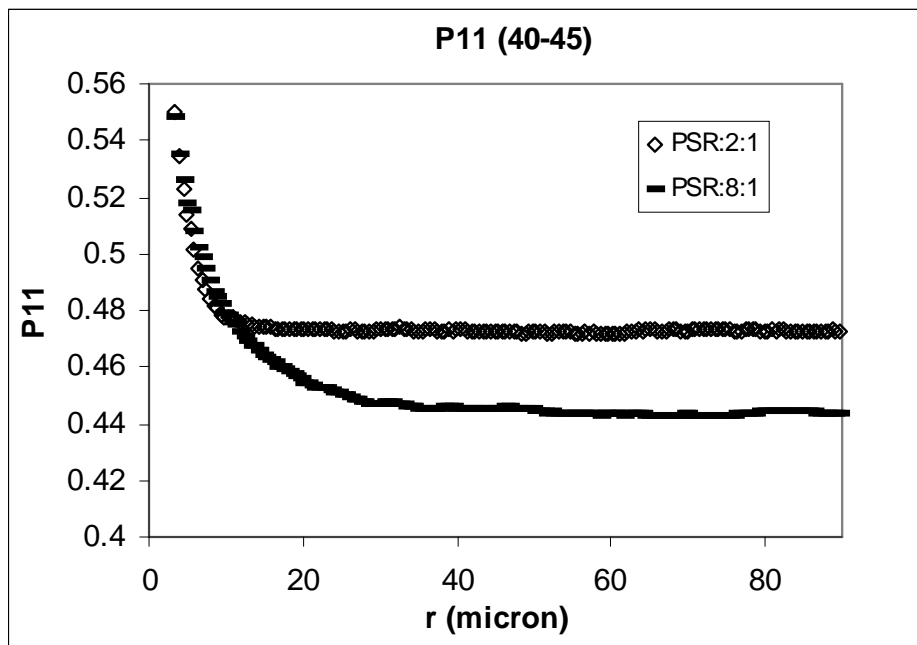


Figure 5.13 Measured P_{11} for two samples of Al-SiC composite

is calculated near 1 that is in agreement with results of (Gokhale,2003). P_{11} for two samples at $40 \pi \varphi \pi 45$ are shown in Figure 5.13. For the case of PSR:2:1 the values of P_{11} reaches to its limit ($\nu_1^2=0.4761$) faster than the values of the sample with PSR:8:1 reaching its limit ($\nu_1^2=0.4489$).

Using the measured two-point probabilities and preparing the simulation code based on the theory described in previous section calculate elastic stiffness matrices for each sample. The mechanical properties of each phase are assumed as follows: (based on previous experimental data):

$$E(\text{Al})=69\ 0\ \text{GPa} , \nu(\text{Al})=0.33 ; \quad E(\text{SiC})=393\text{GPa} , \nu(\text{SiC})=0.19$$

In this simulation both integrals in eq. (4-13) will be calculated, as the samples are considered anisotropic. The second integral includes the two-point statistics information, which has a major role in the calculation of effective elastic properties for anisotropic cases. Therefore the effect of anisotropy as introduced by clustering will be studied in the estimation of elastic properties of these two samples. To validate the simulation results, ultrasonic techniques were used to measure the elastic properties of the two samples.

For the measurements of the fourth rank elastic modulus both mechanical testing and non-destructive testing based on ultrasonic techniques were utilized. Here a brief overview on ultrasounds is discussed.

5.2.1 Ultrasounds technique

Since sound provides valuable information by traveling through the media, it plays a significant role in the nondestructive testing and evaluation of materials.

Ultra-sound is an extension of audible sound with higher magnitude in frequency. The wave length of ultrasounds decreases as a result of increasing the magnitude of the frequency into several MHZ. Therefore, ultrasounds are able to detect the smaller substrate defects, whereas audible sounds detect the relatively large defects in very large material structures. The ultrasound technique uses sound wave with high frequency, typically from 100 KHz to 5 MHz to inspect a sample (Figure 5.14)

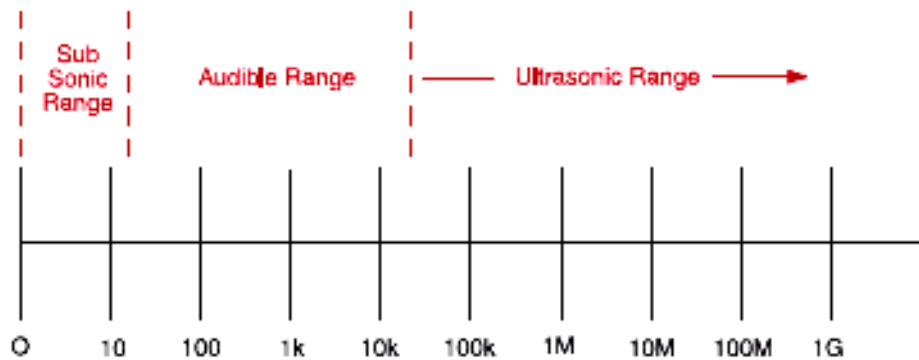


Figure 5.14 Range of frequency in ultrasound

This technique uses two kinds of waves: (a) the longitudinal wave in which the direction of particles displacement and wave propagation are the same. (b) the shear wave in which the direction of particles displacement and wave propagation are perpendicular (Mahesh, 1986).

For this purpose, two transducers were used in the ultrasonic device to propagate the longitudinal and shear wave and measure the time of flight (tof). The following equation will is used to estimate the Lamé's constants by this measurement (Pulse-Echo mode).

$$c_l = \frac{2h}{t_l}$$

$$c_s = \frac{2h}{t_s}$$
(5-5)

where c_l and c_s are the longitudinal and shear wave velocities, and h is the thickness of the sample . Also t_l and t_s are travel time for longitudinal and shear wave respectively.

Lame's constants can be evaluated by the following equations:

$$G = c_s^2 \rho$$

$$\lambda = c_l^2 \rho - 2\mu$$
(5-6)

5.2.2 Results

In this section all the components of the fourth rank elastic stiffness tensor for two samples of Al-SiC composites are calculated and compared with experimental data. For this purpose both integrals in eq. (4-13) are calculated. The statistical results and the contribution of one-point and two-point statistical information for one of the samples are shown in Table 5.3.

Table 5.3 Nonzero terms of elastic stiffness tensor for Al-SiC (PSR: 2:1) to represent the contribution of one-point and two-point statistical information

Elastic Stiffness		Upper Bound	Statistics Result	One-Point	Two-Point	Lower Bound
C_{1111}	C_{11}	221.76	196.81	-16.19	8.76	136.70
C_{2222}	C_{22}	221.76	196.81	-16.19	8.76	136.70
C_{3333}	C_{33}	221.76	214.82	-16.19	-9.25	136.70
C_{1122}	C_{12}	149.56	101.05	19.16	0.94	64.5
C_{1133}	C_{13}	149.56	104.53	19.16	-2.54	64.5
C_{2233}	C_{23}	149.56	104.53	19.16	-2.54	64.5
C_{1212}	C_{44}	69.469	62.82	-2.73	3.90	35.29
C_{1313}	C_{66}	69.469	70.75	-2.73	-4.02	35.29
C_{2323}	C_{55}	69.469	70.75	-2.73	-4.02	35.29

It is observed that the contribution of the second integral is about 30 percent in the calculation of C_{iiii} and about 60 percent in the calculation of C_{ijij} . 1 and 3 indicate transverse and longitudinal (extrusion) directions. For example when i equals to 1, C_{iiii} refers to C_{1111} .

In the previous section, it was shown that I^2_{ijrs} is zero for isotropic composites however it is nonzero and needs to be evaluated by eq. (4-14) in anisotropic composites. As a numerical proof to show how this term is the contribution of two-point function, a numerical example is shown here:

If two different values of C^{upper} or $(C^{upper} + C^{lower})/2$ are used in the calculation of the second integral (I^2_{ijrs}), it is observed that the value of I^2_{ijrs} is calculated to be the same. In other words the calculation of I^2_{ijrs} doesn't depend on the average value of elastic properties. This shows that the second integral is completely the contribution of two-point statistics and shows the morphology of the microstructure, whereas the first integral is the contribution of one-point statistics.

Calculating the inverse of the elastic stiffness matrix calculated above, the elastic modulus and shear modulus in two directions will be calculated from the following matrix (Lai 1993):

$$\begin{bmatrix} \varepsilon_{11} \\ \varepsilon_{22} \\ \varepsilon_{33} \\ 2\varepsilon_{23} \\ 2\varepsilon_{13} \\ 2\varepsilon_{12} \end{bmatrix} = \begin{bmatrix} \frac{1}{E_1} & \frac{-\nu_{21}}{E_1} & \frac{-\nu_{31}}{E_3} & 0 & 0 & 0 \\ \frac{-\nu_{21}}{E_1} & \frac{1}{E_1} & \frac{-\nu_{31}}{E_3} & 0 & 0 & 0 \\ \frac{-\nu_{31}}{E_1} & \frac{-\nu_{31}}{E_1} & \frac{1}{E_3} & 0 & 0 & 0 \\ 0 & 0 & 0 & \frac{1}{G_{13}} & 0 & 0 \\ 0 & 0 & 0 & 0 & \frac{1}{G_{13}} & 0 \\ 0 & 0 & 0 & 0 & 0 & \frac{1}{G_{12}} \end{bmatrix} \begin{bmatrix} \sigma_{11} \\ \sigma_{22} \\ \sigma_{33} \\ 2\sigma_{23} \\ 2\sigma_{13} \\ 2\sigma_{12} \end{bmatrix} \quad (5-7)$$

Inverting the elastic stiffness tensor and comparing to the above tensor, engineering elastic coefficients (E and G) in different planes can be estimated. The calculated values of transverse shear modulus (G_{12}) and the corresponding measured values by Ultra sounds are shown in Table 5.4. In addition Hashin-Shtrikman upper and lower bounds

Table 5.4 Measured and calculated values of transverse elastic shear modulus (G_{12}) for two samples of Al-SiC composite

Transverse Shear Modulus	Voigt	Upper HS	Statistics	SC	Lower HS	Reuss	Ultra Sounds
PSR= 2:1	69.46	41.71	62.82	40.79	39.17	35.5	41.3
PSR= 8:1	72.43	43.94	65.52	42.29	40.92	36.18	37.00

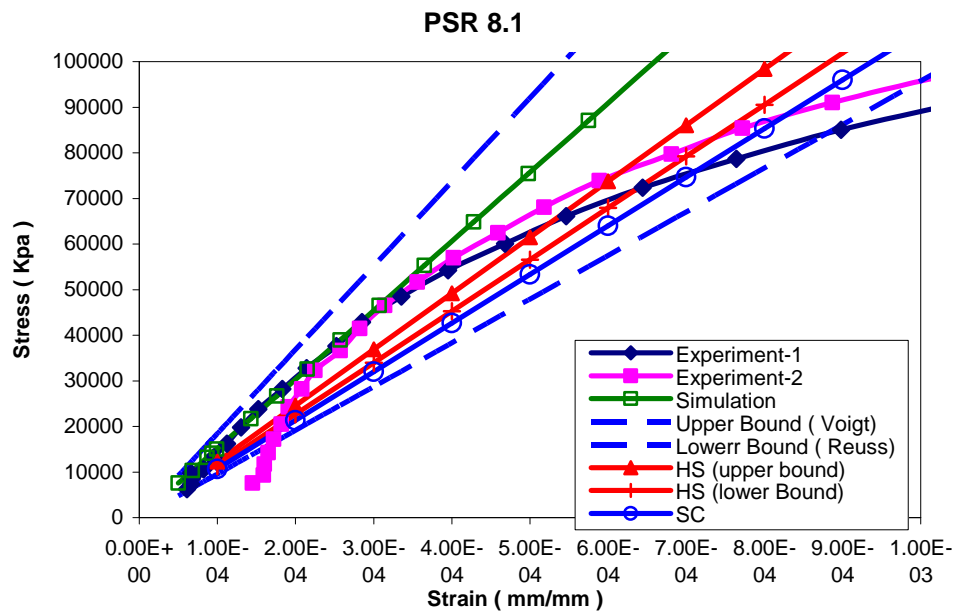
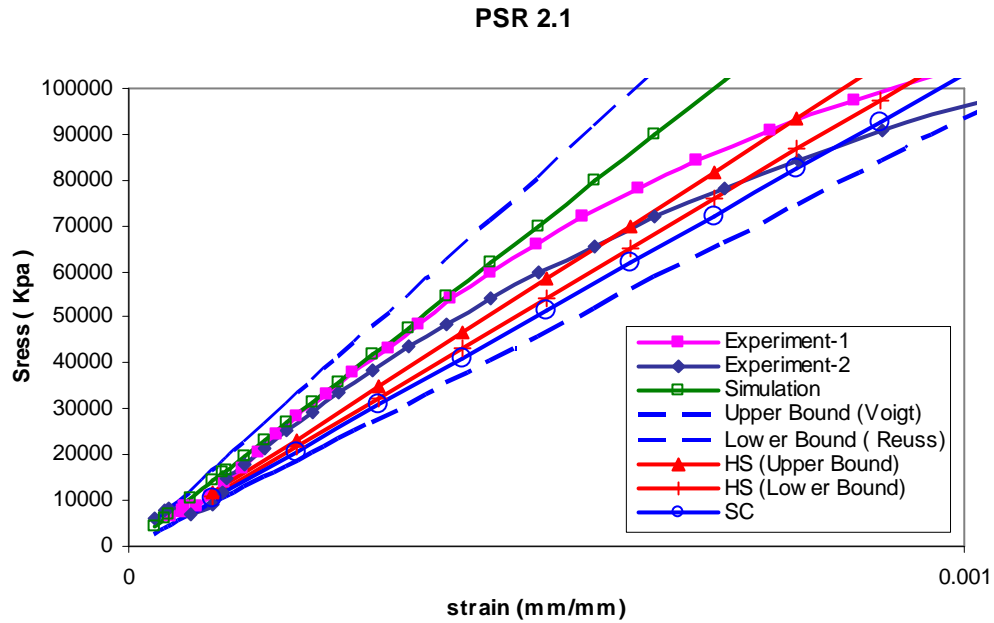


Figure 5.15 Comparing the slope of the elastic region of stress-strain curves with the simulation results and other bounds

(Hashin-Shtrikman, 1962), Voigt and Reuss bounds, and Self-consistent approximation are shown for comparison. The results show that the measured value for shear modulus by ultra sounds has a about 30% error with respect to the statistical calculation. The reason is that the ultra sound measures the elastic properties of the materials including the porosity, whereas in statistical calculation the porosity has not been taken care of in the simulation. Therefore, mechanical testing will be a better tool to verify the statistical mechanics methodology.

Using the simulated values of the longitudinal elastic modulus, the linear behavior of the stress-strain curve in elastic region is shown in Figure 5.15. The stress-strain curves obtained through mechanical testing have been enlarged in elastic region and have been shown in the graphs. In addition, upper bound (Voigt, 1889) and lower bound (Reuss, 1929), Hashin-Shtrikman upper and lower bound, and Self-Consistent approximation are calculated and shown in the Figure for comparison to the simulation and experimental results. It is observed that the linear elastic modulus calculated from the statistical simulation results is the best slope for the experimental stress-strain curves in elastic region. The error is estimated to be between 0.07% and 20%, where 20% error relates to the points that have the largest deviation from experimental data in elastic region. As it is observed from the graph, the other bounds do not provide good approximations for the elastic behavior of the microstructures.

The elastic moduli in two different directions (longitudinal and transverse) are plotted for two samples in Figure 5.16. The micrograph shows that clustering in the sample with PSR 8:1 introduces more anisotropy in the elastic modulus than the other sample. This verifies with the results of the simulation in Figure 5.15. The volume

fraction of the second phase (SiC) in two microstructures with 2:1 and 8:1 PSR is estimated to be 31% and 33% respectively. Although the volume fractions are very close, two-point statistics modeling shows a different degree of anisotropy (about 15% in the two samples). The upper Hashin-Shtrikman bounds for two samples are also shown in this figure and the results show that this bound is not able to distinguish the anisotropy in the system. The upper bounds for both samples show an identical slope. Therefore it can be concluded that the two-point statistics contributes in the calculation of the elastic properties for anisotropic media, whereas it doesn't contribute in the case of isotropic composites.

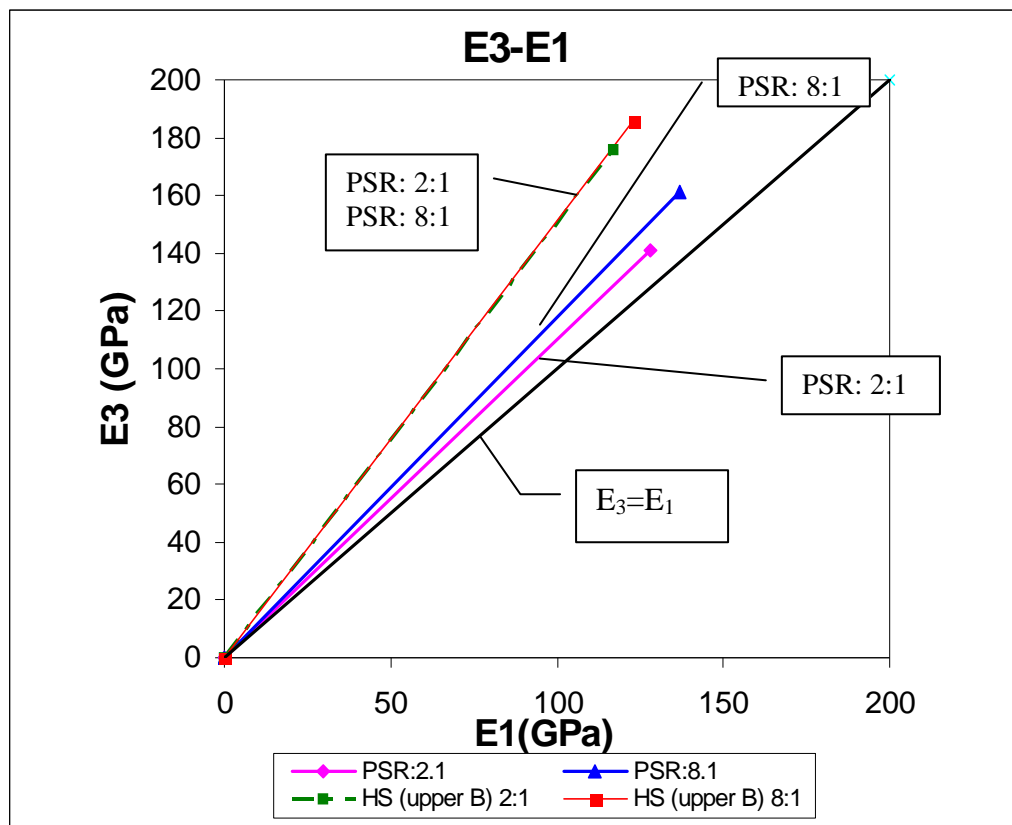


Figure 5.16 Comparison of longitudinal elastic modulus (E_3) vs transverse elastic modulus (E_1) for two samples of Al-SiC composite

CHAPTER 6

HOMOGENIZATION RELATIONS IN POLYCRYSTALLINE MATERIALS

Elastic homogenization relations based on two-point statistics have been applied to two-phase composites in previous chapters. It was shown analytically and numerically that two-point statistics doesn't contribute in the evaluation of elastic properties of isotropic composites. However it has a considerable effect in the case of anisotropy.

In the extension of the research on composite materials, applying statistical continuum mechanics modeling as a homogenization technique, the effect of two-point statistics on elastic properties calculation will be studied in random and textured polycrystalline materials in this section. For this purpose, first a brief review of statistical measurements in polycrystalline materials will be provided and then the methodology will be applied to random and textured polycrystalline materials. A random and textured polycrystalline Al alloy will be digitally constructed in the computer and the effect of one-point and two-point functions will be investigated in detail. Then the effect of rolling on elastic properties of near- α Ti-alloy will be investigated and the contribution of two-point statistics will be studied. These simulations will be compared with experimental results to validate the proposed homogenization technique.

6.1 Statistical Mechanics Modeling for Polycrystalline Microstructures

As it was stated in third chapter, the probability functions can be defined for any state variables in the microstructure such as phase, composition, or lattice orientation. In the case of polycrystalline materials the one-point, two-point and higher order probabilities can be defined for orientations of different crystals. The orientations of polycrystalline materials are conventionally shown by ODF (Orientation Distribution Functions), however in this work the correlation between all the orientations will be considered to be included in the homogenization relationship for elastic properties of polycrystalline materials. Orientation Coherence Function (OCF) which has been introduced by Adams et. al. (1987) and used by Garmestani et. Al. (1998) is the basis to include the spatial orientations of crystals in the computational simulations (Adams et al., 1988, 1990). OCF is the probability density of crystalline orientation g_i at point i and orientation g_j at point j . In other words, OCF represents the correlation between every two grains which are connected to each other by a vector. Therefore two-point OCF requires 9 independent parameters to represent the correlations, where 6 of them are orientational and 3 of them are positional. This was shown in Figure 4.2.

The orientation of crystal lattices can be measured by Backscattered Diffraction (EBSD) which is a technique that measures crystallographic information of the microstructure in Scanning Electron Microscope (SEM).

In this technique a stationary electron strikes a tilted sample and then a pattern will be formed on the fluorescent screen. This pattern can be used to measure crystals orientations, mis-orientations and also texture. The information such as locations, orientations, image quality and confidence index can be stored in a file to visualize the

microstructure. This file including all of this information is called OIM or Orientation Imaging Microscopy. This was first used by Adams and Wright (1993).

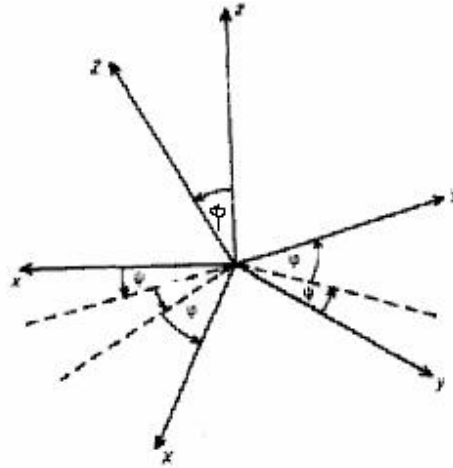


Figure 6.1 Representation of Euler's angles

In the mathematical representation, the orientation of each crystal which is called g can be shown by Euler's angles $(\varphi_1, \Phi, \varphi_2)$, where φ_1 , and φ_2 are rotation with respect to the z-axis and Φ is the rotation with respect to the x-axis of the crystal (Figure 6.2). Euler has proved that each orientation in the 3-dimensional space can be converted to another orientation by 3 single rotations $(\varphi_1, \Phi, \varphi_2)$ about x axis, z axis and x axis respectively. Furthermore, the position of each crystal called p can be shown by 3 variables (r, θ, ϕ) in spherical coordinates. Therefore the specification of each grain can be shown by 6 independent parameters (3 rotations and 3 positions). By having this

information, the arrangement of crystals will be known very accurately and the one-point and two-point statistics can be measured.

When the properties of the reference crystal having the same orientation as the sample coordinates is formulated, the properties of other crystals can be calculated by the following relationship (Morris, 1970 and Bunge, 1982):

$$c'_{i_1 i_2 \mathbf{k} i_n} = a_{i_1 j_1} a_{i_2 j_2} \mathbf{K} a_{i_n j_n} c_{j_1 j_2 \mathbf{k} j_n}, \quad (6-1)$$

where the matrix $[a_{ij}]$ is the transformation matrix for the coordinate $x'y'z'$ of an arbitrary point in the crystal system $K_B = \{X'Y'Z'\}$ expressed by means of the coordinates xyz in the sample coordinate system $K_A = \{XYZ\}$.

Recall the probability for polycrystalline and note that here; the orientation of each crystal is a state variable whereas in composites the state variables are different phases. Several sections with different θ are considered for the measurement of the probabilities. In each section the probabilities are measured for different r and ϕ . Therefore having the statistical information from the microstructure and the elastic properties of each crystal the homogenization technique that was explained in earlier chapters correlates the microstructure to the properties. In the next two sections this methodology will be applied to simulated and real crystalline microstructures.

6.2 Aluminum Alloy Polycrystalline Microstructures

To expand the homogenization technique based on two-point probabilities to polycrystalline materials, a digital microstructure will be simulated for a polycrystalline material in a spherical coordinates and the two-point correlation functions will be

measured in this framework. Recall eq. (3-31) in chapter (3) which was derived to calculate the elastic properties of composites based on two-point statistical information:

$$C_{ijkl} = \langle c_{ijkl} \rangle + \langle \tilde{c}_{ijmn}(x) a_{mnkl}(x) \rangle,$$

where the correlation term can be calculated by the following two integrals(eq. (4-13)):

$$\langle \tilde{c}_{ijku}(x) a_{ku}(x) \rangle = \int_{V'} \partial [K_{kpu} \langle \tilde{c}_{ijku}(x) \tilde{c}_{plrs}(x') \rangle] / \partial x'_l dX' - \int_{V'} K_{kpul}(x, x') \langle \tilde{c}_{ijku}(x) \tilde{c}_{plrs}(x') \rangle dX'$$

In above equation $\langle c_{ijkl} \rangle$ can be obtained using Taylor bound. Two-point probabilities have been defined in the last section for polycrystalline microstructures. Therefore the two integrals can be estimated and the effective stiffness will be calculated. For this purpose the digital sphere is divided into $n_r \times n_\theta \times n_\phi$ crystals to display the simulated polycrystalline microstructure. A random distribution of orientations will be assigned to each crystal and the collection of all orientations will be saved in a file. The elastic properties of a single crystal (Al alloy) with cubic symmetry are assumed to be known and shown by C_{11} , C_{12} , and C_{22} . Having the orientations of each crystal, the elastic constants can be estimated by eq. (6-1) for each grain. Then applying Taylor approximation the average elastic properties is calculated. Therefore deviation in strain and stress tensor, also in elastic modulus and compliance, is assumed to be in each crystal with different orientation comparing to the Taylor average.

Similar to composites, the same method was applied to the polycrystalline microstructure and the stiffness tensor is evaluated. Since the microstructure is assumed to have axial symmetry about Z axis, therefore the measurement of two-point statistics needs to be performed on one section which includes the axis of symmetry (axis z). As a result, 9 independent constants are expected to be calculated. Then this simulation was

extended to textured polycrystalline materials by assigning a specified orientation for a large number of crystals. In this case $\langle 0\ 0\ 1 \rangle$ are assumed to be the texture direction, and the results are shown in Figures 6.2 to Figures 6.4.

In these graphs the degree of texture varies from 0 which refers to a random orientation to 100% which is a completely textured polycrystalline Aluminum. The polycrystalline microstructure includes 120 grains, where some of them have the $\langle 0\ 0\ 1 \rangle$ orientations for the cases of textured microstructures. For example in Figure 6.2, 20%, 40%,...,and 90% means 20%, 40%,..., and 90% of the grains have the same orientations as $\langle 0\ 0\ 1 \rangle$.

As it is observed from the graphs, the upper and lower bounds are very close when the polycrystalline microstructure gets closer to a single crystal (completely textured polycrystalline) and the bounds are apart when the microstructure is completely random.

In Table 6.1, the values of some of the non-zero components of the elastic stiffness matrix for the random and 90% textured microstructures are shown to illustrate the contribution of the one-point and the two-point statistics in the calculation of elastic properties. As it is observed for a random microstructure, the effect of two-point statistics in the calculation of elastic stiffness is very small and varies between 0.04% and 5%. This is in agreement with the results from last chapters where it was stated that the contribution of two-point statistics is negligible in calculating the isotropic microstructure's elastic properties. However the contribution from two-point statistics in textured microstructures is between 20% and 50%. Therefore the statistical microstructural information has a significant contribution in the estimation of elastic properties of textured polycrystalline materials.

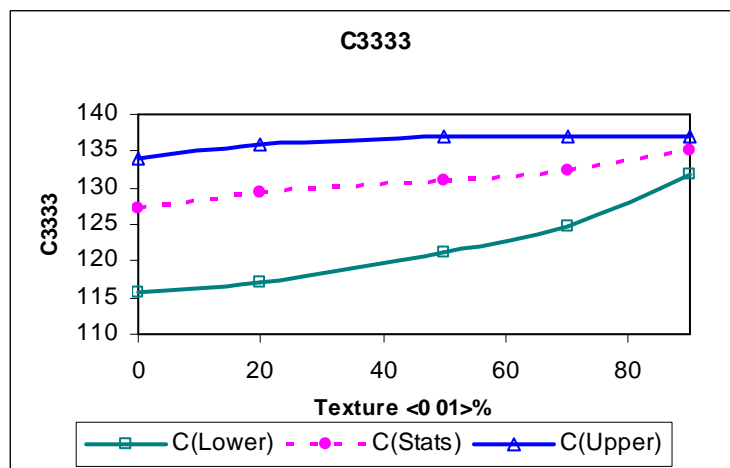
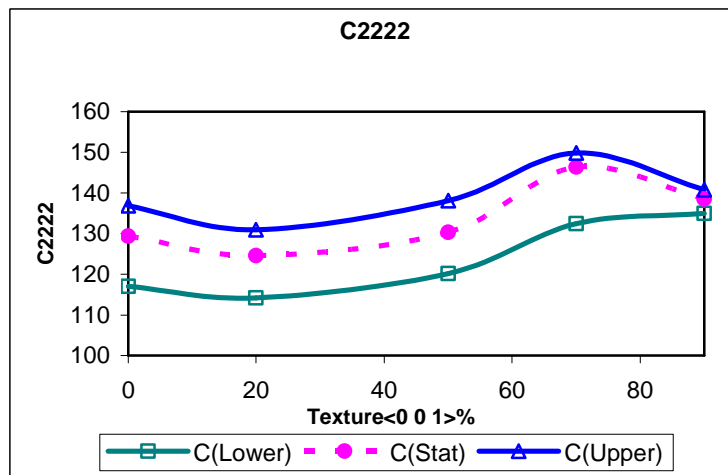
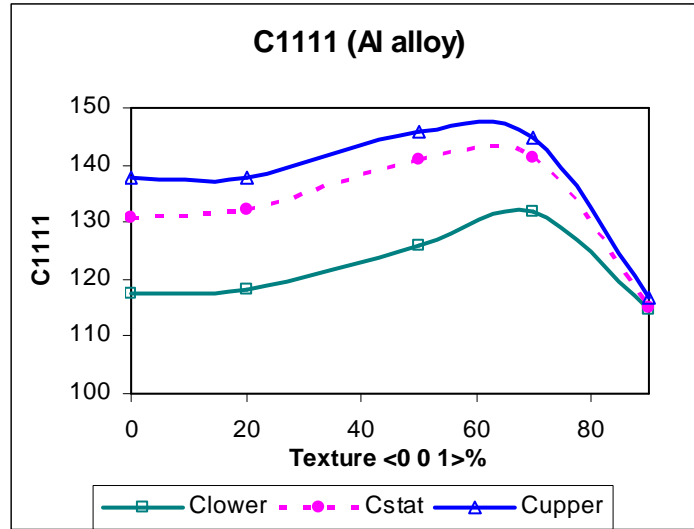


Figure 6.2 Elastic stiffness of Al polycrystalline microstructures in (123) directions for different percentages of texture in $\langle 001 \rangle$ direction

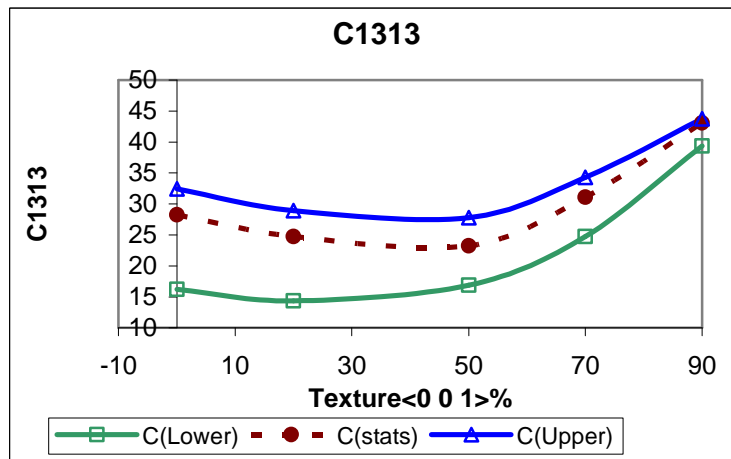
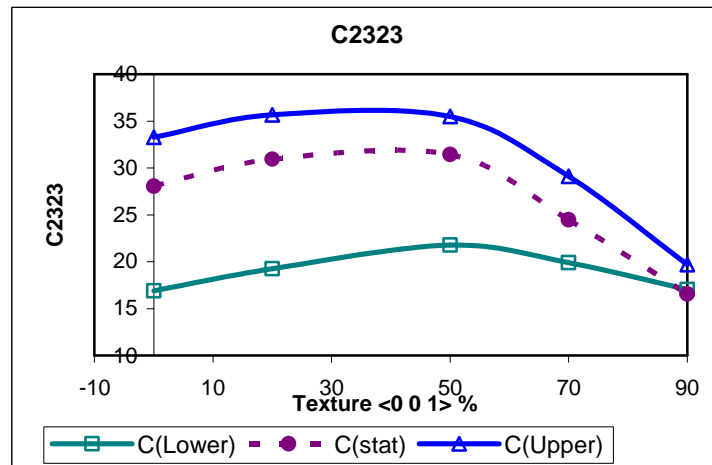
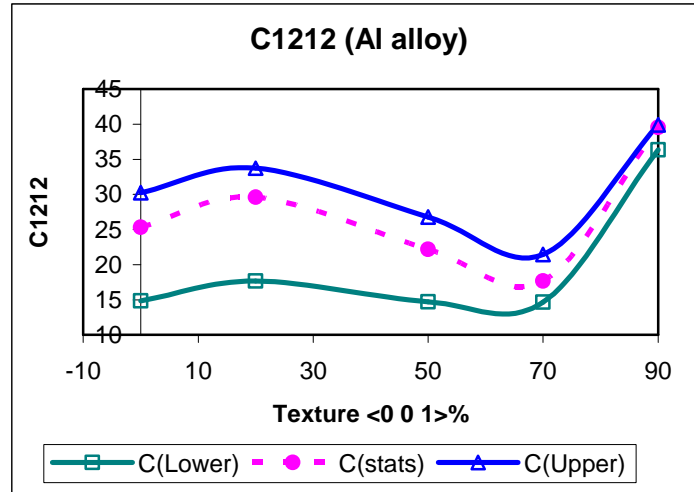


Figure 6.3 Elastic shear stiffness of Al Polycrystalline microstructures for different degree of texture in <0 0 1> direction

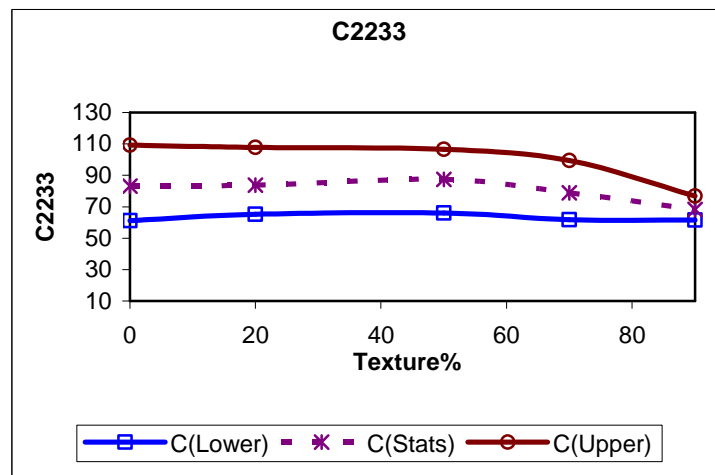
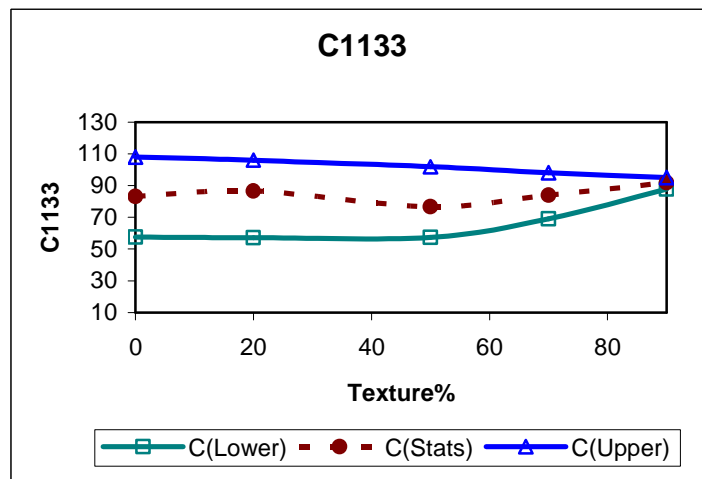
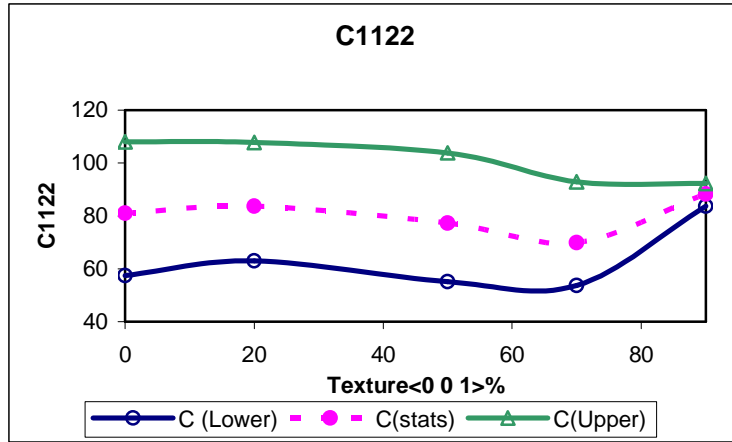


Figure 6.4 Elastic shear stiffness of Al Polycrystalline microstructures for different degree of texture in <0 0 1> direction

Table 6.1 Comparison of contribution of one-point and two-point statistics in elastic stiffness calculation for different samples of simulated polycrystalline Aluminum with different textures

Microstructure		Taylor Bound	Statistical Simulation	One-point	Two-Point	Lower Bound
	C ₁₁₁₁	137.73	130.77	-6.96	-0.0029	117.59
Random	C ₁₁₂₂	108.04	81.08	3.38	-0.16	57.54
	C ₁₂₁₂	30.23	25.32	-5.20	-0.29	14.85
	C ₁₁₁₁	116.74	115.03	-1.45	0.26	114.60
90% Textured	C ₁₁₂₂	92.24	88.23	0.69	-0.33	83.66
	C ₁₂₁₂	39.90	39.35	-0.68	-0.14	36.37

6.3 Near- α Titanium Polycrystalline Microstructures

This method has been applied to near- α Ti alloy in this section. The as-received sample of Ti-1100 (commercial CP-Ti) has the following composition:

Ti + 6% Al + 2.7% Sn + 4% Zr + 0.4% Mo + 0.45% Si

These samples are 5/8" thick plate which were hot rolled and annealed at 600°C for 1 hour. The samples with 3*4*5/8 (inch) were cut from the plate. Then they were cold-rolled with 20% 60%, 80%, and 95% reduction. The samples were additionally

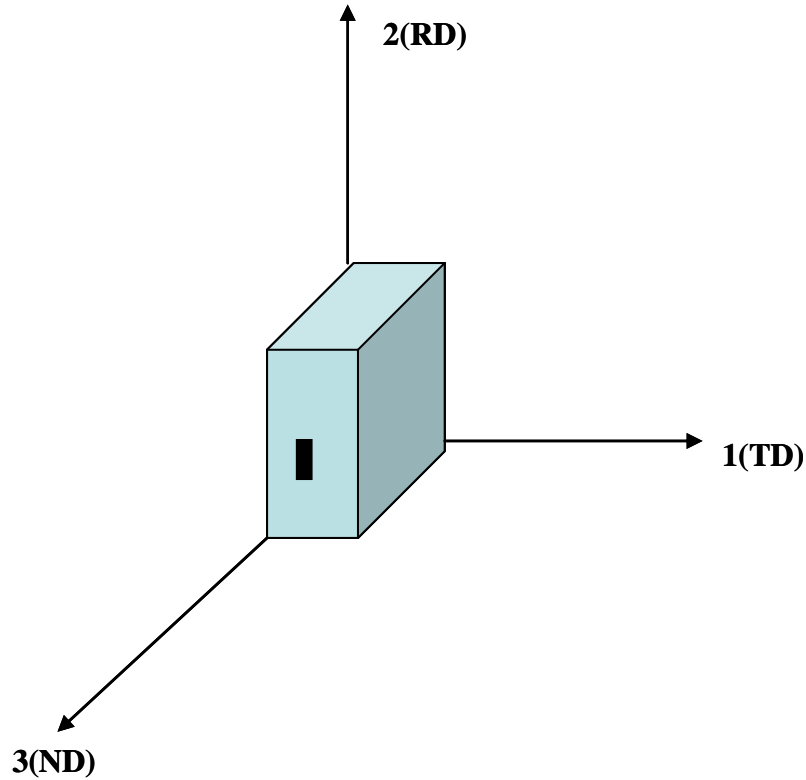
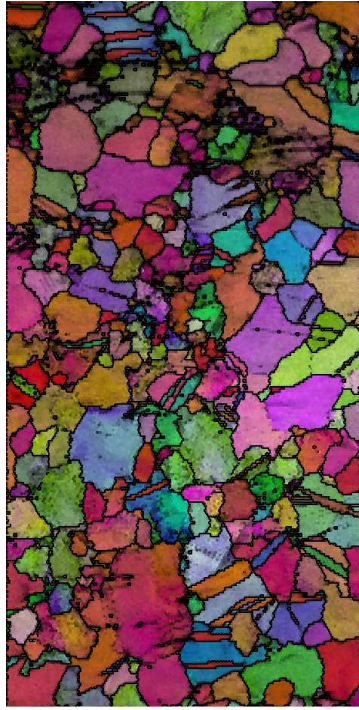


Figure 6.5 Representation of the cross section of the microstructure to measure OIM and two-point statistics

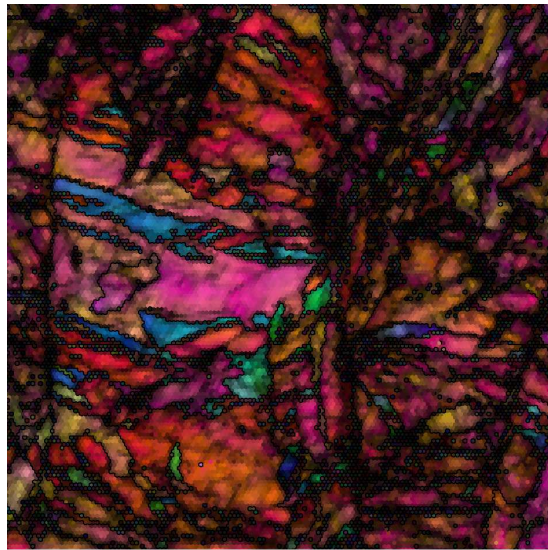
submitted to a conventional duplex annealing (900°C for 30min / 785°C for 15min). In order to evaluate the texture gradient throughout the thickness after the thermo-mechanical processing, each specimen was ground and polished removing 5%, 15%, 30% and 50% from its thickness. The as-received samples and 60% cold rolled samples have been selected here to study.

A perpendicular section to the normal direction (Figure 6.5) has been considered to obtain metallographic information of the microstructure. The information about the



60.00 μm = 30 steps

(a) As received Cp-Ti (CI=0.883; IQ=94)



15.00 μm = 30 steps Boundary levels: 15°
IQ 5.347...107.471, IPF [001]

(a) 60% cold rolled Cp-Ti (CI=0.3; IQ=40)

Figure 6.6 Microstructures of Cp-Ti and their OIM representations

microstructure has been obtained with using OIM. Then the simulation codes written for the simulated polycrystals have been extended to read the data from the OIM file that includes the information about the spatial distribution of the crystals and convert them to two-point statistical information. For this purpose, the microstructure is assumed to be a cube where the microstructural information of the transverse plane (as shown in Figure 6.5) is known. On the other hand, it is assumed that this plane is repeated in every section parallel to transverse plane. The micrographs of two samples are shown in Figure 6.6. Both microstructures show a random distribution of orientations. This micrograph is assumed to be repeated in all the planes perpendicular to ND.

Therefore, in this case also, by applying the homogenization relations, the effect of two-point statistics on the evaluation of the properties has been studied. Note that in previous works by Adams (1999) on polycrystalline materials, the FCC crystal symmetry was assumed, whereas in Ti-1100 alloy the crystal symmetry considered is HCP. The sample symmetry is assumed to be orthorhombic.

The pole figures for the two samples are shown in Figure 6.7. There appears to exist a large component of $\langle 0\ 0\ 1 \rangle$ about 5 degrees to the normal direction (ND) tilted towards transverse direction.

The elastic stiffness matrix has been calculated for both cases. The results for 60% cold rolled sample are shown in table 6.2. The reference crystal has been considered to have anisotropy in direction 3, ($C_{3333} > C_{1111}$) whereas the pole figures show some anisotropy in ND. Therefore the properties in the normal direction (direction 3) are larger than the other direction, since the distribution in transverse plane is assumed to

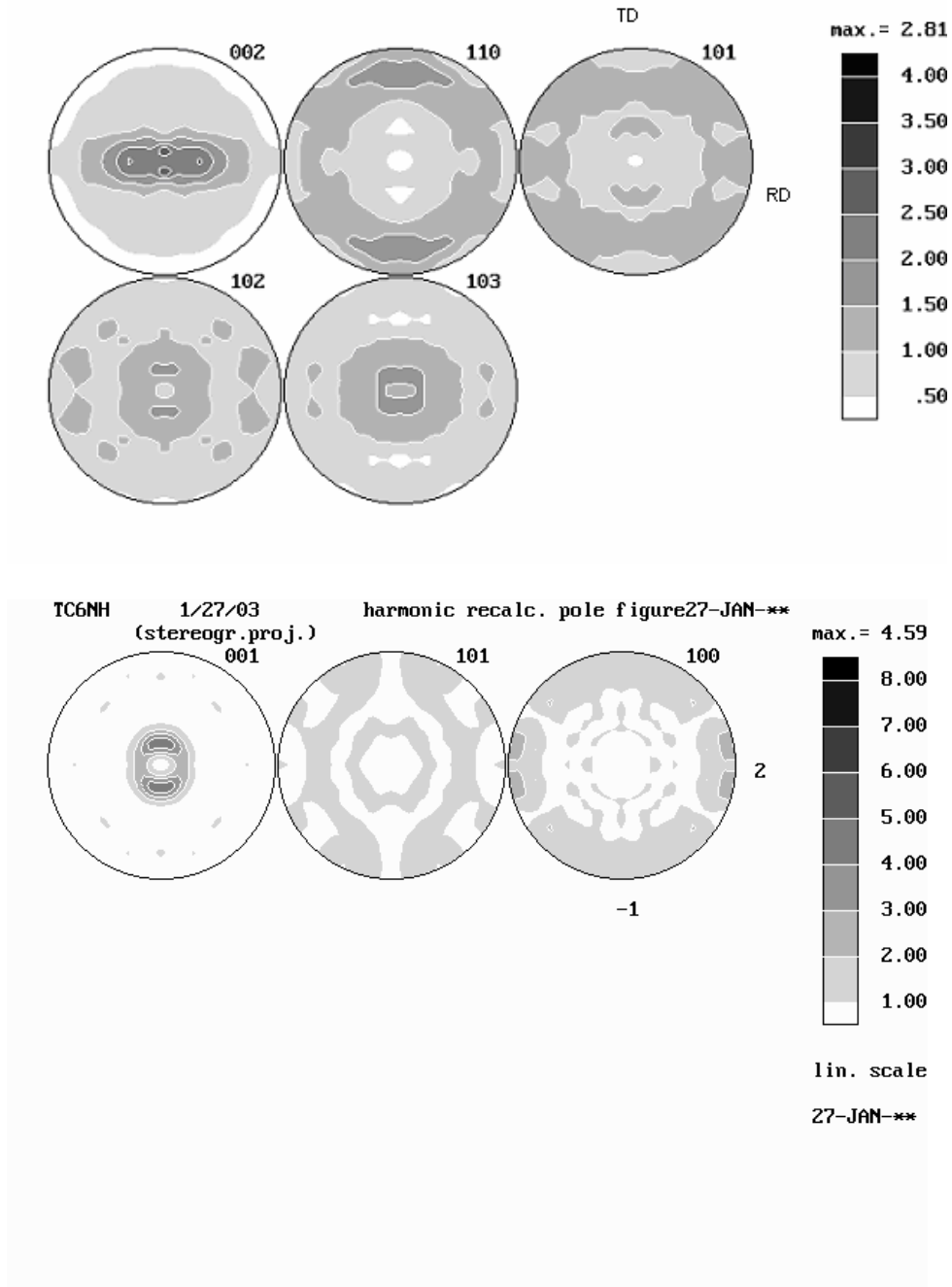


Figure 6.7 Pole figures for two samples of Cp-Ti (As received and 60% cold rolled)

be repeated along axis 3. In addition, since the sample has been rolled in direction 2, it is expected to contain anisotropy in that direction. However, as it was mentioned

earlier, the reference crystal is assumed to be anisotropic in normal direction and in the other hand the pole figures show texture in ND therefore theses

Table 6.2 Elastic stiffness tensor calculated for 60% cold rolled Cp-Ti samples

Stiffness	Taylor Bound	Statistics	One-Point	Two-Point	Lower Bound
$C_{1111}(\text{TD})$	162.655	162.044	-0.645	-0.035	161.337
$C_{2222}(\text{RD})$	165.756	165.282	-0.490	-0.016	164.685
$C_{3333}(\text{ND})$	171.468	170.89	-0.651	-0.0747	170.049
C_{1122}	85.293	83.976	0.153	-0.0212	82.613
C_{2233}	74.383	72.671	0.3520	0.0369	71.1234
C_{1133}	78.789	76.971	0.369	0.0504	75.284
C_{1212}	40.043	39.519	-0.342	0.1811	39.340
C_{2323}	47.921	47.678	-0.239	0.004	47.398
C_{1313}	43.445	43.255	-0.248	-0.057	42.876

assumptions and observations results in diminishing the effect of texture in rolling direction on the properties of the sample. There is no significant texture observed in rolling direction and this verifies the simulation results where there is not much anisotropy observed in the sample in transverse section (in RD) and as a result the contribution of two-point statistics is not significant. In other words the microstructure stays almost isotropic in transverse direction in spite of the applied rolling.

To verify the methodology with experimental results, the elastic modulus for the samples have also been measured by ultrasound techniques and shown in table 6.3. The measured values of elastic modulus and shear modulus by ultrasound are smaller than the predicted values by statistical formulation. The reason is that the porosity is not considered in the computations. On the other hand, since the samples don't have a significant porosity, the difference between the measured values and computational results is less than 15%. Therefore, the statistical estimations are in good agreement with experimental results.

Table 6.3 Elastic modulus of two samples in different directions- Statistical and Ultrasounds measurement

Sample	E_1 (transverse) (Statistics)	E_3 (Normal) (Statistics)	E_1 (transverse) (Ultrasounds)
Cp-Ti	107.53	112.36	90.78
Ti 60% cold rolled	107.53	113.64	91.2

It has been shown in this section that the statistical continuum mechanics modeling is a good tool to correlate the morphology of polycrystalline microstructures to their properties for both cubic and hexagonal crystal. This methodology is applicable in random and textured polycrystalline materials and can be used for inverse structure-properties in future research.

Table 6.4 Elastic shear modulus of two samples of Titanium in transverse plane- Statistical and Ultrasounds measurement

Sample	G (Transverse) (Statistics)	G (Transverse) (Ultrasounds)
Ti-Cp	39.063	30.3
Ti 60% cold rolled	39.52	29.7

It was also observed that rolling did not introduce a significant difference in elastic properties. This maybe due to the original microstructure is in rolled condition and further rolling did not have a significant influence in elastic properties.

CHAPTER 7

CONCLUSIONS AND RECOMMENDATIONS

7.1 Conclusions

In this work statistical mechanics theory is applied to composites and polycrystalline materials to extend the homogenization relations for anisotropic and textured microstructures. Statistical functions are used to represent the microstructure and used the statistical information from the microstructure to establish structure-properties relationships. For this purpose one-point is employed as a volume fraction and two-point statistics as higher order probability functions to represent the heterogeneity in the microstructure. Although there are some works previously done in this area, none of them considered the anisotropy in the microstructure specifically and the effect of two-point statistics was not observed. Therefore the homogenization relations have been extended to anisotropic composites and textured polycrystalline materials and studied the effect of one-point and two-point statistical information from the microstructure on their properties analytically and numerically.

To study the effect of one-point and two-point statistics, several samples of Al-Pb composite were generated in the computer which include isotropic microstructure and anisotropic microstructures with different morphology and measured probability functions. Corson's equation was utilized to fit the measured values and it was observed that the equation works very well for random distribution. The modified Corson's equation was though introduced to capture the anisotropy in the microstructure. That

enabled us to show how to represent anisotropy in the microstructure as an additional parameter for material design and microstructure optimizations.

The results have been compared with some micromechanics models and experimental data. Although there are several micromechanics models to predict the elastic properties, all of them need to have some assumptions for the features of the microstructure. However using two-point statistics enables us to be free of any assumptions. In addition, one of the advantages of statistical mechanics modeling is the use of the homogenization relations to predict the microstructure from the properties for reverse structure-properties problems. This issue has got a lot of attention recently.

It has been shown that the contribution of two-point statistics is very significant in the calculation of elastic properties of anisotropic composites and textured polycrystalline microstructures, though that is negligible in isotropic and random distribution. This was the reason that in previous works by Adams (1995) and Garmestani (2000) the effect of two-point statistics was not observed explicitly in the computations. The composite microstructures were simulated in the computer and it was concluded that structure-property relations are in good agreement with micromechanics models for smaller values of volume fractions of the second phase. Though, the difference becomes larger for higher values of volume fractions. In addition, applying the methodology to samples of Al-SiC, it was observed that two-point statistics information is able to capture the effect of clustering in the microstructure although other micromechanics are not so.

The simulated data and micromechanical results have been compared with experimental data from stress-strain curve in elastic region and the statistical data was the closest value for elastic moduli compared to other micromechanics models. This shows

that statistical functions are good tools to represent the microstructures and are able to capture the morphology of the microstructures.

This methodology was also applied to computer-generated random and textured polycrystalline microstructure, and it was observed that the contribution of two-point statistics for textured polycrystalline microstructures is significant compared to one-point statistics. However in general, the contribution of one-point and two-point statistics is much smaller in textured polycrystalline microstructures than anisotropic composites. The reason is that when the polycrystalline microstructure has a high percentage of texture, it gets closer to single crystal and the upper and lower bounds get closer, therefore statistical information doesn't play a significant role. Finally in this work, the effect of rolling was presented for near- α Titanium and it was observed that not much additional texture was introduced as a result of 60% cold rolling and the elastic properties didn't changes in the results.

7.2 Contributions

These are some of the contributions of this research to computational materials scientific community:

- Extending the homogenization relations for elastic properties of materials based on two-point statistics to anisotropic distribution

- Introducing a new formulation for two-point probability functions in anisotropic composites and defining a new design parameter for materials optimization
- Analytical derivation of one-point and two-point statistics contributions in the calculation of elastic properties of isotropic and anisotropic composites and random and polycrystalline microstructures
- Application of homogenization relations to polycrystalline microstructures with different textures to observe the effect of texture on statistical estimation
- Application of homogenization relations to HCP polycrystalline structures and observe the differences with composites

7.3 Future Works

Here are some works that can be done in extension of this research:

- Application of homogenization relations based on two-point statistics for porous materials
- Extending the homogenization relations based on two-point statistics for plastic deformations

- Using the homogenization relations to solve the reverse problem (predicting microstructure from properties) , MSD (microstructure Sensitive Design)
- Considering three-point probabilities in derivation of homogenization relations and observe its contribution for different types of distribution , isotropic and anisotropic composites and random and textured polycrystalline materials

APPENDIX

A.1 Green's Function Definition

Green's function for the case of isotropic materials is defined by the closed form equation as in the following (Zarka 1986):

$$G_{kp}(x, x') = 1/(8\bar{\mu}\pi|r_{12}|) \left\{ 2\delta_{kp} - \frac{\bar{\lambda} + \bar{\mu}}{\bar{\lambda} + 2\bar{\mu}} \left(\delta_{kp} - \frac{r_{12k}r_{12p}}{|r_{12}|^2} \right) \right\}, \quad (\text{A-1})$$

where $\bar{\lambda}$ and $\bar{\mu}$ are the average values of Lamé's Constants in the composite.

But in the case of orthotropy and texture, there is no closed form, and it can be written in the following numerical form (Bacon, 1979):

$$G_{ij}(x - x') = \frac{1}{8\pi^2|x - x'|} \oint_{|z|=1} (zz)_{ij}^{-1} ds, \quad (\text{A-2})$$

where:

$$(zz)_{ij} = C_{kij}z_kz_l \quad (\text{A-3})$$

$$z_j = \cos \theta T_j + \sin \theta M_j, \quad (\text{A-4})$$

T is the unit vector in the direction of the line connecting two position x and x'. The general expression for the nth derivative of the Green's function is given in the following formulations (Bacon, 1979):

$$G_{ij, s_1 \dots s_n} = (x - x') = \frac{(-1)^N T_{k_1} \dots T_{k_N}}{8\pi^2|x - x'|^{N+1}} \times \oint_{|z|=1} \frac{\partial^N [(zz)_{ij}^{-1} z_{s_1} \dots z_{s_N}]}{\partial Z_{k_1} \dots \partial Z_{k_N}} ds \quad (\text{A-5})$$

$$G_{ij,s}(x-x') = \frac{1}{8\pi^2|x-x'|^2} \times \oint_{|z|=1} \left[T_s (zz)_{ij}^{-1} - z_s F_{ij} \right] ds \quad (\text{A-6})$$

$$G_{ij,sr}(x-x') = \frac{1}{8\pi^2|x-x'|^3} \times \oint \left[2T_s T_r (zz)_{ij}^{-1} - 2(z_s T_r + z_r T_s) F_{ij} + z_s z_r E_{ij} \right] ds \quad (\text{A-7})$$

where:

$$F_{ij} = (zz)_{im}^{-1} (zz)_{kj}^{-1} \left[(zT)_{mk} + (Tz)_{mk} \right] \quad (\text{A-8})$$

$$E_{ij} = \left[(zT)_{mk} + (Tz)_{mk} \right] \left[F_{im} (zz)_{kj}^{-1} + (zz)_{im}^{-1} F_{kj} \right] - 2 (zz)_{im}^{-1} (zz)_{kj}^{-1} (TT)_{mk} \quad (\text{A-9})$$

The resulting integral is a line integral around the circle defined by the tip of the unit vector M for φ on the interval $(0, 2\pi)$.

A.2 First and the Second Derivatives of Green's function

As it was mentioned in last section the Green's function for isotropic composites has a closed form and the first derivative and second derivative can be derived directly:

$$G_{kp,i}(x,x') = 1/(8\bar{\mu}\pi) \left\{ \frac{(K-2)r_{12i}\delta_{kp} + K(r_{12p}\delta_{ki} + r_{12k}\delta_{pi})}{|r_{12}|^3} - 3K \frac{r_{12k}r_{12p}r_{12i}}{|r_{12}|^5} \right\}, \quad (\text{A-10})$$

where

$$K = \frac{\bar{\lambda} + \bar{\mu}}{\bar{\lambda} + 2\bar{\mu}} \quad (\text{A-11})$$

$$\begin{aligned}
G_{kp,ij}(x, x') = & 1/(8\bar{\mu}\pi) \left[\frac{(K-2)\delta_{kp}\delta_{ij} + K(\delta_{pj}\delta_{ki} + \delta_{pi}\delta_{kj})}{|r_{12}|^3} \right. \\
& + \frac{(6-3K)r_{12i}r_{12j}\delta_{kp} - 3K(r_{12p}r_{12j}\delta_{ki} + r_{12k}r_{12j}\delta_{pi}) - 3K(r_{12p}r_{12k}\delta_{ij} + r_{12i}r_{12p}\delta_{kj} + r_{12i}r_{12k}\delta_{pj})}{|r_{12}|^5} \\
& \left. + \frac{15Kr_{12i}r_{12j}r_{12k}r_{12p}}{|r_{12}|^7} \right]
\end{aligned}
\tag{A-12}$$

A.3 Empirical Coefficients in Corson's Equation

It has been proved (Gokhale, 2004) that the scaling parameter “n” is equal to 1 in Corson's equation. Here, the proof is reviewed.

In quantitative analysis of the microstructures, the test lines are thrown in the microstructure to measure some morphological

Suppose P_L is the average number of intersections between all the test lines and boundaries per unit length of test lines and is shown in the following form:

$$P_L = \frac{\text{Number of intersections with boundaries}}{\text{Total length of test lines}} = \lim_{r \rightarrow 0} \left\{ \frac{N[P_{12}(r, \varphi) + P_{21}(r, \varphi)]}{N_r} \right\},
\tag{A-13}$$

where N is the total number of the vectors and N_r is the total length of the test lines.

When r reaches a small values close to zero, the test lines intersect the boundaries of the features (crystals, particles...) not more than once. Therefore the following equation will satisfy:

$$\lim_{r \rightarrow 0} \{P_{12}(r, \varphi)/r\} = P_L/2
\tag{A-14}$$

In the other hand, the probabilities can be measured by Corson's equation which can be written in Taylor series expansion as follows:

$$P_{12} = v_1 v_2 - v_1 v_2 \exp(-c_{12} r^{n_{12}}) = v_1 v_2 (1 - \exp(-c r^n))$$

$$\begin{aligned} P_{12}/r &= \left[v_1 v_2 \left(1 - \left(1 - \left(1 - c r^n + c^2 r^{2n}/2! - c^3 r^{3n}/3! + \dots \right) \right) \right) \right] / r \\ &= v_1 v_2 \left(c r^{n-1} + c^2 r^{2n-1}/2! - c^3 r^{3n-1}/3! + \dots \right) \end{aligned} \quad (\text{A-15})$$

Comparing eq. (A-14) and (A-15) results in:

$$n = 1 \quad (\text{A-16})$$

A.4 Implementation of the Homogenizations Relations in C++ Programming

As it was mentioned in chapter 4, several programs have been implemented to employ the homogenization relations for calculating elastic properties. The program that is shown here is written for general case of anisotropic distributions. The input data are two-point probabilities for Al-SiC composite or any other microstructure and also the properties of each phase. The output is the 4th rank tensor of elastic constants. Green's function has been calculated in another program independently. It is assumed that the samples have axis of symmetry and the measurements for probabilities have been done on just one section. In addition, to apply the homogenization relations to polycrystalline microstructures, the first step was to generate the microstructure in computer with different orientations. First a random orientation is considered and then a percentage of the crystals are assumed to have a specific orientation. This percentage changes from 10% to 90% such that the microstructure shows completely random till almost a single

crystal microstructure. The Green's function and two-point probabilities are calculated in another program separately. Some of the corresponding programs are shown here:

```
#include <stdlib.h>
#include <math.h>
#include <stdio.h>

#define PI 3.141592654

void INDS(int case0);
void Integs_Kkilj();
void matrix(double leimina, double miu, double cc[3][3][3][3]); /*PRODUCING
MATRIX FOR STIFFNESS*/
void read_probabilitiesfile();
int del(int i,int j);

double Kisjr(int n0,int i0,int m0,int j0,double rs10,double rs20,double rs30);
double f(double teta,double phi,double r,int i0);
double g( double teta);
double h(double teta,double phi);

/*CASE 6 : Al, Sic */
Double
    lambda1=51.084,lambda2=152.60,miu1=26,miu2=165;

double

    p11[18][1000], p12[18][1000], p22[18][600],
    cp1[3][3][3][3], cp2[3][3][3][3],
    teta[251],phi[1081],r[1000],
    m11[10], m12[10], m21[10], m22[10],n11[10], n12[10], n21[10], n22[10],
    vol1,vol2, Kc[3][3][3][3],amiu,alambda,K;

int
    nteta=30; nphi=36*10,
    i_count/* the number of rs that have been read from p's file*/
    ind1, ind2, ind3, ind4, num,case0;

char    str[25];

FILE    *fp1,*fpcc1,*fpt;

////*TERM 1        Integral over surface */////
```

```

void Integs_Kkilj()
{
    int k0,i0,j0,l0;

    amiu=miu1*vol1+miu2*vol2;
    alambda=lambda1*vol1+lambda2*vol2;
    K=(alambda+amiu)/(alambda+2*amiu);

    /* Kc[2][2][2][2]=Integral(Kkpu dA^m) Integrated Anaytically in Spherical
    Coordinates on a small sphere around X-X'=0 (81-27= 54 terms)(27 terms has
    symmetry in Kkpu) */

    // These values are for the sphere surrounding r=0 , but the surface vector is
    outward, so in calculation they have to be multiplied by negative sign.
    for (k0=0;k0<=2;k0++)
        for (i0=0;i0<=2;i0++)
            for (l0=0;l0<=2;l0++)
                for (j0=0;j0<=2;j0++)
                    Kc[k0][i0][l0][j0]=0;

    Kc[0][1][0][1]= - ( 4/3 - 4*K/5 ) / (8*amiu);
    Kc[1][0][1][0]= - ( 4/3 - 4*K/5 ) / (8*amiu);
    Kc[0][2][0][2]= - ( 4/3 - 4*K/5 ) / (8*amiu);
    Kc[2][0][2][0]= - ( 4/3 - 4*K/5 ) / (8*amiu);
    Kc[1][2][1][2]= - ( 4/3 - 4*K/5 ) / (8*amiu);
    Kc[2][1][2][1]= - ( 4/3 - 4*K/5 ) / (8*amiu);

    Kc[0][1][1][0]= Kc[1][1][0][0]= ( 2*K/15+2/3 ) / (8*amiu);
    Kc[0][2][2][0]= Kc[2][2][0][0]= ( 2*K/15+2/3 ) / (8*amiu);
    Kc[1][2][2][1]= Kc[2][2][1][1]= ( 2*K/15+2/3 ) / (8*amiu);

    Kc[0][0][1][1]= Kc[1][0][0][1]= ( 2*K/15+2/3 ) / (8*amiu);
    Kc[0][0][2][2]= Kc[2][0][0][2]= ( 2*K/15+2/3 ) / (8*amiu);
    Kc[1][1][2][2]= Kc[2][1][1][2]= ( 2*K/15+2/3 ) / (8*amiu);

    Kc[0][0][0][0]= ( 16*K/15 ) / (8*amiu);
    Kc[1][1][1][1]= ( 16*K/15 ) / (8*amiu);
    Kc[2][2][2][2]= ( 16*K/15 ) / (8*amiu);
}

```

```

void main()
{
    double
        F[3][3][3][3][3][3][3][3], S_Integ[3][3][3][3], V_Integ[3][3][3][3],
        cc[3][3][3][3], cc1[3][3][3][3], ccu[3][3][3][3],
        cc2[3][3][3][3],ccb[3][3][3][3],cclo[3][3][3][3],del00,del11,del22,
        ttemp[3][3][3][3], term1,term2,term3,term4;
        p11_term1,p12_term1,p22_term1;

    int
        i,j,k,l, ii, jj, kk, ll, count=0, shomar;

    FILE *fpccul;

    /*reading volume fractions and probabilities */
    read_probabilitiesfile();

    for (i=0;i<=2;i++)
    for (j=0;j<=2;j++)
    for (k=0;k<=2;k++)
    for (l=0;l<=2;l++)
    {

        cc[i][j][k][l]=0;
        cc1[i][j][k][l]=0;
        cc2[i][j][k][l]=0;
        ccb[i][j][k][l]=0;cclo[i][j][k][l]=0;
        cp1[i][j][k][l]=0; cp2[i][j][k][l]=0;
        V_Integ[i][j][k][l]=0;

    }

    /*INPUT DATA: GREENS FUNCTION DATA
    EMPRICAL PARAMETERS
    MATERIAL PROPERTIES, VOLUME FRACTION FOR DIFFERENT
    PHASES

    THIS PROGRAM IS FOR TWO ISOTROPIC PHASES IN AN
    ANISOTROPIC COMPOSITE,

```

THE PROBABILITY DISTRIBUTION FUNCTIONS ARE CONSIDERED
ORIENTATION DEPENDENT AND GREENS FUNCTIONS ARE ALSO
CALCULATED IN THE SAME WAY.

*/

//////////INPUT DATA//////////

sprintf(str,"res2.1-%d-%d-AlSiC.dat",nteta,nphi);

fp1=fopen(str,"w");

if(fp1==NULL){printf("result.dat can't be opened to write.\n");

exit(1);}

fprintf(fp1,"nteta=%d nphi=%d\n",nteta,nphi);

fprintf(fp1,"indices Cupper C(statistical) S-integ1 V-integral Clower \n
\n");

matrix(lambda1, miu1, cc1);

matrix(lambda2, miu2, cc2);

Integs_Kkilj();

for(i=0;i<=2;i++)

for(j=0;j<=2;j++)

for(k=0;k<=2;k++)

for(l=0;l<=2;l++)

printf("%f\n",Kc[i][j][k][l]);

for(i=0;i<=2;i++)

for(j=0;j<=2;j++)

for(k=0;k<=2;k++)

for(l=0;l<=2;l++)

{

ccb[i][j][k][l]=vol1*cc1[i][j][k][l]+vol2*cc2[i][j][k][l];

ccu[i][j][k][l]=ccb[i][j][k][l];

if (ccb[i][j][k][l]==0)

cclo[i][j][k][l]=cc1[i][j][k][l]*cc2[i][j][k][l]/(vol1*cc2[i][j][k][l]+vol2*cc1[i][j][k][l]);

else cclo[i][j][k][l]=0.0;

}

del00=ccb[0][0][0][0]-cclo[0][0][0][0];

del11=ccb[1][1][1][1]-cclo[1][1][1][1];

del22=ccb[2][2][2][2]-cclo[2][2][2][2];

ccu[0][0][1][1]=cclo[0][0][1][1]+sqrt(del00*del11);

ccu[1][1][0][0]=ccu[0][0][1][1];

```
ccu[0][0][2][2]=cclo[0][0][2][2]+sqrt(del00*del22);
ccu[2][2][0][0]=ccu[0][0][2][2];
```

```
ccu[1][1][2][2]=cclo[1][1][2][2]+sqrt(del11*del22);
ccu[2][2][1][1]=ccu[1][1][2][2];
```

```
cclo[1][1][2][2]=ccb[1][1][2][2]-sqrt(del11*del22);
cclo[2][2][1][1]=cclo[1][1][2][2];
```

```
cclo[0][0][2][2]=ccb[0][0][2][2]-sqrt(del00*del22);
cclo[2][2][0][0]=cclo[0][0][2][2];
```

```
cclo[0][0][1][1]=ccb[0][0][1][1]-sqrt(del00*del11);
cclo[1][1][0][0]=cclo[0][0][1][1];
```

```
for(i=0;i<=2;i++)
for(j=0;j<=2;j++)
for(k=0;k<=2;k++)
for(l=0;l<=2;l++)
{
    cp1[i][j][k][l]=cc1[i][j][k][l]-ccb[i][j][k][l];
    cp2[i][j][k][l]=cc2[i][j][k][l]-ccb[i][j][k][l];
}
```

```
shomar=0;
```

```
/* Integration on the sphere volume*/
```

```
teta[0]=0;
for (i=0;i<=(nteta-1);i++) teta[i+1]=teta[i]+2*PI/nteta;
```

```
phi[0]=0;
for (i=0;i<=(nphi-1);i++) phi[i+1]=phi[i]+PI/nphi;
```

```
for (case0=0;case0<=8;case0++)
{
    INDS(case0);
    term1=g(teta[0]);
    term2=0;
    for (i=1;i<=(nteta-1);i=i+2)
    term2=term2+g(teta[i]);
    term3=0;
    for (i=2;i<=(nteta-2);i=i+2)
```

```

        term3=term3+g(teta[i]);
        term4=g(teta[nteta]);
        V_Integ[ind1][ind2][ind3][ind4]=(term1+4*term2+2*term3+term4)*(teta[
nteta]-teta[0])/(3*nteta);
    }

    p11_term1=vol1*vol1+vol1*vol2; //v1
    p12_term1=vol1*vol2-vol1*vol2;//0
    p22_term1=vol2*vol2+vol1*vol2;//v2

    for(i=0;i<=2;i++)
    for(j=0;j<=2;j++)
    for(k=0;k<=2;k++)
    for(l=0;l<=2;l++)
    {
        S_Integ[i][j][k][l]=0.0;
        for(ii=0;ii<=2;ii++)
        for(jj=0;jj<=2;jj++)
        for(kk=0;kk<=2;kk++)
        for(ll=0;ll<=2;ll++)
        {
            F[i][j][kk][ll][ii][jj][k][l]=
            cp1[i][j][kk][ll]*cp1[ii][jj][k][l]*p11_term1+
            cp1[i][j][kk][ll]*cp2[ii][jj][k][l]*p12_term1+
            cp2[i][j][kk][ll]*cp1[ii][jj][k][l]*p12_term1+
            cp2[i][j][kk][ll]*cp2[ii][jj][k][l]*p22_term1;
            ttemp[i][j][k][l]= F[i][j][kk][ll][ii][jj][k][l]*(-Kc[i][kk][jj][ll]);
            // The values that are calculated for Kc are the values over a sphere
            surroundind r=0 but the normal unit is outward
            S_Integ[i][j][k][l]=S_Integ[i][j][k][l]+ttemp[i][j][k][l];
        }
    }

    //////////////////////////////////////

    for(i=0;i<=2;i++)
    for(j=0;j<=2;j++)
    for(k=0;k<=2;k++)
    for(l=0;l<=2;l++)
    {
        cc[i][j][k][l]=ccb[i][j][k][l]+S_Integ[i][j][k][l]-V_Integ[i][j][k][l];
        fprintf(fp1, "%d %d %d %d %f %f %f %f %f\n",i+1,j+1,k+1,l+1,
        ccu[i][j][k][l],cc[i][j][k][l],
        S_Integ[i][j][k][l],V_Integ[i][j][k][l],cclo[i][j][k][l]);
    }

    fclose(fp1);

```

```

        return;
    } //main

double Kisjr(int n0,int i0,int m0,int j0,double rs10,double rs20,double rs30)
{
    double rr,term1,term2,term3,term4,term5,r12[3],value;

    r12[0]=rs10;
    r12[1]=rs20;
    r12[2]=rs30;
    rr=sqrt(pow(rs10,2)+pow(rs20,2)+pow(rs30,2));

    term1=15*K*r12[m0]*r12[i0]*r12[n0]*r12[j0]/pow(rr,7);
    term2=( -3*K*(
    r12[m0]*r12[i0]*del(n0,j0)+r12[n0]*r12[i0]*del(m0,j0)+r12[m0]*r12[n0]*del(i0,
    j0) ) -3*K*(r12[i0]*r12[j0]*del(n0,m0) ) )/pow(rr,5);

    term3= ( K*del(n0,m0)*del(i0,j0) )/pow(rr,3);
    term4=(K-1)*( del(n0,j0)*del(m0,i0)+del(n0,i0)*del(m0,j0)) /pow(rr,3);
    term5=(3-3*K)*( r12[m0]*r12[j0]*del(n0,i0)+ r12[n0]*r12[j0]*del(i0,m0) )
    /pow(rr,5);
    value=(term1+term2+term3+term4+term5)/(8*3.1415926*amiu);
    return value;
}

//SUBROTINES

void matrix(double leimina, double miu, double cc[3][3][3][3])
{
    int i,j,k,l;

    for(i=0;i<=2;i++)
    for(j=0;j<=2;j++)
    for(k=0;k<=2;k++)
    for(l=0;l<=2;l++)
    cc[i][j][k][l]=leimina*del(i,j)*del(k,l)+miu*del(i,k)*del(j,l)
    +miu*del(i,l)*del(j,k);
    return;
}

void read_probabilitiesfile()
{
    FILE *fp,*fpr,*fp1;
    int i0;

```



```

        (fabs(p11[9][i_count]-vol1*vol1)>=dif) ||
        (fabs(p11[10][i_count]-vol1*vol1)>=dif) ||
        (fabs(p11[11][i_count]-vol1*vol1)>=dif) ||
        (fabs(p11[12][i_count]-vol1*vol1)>=dif) ||
        (fabs(p11[13][i_count]-vol1*vol1)>=dif) ||
        (fabs(p11[14][i_count]-vol1*vol1)>=dif) ||
        (fabs(p11[15][i_count]-vol1*vol1)>=dif) ||
        (fabs(p11[16][i_count]-vol1*vol1)>=dif) ||
        (fabs(p11[17][i_count]-vol1*vol1)>=dif));

    fp1=fopen("filep.dat","w");
    for (num=0;num<=17;num++)
    for (i0=0;i0<=i_count;i0++)
    fprintf(fp1,"%lf %lf %lf\n ", p11[num][i0],p12[num][i0],p22[num][i0]);
    fclose(fp1);

    as=i_count%2;
    if (as==0) i_count=i_count;
    else i_count=i_count-1;
    fclose(fp);
    printf("i_count=%d\n",i_count);
}

int del(int i, int j)
{
    if(i==j)return 1;
    return 0;
}

double g(double teta)
{
    double gt,term1,term2,term3,term4;
    int i;

    term1=h(teta,phi[0]);
    term2=0;
    for (i=1;i<=(nphi-1);i=i+2) //+2
        term2=term2+h(teta,phi[i]);
    term3=0;
    for (i=2;i<=(nphi-2);i=i+2) //+2
        term3=term3+h(teta,phi[i]);
    term4=h(teta,phi[nphi]);

    gt=(term1+4*term2+2*term3+term4)*(phi[nphi]-phi[0])/(3*nphi);
}

```

```

    return gt;
}

double h(double teta,double phi)
{
    double htp,term1,term2,term3,term4;
    int i;

    if ( ( (phi >=0)      && (phi<( 5*PI/180)) ) || ( (phi >175*PI/180)  &&
    (phi<=(180*PI/180)) ) ) num=0;
    else if ( ( (phi >=( 5*PI/180)) && (phi<(10*PI/180)) ) || ( (phi >(170*PI/180))
    && (phi<=(175*PI/180)) ) ) num=1;
    else if ( ( (phi >=(10*PI/180)) && (phi<(15*PI/180)) ) || ( (phi >(165*PI/180))
    && (phi<=(170*PI/180)) ) ) num=2;
    else if ( ( (phi >=(15*PI/180)) && (phi<(20*PI/180)) ) || ( (phi >(160*PI/180))
    && (phi<=(165*PI/180)) ) ) num=3;
    else if ( ( (phi >=(20*PI/180)) && (phi<(25*PI/180)) ) || ( (phi >(155*PI/180))
    && (phi<=(160*PI/180)) ) ) num=4;
    else if ( ( (phi >=(25*PI/180)) && (phi<(30*PI/180)) ) || ( (phi >(150*PI/180))
    && (phi<=(155*PI/180)) ) ) num=5;
    else if ( ( (phi >=(30*PI/180)) && (phi<(35*PI/180)) ) || ( (phi >(145*PI/180))
    && (phi<=(150*PI/180)) ) ) num=6;
    else if ( ( (phi >=(35*PI/180)) && (phi<(40*PI/180)) ) || ( (phi >(140*PI/180))
    && (phi<=(145*PI/180)) ) ) num=7;
    else if ( ( (phi >=(40*PI/180)) && (phi<(45*PI/180)) ) || ( (phi >(135*PI/180))
    && (phi<=(140*PI/180)) ) ) num=8;
    else if ( ( (phi >=(45*PI/180)) && (phi<(50*PI/180)) ) || ( (phi >(130*PI/180))
    && (phi<=(135*PI/180)) ) ) num=9;
    else if ( ( (phi >=(50*PI/180)) && (phi<(55*PI/180)) ) || ( (phi >(125*PI/180))
    && (phi<=(130*PI/180)) ) ) num=10;
    else if ( ( (phi >=(55*PI/180)) && (phi<(60*PI/180)) ) || ( (phi >(120*PI/180))
    && (phi<=(125*PI/180)) ) ) num=11;
    else if ( ( (phi >=(60*PI/180)) && (phi<(65*PI/180)) ) || ( (phi >(115*PI/180))
    && (phi<=(120*PI/180)) ) ) num=12;
    else if ( ( (phi >=(65*PI/180)) && (phi<(70*PI/180)) ) || ( (phi >(110*PI/180))
    && (phi<=(115*PI/180)) ) ) num=13;
    else if ( ( (phi >=(70*PI/180)) && (phi<(75*PI/180)) ) || ( (phi >(105*PI/180))
    && (phi<=(110*PI/180)) ) ) num=14;
    else if ( ( (phi >=(75*PI/180)) && (phi<(80*PI/180)) ) || ( (phi >(100*PI/180))
    && (phi<=(105*PI/180)) ) ) num=15;
    else if ( ( (phi >=(80*PI/180)) && (phi<(85*PI/180)) ) || ( (phi >( 95*PI/180))
    && (phi<=(100*PI/180)) ) ) num=16;
    else num=17;

    test=0;
}

```

```

term1=f(teta,phi,r[0],0);

term2=0;
for (i=1;i<=(i_count-1);i=i+2) term2=term2+f(teta,phi,r[i],i);

term3=0;
for (i=2;i<=(i_count-2);i=i+2) term3=term3+f(teta,phi,r[i],i);

term4=f(teta,phi,r[i_count],i_count);

htp=(term1+4*term2+2*term3+term4)*(r[i_count]-r[0])/(3*i_count);

return htp;
}

```

```

double f(double teta,double phi,double r, int i0)
{
double func,Kvar,Fvar, T[3]={0,0,0},sum1, F[3][3][3][3][3][3][3];
int i,j,s,q;

T[0]=r*sint(phi)*cost(teta);

T[1]=r*sint(phi)*sint(teta);
T[2]=r*cost(phi);
sum1=0;

for (i=0;i<=2;i++)
for (s=0;s<=2;s++)
for(j=0;j<=2;j++)
for (q=0;q<=2;q++)
{
F[ind1][ind2][i][s][j][q][ind3][ind4]=
cp1[ind1][ind2][i][s]*cp1[j][q][ind3][ind4]*p11[num][i0]+
cp1[ind1][ind2][i][s]*cp2[j][q][ind3][ind4]*p12[num][i0]+
cp2[ind1][ind2][i][s]*cp1[j][q][ind3][ind4]*p12[num][i0]+
cp2[ind1][ind2][i][s]*cp2[j][q][ind3][ind4]*p22[num][i0];

Kvar=Kisjr(i,j,s,q,T[0],T[1],T[2]);
Fvar=F[ind1][ind2][i][s][j][q][ind3][ind4];
sum1=sum1+Kvar*Fvar;
} //i s j q

test=test+1;
func=sum1*pow(r,2)*sint(phi);
return func;
}

```

```
}
```

```
void INDS(int case0)
```

```
{  
    if (case0== 0) {ind1=0;ind2=0;ind3=0;ind4=0;}  
    else if (case0== 1) {ind1=1;ind2=1;ind3=1;ind4=1;}  
    else if (case0== 2) {ind1=2;ind2=2;ind3=2;ind4=2;}  
    else if (case0== 3) {ind1=0;ind2=1;ind3=0;ind4=1;}  
    else if (case0== 4) {ind1=1;ind2=2;ind3=1;ind4=2;}  
    else if (case0== 5) {ind1=0;ind2=2;ind3=0;ind4=2;}  
    else if (case0== 6) {ind1=1;ind2=1;ind3=2;ind4=2;}  
    else if (case0== 7) {ind1=0;ind2=0;ind3=2;ind4=2;}  
    else if (case0== 8) {ind1=0;ind2=0;ind3=1;ind4=1;};  
    return;  
}
```

```
*****  
/* This program is written to produce the polycrystalline microstructures with different  
textures (10% to 90%), and calculate the correlation terms for those microstructures*/
```

```
#include"firstinteg.h"  
#include"ghte.h"  
#include "vardef.h"  
#include"mathfunc.h"
```

```
//read greensfunction.dat  
// read orientation.dat
```

```
//THIS PROGRAM IS WRITTEN TO CALCULATE THE first integral in <c a>
```

```
////////////////////////////////////  
/*VARIABLES*/
```

```
float a[3][3],  
phi1[10000],phi2[10000],PHI[10000],*r,*r[10000],**teta[10000]/*teta,*phi;  
float fr,fteta,fphi,fphi1,fPHI,fphi2;  
float Rf,XtalVf[1000];  
float *p;  
float CTaylor[3][3][3][3],CC[1000][6][6],C1_INV[6][6],Ctotal_INV[6][6];  
int nr,gR_1,gR_2,gR_3,nteta1=10;
```

```

float F[3][3][3][3],CCt[6][6],C_L66[6][6];
////////////////////////////////////

void caseNcall(caseN0);

void main()
{
    int
        i0,j0,caseN,jpV,kpV,i,j,k,l,ip,jp,kp,lp,s,q,g1,g2,g,i_c,
        int shomar,ir,it,iph;
    double
        Clo[3][3][3][3],VC_term[3][3][3][3],Cup[3][3][3][3];
    char
        str[101],strr[102],str2[100];
    float
        SUM,varp,cR[3][3][3][3],CStat[3][3][3][3],S_Integ[3][3][3][3],
        term1,term2,term3,term4,GF,delteta1, del00,del11,del22, rr,phii;

    FILE
        *fpp,*ft,*fp2,*fp3,*ftaylor;

    //READING INPUT DATA
        ft=fopen("orientation.dat","r");
    if(ft==NULL){printf("orientations.dat can't be opened to be read.\n");
    exit(1);}
    fscanf(ft,"%s \n",str);
    fscanf(ft,"%d \n",&Ntotal);
    fscanf(ft,"%s\n",str);
    fscanf(ft,"%d\n",&Ototal);

    fpG=fopen("Greensfunctions.dat","r");
    if(fpG==NULL){printf("Greensfuncns.dat can't be opened to be read.\n");
    exit(1);}
    fscanf(fpG,"%s %s %s\n",str,str,str);

    fscanf(fpG,"%d %d %d\n",&nrr,&nteta_I,&nphi);
    for (i=0;i<=2;i++)
    for (s=0;s<=2;s++)
    for(j=0;j<=2;j++)

```

```

for (q=0;q<=2;q++)
    for (ir=0;ir<=(nrr);ir++)
        for (it=0;it<=(nteta_I);it++)
            for (iph=0;iph<=(nphi);iph++)
                {
                    fscanf(fpG,"%f",&GF);
                    Kisjr[i][j][s][q][it][iph][ir]=GF;
                }
fclose(fpG);

r=malloc((Ntotal+1)*sizeof(float));
teta=malloc((Ntotal+1)*sizeof(float));
phi=malloc((Ntotal+1)*sizeof(float));

for (g=1;g<=(Ototal-1);g++)      XtalVf[g]=1./(Ntotal);

XtalVf[Ototal]=(Ntotal-Ototal+1.)*1./(Ntotal);

delphi=PI/nphi;
delteta=(2*PI)/nteta_I;

// When we want to calculate S_integ. In that case we just need to calculate the
// surface integral on 1/8 of the sphere

for (ip=0;ip<=2;ip++)
    for (jp=0;jp<=2;jp++)
        for (kp=0;kp<=2;kp++)
            for (lp=0;lp<=2;lp++)
                {
                    CTaylor[ip][jp][kp][lp]=0;
                    cR[ip][jp][kp][lp]=0; /*Reference Crystal*/
                    Clo[ip][jp][kp][lp]=0;
                    VC_term[ip][jp][kp][lp]=0;
                }

//Aluminium Single Crystal Cubic
cR[0][0][0][0]=cR[1][1][1][1]=cR[2][2][2][2]=108.2;
cR[0][1][0][1]=cR[0][1][1][0]=cR[1][0][0][1]=cR[1][0][1][0]=46.1;
cR[0][2][0][2]=cR[0][2][2][0]=cR[2][0][0][2]=cR[2][0][2][0]=46.1;
cR[1][2][1][2]=cR[1][2][2][1]=cR[2][1][1][2]=cR[2][1][2][1]=46.1;

cR[0][0][1][1]=cR[1][1][0][0]=cR[0][0][2][2]=cR[2][2][0][0]=cR[1][1][2][2]=cR
[2][2][1][1]=93.4;

fscanf(ft,"%s %s %s %s %s\n",str,str,str,str,str);

```

```

for (i=0;i<=Ntotal-1;i++)
{
    fscanf(ft,"%d %f %f %f %f %f
    %f\n",&g,r+i,teta+i,phi+i,phi1+i,PHI+i,phi2+i);
    printf("%d %d %f %f %f %f %f
    %f\n",i,g,r[i],teta[i],phi[i],phi1[i],PHI[i],phi2[i]);
}

fclose(ft);

p=malloc((Ototal+1)*(Ototal+1)*sizeof(float));

SUM=0;
shomar=0;
for (i=1;i<=(Ototal);i++)
    for (j=1;j<=(Ototal);j++)
    {
        if (i==j) {
            p[i*Ototal+j]=XtalVf[i]; //XtalVf[i]=XtalVf[j]
            shomar=shomar+1;
            SUM=SUM+p[i*Ototal+j];
        }
        else p[i*Ototal+j]=0;
    }

c=malloc((Ototal+1)*81*sizeof(float));
cp=malloc((Ototal+1)*81*sizeof(float));

for (ip=0;ip<=2;ip++)
    for (jp=0;jp<=2;jp++)
        for (kp=0;kp<=2;kp++)
            for (lp=0;lp<=2;lp++)
                for (g=1;g<=Ototal;g++)
    {
        i_c=(27*(Ototal))*ip+(9*(Ototal))*jp+(3*(Ototal))*kp+((Ototal))*lp+g;
        c[i_c]=0;
    }

for (ip=0;ip<=2;ip++)
    for (jp=0;jp<=2;jp++)
        for (kp=0;kp<=2;kp++)
            for (lp=0;lp<=2;lp++)
    {

```

```

for (g=1;g<=(Ototal);g++)
{
    XtalRotMatrix(phi1[g]*PI/180,PHI[g]*PI/180,phi2[g]*PI/180);
    //CALCULATING THE COMPONENT OF ROTATION
    MATRIX

    i_c=(27*(Ototal))*ip+(9*(Ototal))*jp+(3*(Ototal))*kp+(Ototal)*lp
    +g;
    c[i_c]=0;
    for (i=0;i<=2;i++)
    for (j=0;j<=2;j++)
    for (k=0;k<=2;k++)
    for (l=0;l<=2;l++)
    //THE STIFFNESS OF EACH CRYSTALL BY CONSIDERING
    IT'S ORIENTATION
    {

        c[i_c]=c[i_c]+a[ip][i]*a[jp][j]*a[kp][k]*a[lp][l]*cR[i][j][k]
        [l];
        //CALCULATING TAYLOR BY ASSIGNING EQUAL
        WEIGHT FOR EACH XTAL

    }

    IJ_Value(ip,jp,kp,lp);
    CC[g][I][J]=c[i_c];

    CTaylor[ip][jp][kp][lp]=CTaylor[ip][jp][kp][lp]+c[i_c]*XtalVf[g];
    }

}

ftaylor=fopen("CTaylor.dat","w");
if(ftaylor==NULL){printf("CTaylor.dat can't be opened to to write.\n");
exit(1);}
for (ip=0;ip<=2;ip++)
for (jp=0;jp<=2;jp++)
for (kp=0;kp<=2;kp++)
for (lp=0;lp<=2;lp++)
fprintf(ftaylor,"%d%d%d%d %f\n",ip,jp,kp,lp,CTaylor[ip][jp][kp][lp]);

fclose(ftaylor);

for (i0=0;i0<=5;i0++)
for (j0=0;j0<=5;j0++)
    Ctotal_INV[i0][j0]=0;

```

```

for (g=1;g<=Ototal;g++)
{
    for (i0=0;i0<=5;i0++)
        for (j0=0;j0<=5;j0++)            CCt[i0][j0]=CC[g][i0][j0];

    Inverse_FUNC(CCt,C1_INV); //inverse of C for each crystal
    for (i0=0;i0<=5;i0++)
        for (j0=0;j0<=5;j0++)
            Ctotal_INV[i0][j0]=Ctotal_INV[i0][j0]+XtalVf[g]*C1_INV[i0][j0];
}
Inverse_FUNC(Ctotal_INV,C_L66);

for (I=0; I<=5;I++)
for (J=0; J<=5;J++)
{
    ijk1_Value(I,J);
    Clo[I1][J1][K1][L1]=C_L66[I][J];
    Clo[J1][I1][K1][L1]=Clo[I1][J1][K1][L1];
    Clo[J1][I1][L1][K1]=Clo[I1][J1][K1][L1];
    Clo[I1][J1][K1][L1]=Clo[I1][J1][K1][L1];
}

//Calculating Upper and Lower BDS (DEGRADED BOUNDS)

for (i=0;i<=2;i++)
for (j=0;j<=2;j++)
for (k=0;k<=2;k++)
for (l=0;l<=2;l++)
Cup[i][j][k][l]=CTaylor[i][j][k][l];

del00=CTaylor[0][0][0][0]-Clo[0][0][0][0];
del11=CTaylor[1][1][1][1]-Clo[1][1][1][1];
del22=CTaylor[2][2][2][2]-Clo[2][2][2][2];

Cup[0][0][1][1]=Clo[0][0][1][1]+sqrt(del00*del11);
Cup[1][1][0][0]=Cup[0][0][1][1];

Cup[0][0][2][2]=Clo[0][0][2][2]+sqrt(del00*del22);
Cup[2][2][0][0]=Cup[0][0][2][2];

Cup[1][1][2][2]=Clo[1][1][2][2]+sqrt(del11*del22);
Cup[2][2][1][1]=Cup[1][1][2][2];

```

```

Clo[1][1][2][2]=CTaylor[1][1][2][2]-sqrt(del11*del22);
Clo[2][2][1][1]=CTaylor[1][1][2][2];

Clo[0][0][2][2]=CTaylor[0][0][2][2]-sqrt(del00*del22);
Clo[2][2][0][0]=CTaylor[0][0][2][2];

Clo[0][0][1][1]=CTaylor[0][0][1][1]-sqrt(del00*del11);
Clo[1][1][0][0]=Clo[0][0][1][1];

for(ip=0;ip<=2;ip++)
for (jp=0;jp<=2;jp++)
for (kp=0;kp<=2;kp++)
for (lp=0;lp<=2;lp++)
for (g=1;g<=Ototal;g++)
{
    i_c=(27*(Ototal))*ip+(9*(Ototal))*jp+(3*(Ototal))*kp+((Ototal))*lp+g;
    cp[i_c]=c[i_c]-CTaylor[ip][jp][kp][lp];
    printf("C=%f CTaylor=%f
    Cp=%f\n",c[i_c],CTaylor[ip][jp][kp][lp],cp[i_c]);
}

free(r);
free(teta);
free(phi);
/*****
/* Integration on the sphere volume*/
rr_I=malloc((nrr+1)*sizeof(float));
teta_I=malloc((nteta_I+1)*sizeof(float));
teta1_I=malloc((nteta1+1)*sizeof(float));
phi_I=malloc((nphi+1)*sizeof(float));

delteta1=2*PI/nteta1;

Rf=20; //we ahve to read it from the 2pgenerate program
delrr=Rf/nrr;

teta_I[0]=0;
for (i=0;i<=(nteta_I-1);i++)
{
    teta_I[i+1]=teta_I[i]+delteta;
}
teta1_I[0]=0;
for (i=0;i<=(nteta1-1);i++) teta1_I[i+1]=teta1_I[i]+delteta1;

```

```

phi_I[0]=0;
for (i=0;i<=(nphi-1);i++) phi_I[i+1]=phi_I[i]+delphi;

rr_I[0]=0.03;
for (i=0;i<=(nrr-1);i++) {rr_I[i+1]=rr_I[i]+delrr;

for (jpV=0;jpV<=18;jpV++)
  for (kpV=0;kpV<=40;kpV++)
    for (g1=1;g1<=Ototal;g1++)
      for (g2=1;g2<=Ototal;g2++)
        pV[jpV][kpV][g1][g2]=0;

//READING PROBABILITIS FUNCTUINS
phii=0;
for (jpV=0;jpV<=18;jpV++)//phii loop
{
  rr=0.05;
  for (kpV=0;kpV<=40;kpV++)//rr loop
  {
    sprintf(strr,"prob-%3.1f-%3.2f",phii,rr);
    printf("%s\n",strr);
    if( (fpp = fopen(strr, "r" ) ) == NULL )
    { exit( 1 ); printf("%s couldnt be opened\n",strr);}

    for (i=0;i<=4;i++) fscanf(fpp,"%s \n",str2);
    /* Cycle until end of file reached: */
    while( !feof( fpp ) )
    {
      fscanf(fpp,"%d %d %f",&g1,&g2,&varp);
      pV[jpV][kpV][g1][g2]=varp;
      printf("%f\n",pV[jpV][kpV][g1][g2]);
    }
    fclose(fpp);
    rr=rr+0.2;
  }// rr loop
  phii=phii+10;
} //phii loop

fp3=fopen("Results.dat","w");
if(fp3==NULL){printf("Results.dat can't be opened to write.\n");
exit(1);}

```

```

fprintf(fp3," ijkl cTaylor      cstat      S-integ  CLower  \n");

for (caseN=1;caseN<=8;caseN++)
{
    caseNcall(caseN);
    for (i=0;i<=2;i++)
    for (s=0;s<=2;s++)
    for(j=0;j<=2;j++)
    for (q=0;q<=2;q++)
    {
        F[i][s][j][q]=0;
        for (g1=1;g1<=(Ototal);g1++)
        for ( g2=1;g2<=(Ototal);g2++)

            F[i][s][j][q]=F[i][s][j][q]+cp[(27*(Ototal))*ind1+(9*(Ototal))*ind
            2+(3*(Ototal))*i+((Ototal))*s+g1]*cp[(27*(Ototal))*j+(9*(Ototal)
            )*q+(3*(Ototal))*ind3+((Ototal))*ind4+g2]*p[g1*((Ototal))+g2];

    }

    term1=g_I(teta_I[0]);
    term2=0;
    for (i=1;i<=((nteta_I-1)-2);i=i+2)
        term2=term2+g_I(teta_I[i]);
    term3=0;
    for (i=2;i<=((nteta_I-1)-1);i=i+2)
        term3=term3+g_I(teta_I[i]);
    term4=g_I(teta_I[nteta_I-1]);

    S_Integ[ind1][ind2][ind3][ind4]=(term1+4*term2+2*term3+term4)*(teta_
    I[nteta_I]-teta_I[0])/(3*nteta_I);

    Calculate_secondInteg();

    CStat[ind1][ind2][ind3][ind4]=CTaylor[ind1][ind2][ind3][ind4]+S_Integ[i
    nd1][ind2][ind3][ind4]-V_Integ[ind1][ind2][ind3][ind4];

    fprintf(fp3, "%d%d%d%d  %f  %f  %f  %f
    %f\n",ind1,ind2,ind3,ind4,Cup[ind1][ind2][ind3][ind4],CStat[ind1][ind2][
    ind3][ind4],S_Integ[ind1][ind2][ind3][ind4],V_Integ[ind1][ind2][ind3][in
    d4],Clo[ind1][ind2][ind3][ind4]);
}

fclose(fp3);
free(teta_I);

```

```

    free(phi_I);
    free(rr_I);

    free(p);
    free(c);
    free(cp);
}

void XtalRotMatrix(float phi1, float PHI,float phi2)
{
    a[0][0]=cos(phi1)*cos(phi2)-sin(phi1)*sin(phi2)*cos(PHI);
    a[0][1]=sin(phi1)*cos(phi2)+cos(phi1)*sin(phi2)*cos(PHI);
    a[0][2]=sin(phi2)*sin(PHI);
    a[1][0]=-cos(phi1)*sin(phi2)-sin(phi1)*cos(phi2)*cos(PHI);
    a[1][1]=-sin(phi1)*sin(phi2)+cos(phi1)*cos(phi2)*cos(PHI);
    a[1][2]=cos(phi2)*sin(PHI);
    a[2][0]=sin(phi1)*sin(PHI);
    a[2][1]=-cos(phi1)*sin(PHI);
    a[2][2]=cos(PHI);
}

float Kijs(int i_n,int j_n,int s_n,float teta,float phi)
{
    float value,term1,term2,term3,term4;
    int i;
    term1=Integrand(i_n,j_n,s_n,teta,phi,teta1_I[0]);
    term2=0;
    for (i=1;i<=(nteta1-1);i=i+2)
        term2=term2+Integrand(i_n,j_n,s_n,teta,phi,teta1_I[i]);

    term3=0;
    for (i=2;i<=(nteta1-2);i=i+2)
        term3=term3+Integrand(i_n,j_n,s_n,teta,phi,teta1_I[i]);

    term4=Integrand(i_n,j_n,s_n,teta,phi,teta1_I[nteta1]);
    value=(term1+4*term2+2*term3+term4)*(teta1_I[nteta1]-teta1_I[0])/(3*nteta1);
    return value;
}

```

```

float Integrand(int i_n,int j_n,int s_n,float teta, float phi, float teta1)
{
    float value,numi,domin;

    z[3]={0,0,0},zz1[3][3]={0,0,0,0,0,0,0,0,0},T[3]={0,0,0},zz[3][3]={0,0,0,0,0,0,0,0,0,0},
    Tz[3][3]={0,0,0,0,0,0,0,0,0},zT[3][3]={0,0,0,0,0,0,0,0,0},TT[3][3]={0,0,0,0,0,0,0,0,0},
    FF[3][3]={0,0,0,0,0,0,0,0,0},
    E[3][3]={0,0,0,0,0,0,0,0,0};
    int s0,r0,i0,j0,m0,w0,k0,l,k;

    T[0]=sint(phi)*cost(teta);//unit vector  rr0*sint(phi)*cost(teta)/rr0
    T[1]=sint(phi)*sint(teta);
    T[2]=cost(phi);

    z[0]=sint(teta)*cost(teta1)-cost(phi)*cost(teta)*sint(teta1);
    z[1]=-cost(teta)*cost(teta1)-sint(teta)*cost(phi)*sint(teta1);
    z[2]=sint(phi)*sint(teta1);
    //Calculation of zz[3][3]
    for(s0=0;s0<=2;s0++)
    for(r0=0;r0<=2;r0++)
    {
        zz[s0][r0]=0;
        for (l=0;l<=2;l++)
        for (k=0;k<=2;k++)
            zz[s0][r0]=zz[s0][r0]+CTaylor[k][s0][r0][l]*z[k]*z[l];
    }
    //calculation of zz1[3][3]

    for(i0=0;i0<=2;i0++)
    for (j0=0;j0<=2;j0++)//(j0=0;j0<=2;j0++)
    {
        numi=0.0;
        domin=0.0;
        for (s0=0;s0<=2;s0++)
        for (m0=0;m0<=2;m0++)
        for (w0=0;w0<=2;w0++)
        for (r0=0;r0<=2;r0++)
            numi=numi+e(i0,s0,m0)*e(j0,r0,w0)*zz[s0][r0]*zz[m0][w0];

        for (s0=0;s0<=2;s0++)
        for (m0=0;m0<=2;m0++)
        for (w0=0;w0<=2;w0++)
            domin=domin+2*e(s0,m0,w0)*zz[0][s0]*zz[1][m0]*zz[2][w0];
        zz1[i0][j0]=numi/domin; /*z-1*/
    }

    // Calculation of zT[2][2],Tz[2][2],TT[3][3] to evaluate FF

```

```

for (m0=0;m0<=2;m0++)
for (k0=0;k0<=2;k0++)
{
    zT[m0][k0]=0;
    Tz[m0][k0]=0;
    TT[m0][k0]=0;
    for (i0=0;i0<=2;i0++)
    for (j0=0;j0<=2;j0++)
    {
        zT[m0][k0]=zT[m0][k0]+z[i0]*CTaylor[i0][m0][j0][k0]*T[j0];
        Tz[m0][k0]=Tz[m0][k0]+T[i0]*CTaylor[i0][m0][j0][k0]*z[j0];

        TT[m0][k0]=TT[m0][k0]+T[i0]*CTaylor[i0][m0][j0][k0]*T[j0];
        //sum on i,j
    }
}
//Evaluation of FF[3][3]

for (i0=0;i0<=2;i0++)
for (j0=0;j0<=2;j0++)
{
    FF[i0][j0]=0;
    for (m0=0;m0<=2;m0++)
    for (k0=0;k0<=2;k0++)

        FF[i0][j0]=FF[i0][j0]+zz1[i0][m0]*zz1[k0][j0]*(zT[m0][k0]+Tz[m0][k0])
}

//Evaluation of E[3][3]

for (i0=0;i0<=2;i0++)
for (j0=0;j0<=2;j0++)
{
    E[i0][j0]=0;
    for (m0=0;m0<=2;m0++)
    for (k0=0;k0<=2;k0++)
        E[i0][j0]=E[i0][j0]+( zT[m0][k0]+Tz[m0][k0] )*(
        FF[i0][m0]*zz1[k0][j0]+zz1[i0][m0]*FF[k0][j0] )-
        2*zz1[i0][m0]*zz1[k0][j0]*TT[m0][k0];//sum on m,k
}
value=1/(2*8*PI*PI/*pow(rr0,2)*/)*( T[s_n]*zz1[i_n][j_n]-(z[s_n]*FF[i_n][j_n])
    +T[i_n]*zz1[s_n][j_n]-(z[i_n]*FF[s_n][j_n])
    );
return value;

```

```

}

float f_I(float teta,float phi/*,float rr0*/)
{
    float func, T[3]={0,0,0},sum1;
    int i,j,s,q;

    sum1=0;
    for (i=0;i<=2;i++)
    for (s=0;s<=2;s++)
    for(j=0;j<=2;j++)
    for (q=0;q<=2;q++)
    {
        sum1=sum1+Kijs(i,j,s,teta,phi)*F[i][s][j][q]*(-
        rhat(q,teta,phi)*sint(phi));//the unit vector is toward the center so rhat has
        to be negative

    }//i s j q

    func=sum1;

    return func;
}

float g_I(float teta)
{
    float gt, term1,term2,term3,term4;
    int i;

    term1=f_I(teta,phi_I[0]);
    term2=0;
    for (i=1;i<=(nphi-1);i=i+2) //+2
        term2=term2+f_I(teta,phi_I[i]);

    term3=0;
    for (i=2;i<=(nphi-2);i=i+2) //+2
    term3=term3+f_I(teta,phi_I[i]);
    term4=f_I(teta,phi_I[nphi]);

    gt=(term1+4*term2+2*term3+term4)*(phi_I[nphi]-phi_I[0])/(3*nphi);
    return gt;
}

```

```

float rhat(int q_A,float teta_A,float phi_A)
{
    float value;
    if (q_A==0) value=cost(teta_A)*sint(phi_A);
    if (q_A==1) value=sint(teta_A)*sint(phi_A);
    if (q_A==2) value=cost(phi_A);
    return value;
}

void caseNcall(caseN0)
{
    if (caseN0==0) {ind1=0;ind2=0;ind3=0;ind4=0;}
    else if (caseN0==1) {ind1=1;ind2=1;ind3=1;ind4=1;}
    else if (caseN0==2) {ind1=2;ind2=2;ind3=2;ind4=2;}
    else if (caseN0==3) {ind1=0;ind2=0;ind3=1;ind4=1;}
    else if (caseN0==4) {ind1=1;ind2=1;ind3=2;ind4=2;}
    else if (caseN0==5) {ind1=0;ind2=0;ind3=2;ind4=2;}
    else if (caseN0==6) {ind1=0;ind2=1;ind3=0;ind4=1;}
    else if (caseN0==7) {ind1=1;ind2=2;ind3=1;ind4=2;}
    else if (caseN0==8) {ind1=0;ind2=2;ind3=0;ind4=2;}
}

#include "vardef.h"
#include "mathfunc.h"

float fV_I(float teta,float phi,float rr0);
float gV_I(float teta);
float hV_I(float teta,float phi);

float S_total[3][3][3][3],test;
int iTETA,iPHI,iR,IpV,JpV,KpV,g1,g2;

*****
/*This program is written to calculate the second integral in <c a> in polycrystalline
microstructures*/

void Calculate_secondInteg()
{
    FILE *fp2;
    float term1,term2,term3,term4,term_extra;
    int ip,jp,kp,lp,i_c;

```

```

fp2=fopen("c-cp-data2.dat","w");
if(fp2==NULL){printf("c-cp-data2.dat can't be opened to to write.\n");
exit(1);}
for (ip=0;ip<=2;ip++)
    for (jp=0;jp<=2;jp++)
        for (kp=0;kp<=2;kp++)
            for (lp=0;lp<=2;lp++)
                for (g1=1;g1<=(Ototal);g1++)

                    {

i_c=(27*(Ototal))*ip+(9*(Ototal))*jp+(3*(Ototal))*kp+((Ototal))*lp+g1;

                                                                    fprintf(fp2,"%f %f\n",c[i_c],cp[i_c]);
                    }

fclose(fp2);

iTETA=0;
    term1=gV_I(teta_I[iTETA]);
    printf("term1=%f\n",term1);
    term2=0;
    for (iTETA=1;iTETA<=((nteta_I-1)-2);iTETA=iTETA+2)
        term2=term2+gV_I(teta_I[iTETA]);
        printf("term2=%f\n",term2);

    term3=0;
    for (iTETA=2;iTETA<=((nteta_I-1)-1);iTETA=iTETA+2)
        term3=term3+gV_I(teta_I[iTETA]);
        printf("term3=%f\n",term3);

    iTETA=nteta_I-1;
    term4=gV_I(teta_I[iTETA]);

    iTETA=nteta_I;
    term_extra=gV_I(teta_I[iTETA]);

    printf("term4=%f\n",term4);

    V_Integ[ind1][ind2][ind3][ind4]=(term1+4*term2+2*term3+term4)*(teta_I[nteta_I]-teta_I[0])/(3*nteta_I);

}

```

```

float gV_I(float teta)
{
    float gt,term1,term2,term3,term4;

    iPHI=0;
    term1=hV_I(teta,phi_I[iPHI]);
    term2=0;
    for (iPHI=1;iPHI<=(nphi-1);iPHI=iPHI+2) term2=term2+hV_I(teta,phi_I[iPHI]);

    term3=0;
    for (iPHI=2;iPHI<=(nphi-2);iPHI=iPHI+2) term3=term3+hV_I(teta,phi_I[iPHI]);
    iPHI=nphi;
    term4=hV_I(teta,phi_I[iPHI]);

    gt=(term1+4*term2+2*term3+term4)*(phi_I[nphi]-phi_I[0])/(3*nphi);
    return gt;
}

```

```

float hV_I(float teta,float phi)
{
    float htp,term1,term2,term3,term4;

    if (phi==0) JpV=0;
    else if ( (phi>0) && ( phi<=(10*PI/180) ) ) JpV=1;
    else if ( (phi>(10*PI/180)) && (phi<=(20*PI/180)) ) JpV=2;
    else if ( (phi>(20*PI/180)) && (phi<=(30*PI/180)) ) JpV=3;
    else if ( (phi>(30*PI/180)) && (phi<=(40*PI/180)) ) JpV=4;
    else if ( (phi>(40*PI/180)) && (phi<=(50*PI/180)) ) JpV=5;
    else if ( (phi>(50*PI/180)) && (phi<=(60*PI/180)) ) JpV=6;
    else if ( (phi>(60*PI/180)) && (phi<=(70*PI/180)) ) JpV=7;
    else if ( (phi>(70*PI/180)) && (phi<=(80*PI/180)) ) JpV=8;
    else if ( (phi>(80*PI/180)) && (phi<=(90*PI/180)) ) JpV=9;
    else if ( (phi>(90*PI/180)) && (phi<=(100*PI/180)) ) JpV=10;
    else if ( (phi>(100*PI/180)) && (phi<=(110*PI/180)) ) JpV=11;
    else if ( (phi>(110*PI/180)) && (phi<=(120*PI/180)) ) JpV=12;
    else if ( (phi>(120*PI/180)) && (phi<=(130*PI/180)) ) JpV=13;
    else if ( (phi>(130*PI/180)) && (phi<=(140*PI/180)) ) JpV=14;
    else if ( (phi>(140*PI/180)) && (phi<=(150*PI/180)) ) JpV=15;
    else if ( (phi>(150*PI/180)) && (phi<=(160*PI/180)) ) JpV=16;
    else if ( (phi>(160*PI/180)) && (phi<=(170*PI/180)) ) JpV=17;
    else if ( (phi>(170*PI/180)) && (phi<=(180*PI/180)) ) JpV=18;

    iR=0;
    term1=fV_I(teta,phi,rr_I[iR]);

```

```

term2=0;
for (iR=1;iR<=(nrr-1);iR=iR+2)
{
    term2=term2+fV_I(teta,phi,rr_I[iR]);
}

term3=0;
for (iR=2;iR<=(nrr-2);iR=iR+2) /*+2*/
{ term3=term3+fV_I(teta,phi,rr_I[iR]);
}
iR=nrr;

term4=fV_I(teta,phi,rr_I[iR]);

htp=(term1+4*term2+2*term3+term4)*(delrr)/3;

return htp;
}

```

```

float fV_I(float teta,float phi,float rr0)
{
    float func,T[3]={0,0,0},sum1;
    int i,j,s,q;

    if (rr0<=0.05) KpV=0;
    else if ( (rr0>0.05) && (rr0<=0.25) ) KpV=1;
    else if ( (rr0>0.25) && (rr0<=0.45) ) KpV=2;
    else if ( (rr0>0.45) && (rr0<=0.65) ) KpV=3;
    else if ( (rr0>0.65) && (rr0<=0.85) ) KpV=4;
    else if ( (rr0>0.85) && (rr0<=1.05) ) KpV=5;
    else if ( (rr0>1.05) && (rr0<=1.25) ) KpV=6;
    else if ( (rr0>1.25) && (rr0<=1.45) ) KpV=7;
    else if ( (rr0>1.45) && (rr0<=1.65) ) KpV=8;
    else if ( (rr0>1.65) && (rr0<=1.85) ) KpV=9;
    else if ( (rr0>1.85) && (rr0<=2.05) ) KpV=10;
    else if ( (rr0>2.05) && (rr0<=2.25) ) KpV=11;
    else if ( (rr0>2.25) && (rr0<=2.45) ) KpV=12;
    else if ( (rr0>2.45) && (rr0<=2.65) ) KpV=13;
    else if ( (rr0>2.65) && (rr0<=2.85) ) KpV=14;
    else if ( (rr0>2.85) && (rr0<=3.05) ) KpV=15;
    else if ( (rr0>3.05) && (rr0<=3.25) ) KpV=16;
    else if ( (rr0>3.25) && (rr0<=3.45) ) KpV=17;
    else if ( (rr0>3.45) && (rr0<=3.65) ) KpV=18;
    else if ( (rr0>3.65) && (rr0<=3.85) ) KpV=19;
    else if ( (rr0>3.85) && (rr0<=4.05) ) KpV=20;
    else if ( (rr0>4.05) && (rr0<=4.25) ) KpV=21;
}

```

```

else if ( (rr0>4.25) && (rr0<=4.45) ) KpV=22;
else if ( (rr0>4.45) && (rr0<=4.65) ) KpV=23;
else if ( (rr0>4.65) && (rr0<=4.85) ) KpV=24;
else if ( (rr0>4.85) && (rr0<=5.05) ) KpV=25;
else if ( (rr0>5.05) && (rr0<=5.25) ) KpV=26;
else if ( (rr0>5.25) && (rr0<=5.45) ) KpV=27;
else if ( (rr0>5.45) && (rr0<=5.65) ) KpV=28;
else if ( (rr0>5.65) && (rr0<=5.85) ) KpV=29;
else if ( (rr0>5.85) && (rr0<=6.05) ) KpV=30;
else if ( (rr0>6.05) && (rr0<=6.25) ) KpV=31;
else if ( (rr0>6.25) && (rr0<=6.45) ) KpV=32;
else if ( (rr0>6.45) && (rr0<=6.65) ) KpV=33;
else if ( (rr0>6.65) && (rr0<=6.85) ) KpV=34;
else if ( (rr0>6.85) && (rr0<=7.05) ) KpV=35;
else if ( (rr0>7.05) && (rr0<=7.25) ) KpV=36;
else if ( (rr0>7.25) && (rr0<=7.45) ) KpV=37;
else if ( (rr0>7.45) && (rr0<=7.65) ) KpV=38;
else if ( (rr0>7.65) && (rr0<=7.85) ) KpV=39;
else KpV=40;

```

```

sum1=0;
for (i=0;i<=2;i++)
    for (s=0;s<=2;s++)
        for(j=0;j<=2;j++)
            for (q=0;q<=2;q++)
                {

```

```

                    S_total[i][s][j][q]=0;

```

```

                    for (g1=1;g1<=Ototal;g1++)
                        for ( g2=1;g2<=Ototal;g2++)

```

```

                            S_total[i][s][j][q]=S_total[i][s][j][q]+cp[(27*((Ototal-1)+1))*ind1+(9*((Ototal-1)+1))*ind2+(3*((Ototal-1)+1))*j+((Ototal-1)+1)*q+g1]*cp[(27*((Ototal-1)+1))*i+(9*((Ototal-1)+1))*s+(3*((Ototal-1)+1))*ind3+((Ototal-1)+1)*ind4+g2]*pV[JpV][KpV][g1][g2];

```

```

                    sum1=sum1+Kisjr[i][j][s][q][iTETA][iPHI][iR]/*Kisjr(i,j,s,q,teta,phi,rr0)/*S_total[i][s][j][q];

```

```

                }//i s j q
            func=sum1*pow(rr0,2)*sint(phi);

```

```
}    return func;
```

REFERENCES

- Adams, B.L., Canova, G.R., and Molinari, A., 1989. "A Statistical Formulation of Viscoplastic Behavior in Heterogeneous Polycrystals.", *Textures and Microstructures* 11, 57-71.
- Adams, B.L., Morris, P.R., Wang, T.T., Willden, K.S., and Wright, S.I., 1987. "Description of Orientation Coherence in Polycrystalline Materials.", *Acta Metall* 35, 2935-2946.
- Adams, B. L., Zhao, J. and Grimmer, H.,1990. "Discussion of the of Rpresentation of Intercrystalline Mis-Orientation in Cubic Materials.", *Acta Crystall.* A46, 620-622
- Adams, B. L. Wright, S. I. and Kunze, K., 1993. "Orientation Imaging: The Emergence of a New Microscopy.", *Met. Trans.* A24, 8 19-831
- Adams, B.L., Lyon, M.B., Kalidindi, S.R., and Garmestani, H., 2002. "Spectral Integration of Microstructure and Design.", *Materials Science Forum*, 408-412, 493-498.
- Bacon, D.J., Barnett, D.M., and Scattergood, R.O.1978. "Anisotropic Continuum Theory of Lattice Defects.", *Progress in Materials Science*, 23, 51-262.
- Beran, M., 1965. "Use of Variational Approach to Determine Bounds for Effective Permittivity in Random Media.", *Nuovo Cimento*, 38, 771-782.
- Beran, M., and Molyneux. J., 1966. "Use of Classical Variational Principles to Determine Bounds for the Effective Bulk Modulus in Heterogeneous Media.", *Quart. Appl. Math.* 24, 107-118.
- Beran, M. J., 1968. *Statistical Continuum Theories*, Interscience Publishers, NewYork.
- Beran, M.J., Mason, T.A., Adams, B.L., and Olsen, T., 1996. "Bounding Elastic Constants of an Orthotropic Polycrystal using Measurements of the Microstructure.", *J. Mech. Phys. Solids* 44, 1543-1563.
- Bishop, J.F.W., Hill, R., 1928. "A Theoretical Derivation of the Plastic Properties of a Polycrystalline Face-centred.", *Phil. Mag.* 42.
- Brush, Don O., and Almroth, Bo O., 1975. *Buckling of Bars, Plates, and Shells*, Mc Grow-Hill, USA.
- Bunge, H.J., 1982. *Texture Analysis in Materials Science*, Cuvillier Verlag

- Corson, P.B., 1974a. "Correlation Functions for Predicting Properties of Heterogeneous Materials: I. Experimental Measurement of Spatial Correlation Functions in Multiphase Solids.", *J. Applied Physics*, 45, 3159-3164.
- Corson, P.B., 1974b. "Correlation functions for Predicting Properties of Heterogeneous materials. II. Empirical Construction of Spatial Correlation Functions for Two-phase Slids.", *J. Applied Physics* 45.
- Garmestani, H., Lin, S., and Adams, B.L., 1998. "Statistical Continuum Theory for Inelastic Behavior of Two-phase Medium.", *Int. J. Plasticity* 14, 719-731.
- Garmestani, H., Kalu, P., and Dingley, D., 1998. "Micro-characterization of Al-8090 Superplastic Materials Using Orientation Imaging Microscopy.", *Journal of Materials Science and Engineering A*. 242:1-2, 284-291.
- Garmestani, H., Lin, S., 2000. "Statistical Continuum Mechanics Analysis of an Elastic Two-isotropic-phase Composite Material.", *Journal of Composites: Part B* 31, 39-46.
- Garmestani, H., Lin, S., Adams, B., and Ahzi, S.I, 2001. "Statistical Continuum Theory for Texture Evolution of Polycrystals.", *Journal of the Mechanics and physics of Solids* 49, 589-607.
- Hashin, Z., 1962. "The elastic Moduli of Heterogeneous Materials.", *Journal of Applied Mechanics*, 143-150.
- Hashin, Z. , and Shtrikman S. , 1962. "On Some Variational Principles in Anisotropic And Homogeneous Elasticity.", *J. Mech. And phys. Solids*, vol 10, pp 335, 342.
- Hashin, Z., and Shtrikman, S., 1963. "A Variational Approach to the Theory of the Elastic Behavior of Multiphase Materials", *J. Mech. And phys. Solids*, vol 11, 127-140.
- Hill, R., 1952. "The elastic behavior of a crystalline aggregate", *Proc. Phys. Soc. A* 65, 349.
- Hill, R. , 1965. "A Self Consistent Mechanics of Composite Materials", *Journal of the Mechanics and Physics of Solids*, Vol. 13, 213-222.
- Hill, R., 1967. "The Essential Structure of Constitutive Laws for Metal Composites and Polycrystals", *J. Mech. Phys. Solids* 15, 79.
- Hirth, J. P. and Lothe J., 1968. *Theory of Dislocations*, McGraw-Hill, New York, 401.
- Johnson, W.S. and Birt, M.J., 1991. "Comparison of Some Micromechanics Models for Discontinuously Reinforced Metal Matrix Composites.", *Journal of Composites Technology and Research*, 13,3, PP 161-167.

- Kroner, E., 1972. "Statistical Continuum Mechanics.", Springer Verlag, Wien., NY.
- Kroner, E. 1977. "Bounds for Effective Elastic Moduli of Disordered Materials.", J. Mech. Phys. Solids 25, 137-55.
- Kroner, E., Gittus, J., and Zarka, J., 1987. "Modeling Small Deformations of Polycrystals.", Elsevier Applied Science Publishers ed. New York, 229.
- Lai, W. M., Rubin, D., and Krempel, E., 1993. Introduction to Continuum Mechanics, Butterworth-Heinemann Ltd .
- Lin, S., Garmestani, H., and Adams, B., 2000. "The Evolution of Probability Functions in an Inelastically Deforming Two-phase Medium.", International Journal of Solids and Structures. 37: 3, 423.
- Mahesh, C. B., 1986. "Principles and Methods of Ultrasonic Characterization of Materials.", Advanced Ceramic Materials, 1,4, 311-323.
- Mason, A.T., Adams, B.L., 1999. "Use of Microstructural Statistics in Predicting Polycrystalline Material Properties.", Metallurgical and Materials transactions A 30, 969-977.
- Maxwell, J.C., 1873. Treatise on Electricity and Magnetism, Clarendon Press, Oxford.
- Nemat-Nasser, S., Hori, M., 1999. Micromechanics: Overall Properties of Heterogeneous Materials, Elsevier, NY.
- Miller, M.N., 1969. "Bounds for Effective Bulk Modulus of Heterogeneous Materials.", J. Math. Phys. 10, 11.
- Morris, P.R., 1970. "Elastic constants of polycrystals.", Int. J. Engeng. Sci. 8, 49-61.
- Proust, G., 2005. "Identifying the Complete Space of Feasible Anisotropic Properties in Polycrystalline Microstructures.", PhD thesis at Drexel University.
- Reuss, A., 1929. "Berechnung der fließgrenze von mischkristallen auf grund der plastizitätsbedingung für einkristalle.", Math. Mech. 9, 49-58.
- Saheli, G., Garmestani, H., and Adams, B.L, 2004. "Microstructure Design of a Two-phase Composite Using Two-point Correlation Functions.", Journal of Computer Aided Design, 11, No.2-3, 103-115.
- Sokolnikof, I.S., 1956. Mathematical Theory of Elasticity, Mc Grow Hill, NY.

- Torquato, S., Stell, G., 1982. "Microstructure of Two-phase Random Media: I. The N-Point Probability Functions.", *J. Chem. Phys.* 77:4, 2071-2077.
- Torquato, S., Stell, G., 1985. "Microstructure of Two-phase Random Media: The N-Point Matrix Probability Functions for Impenetrable Spheres", *J. Chem. Phys.*, 82, 980-987.
- Tewari, A., Gokhale, A.M., Spowart, J.E., Miracle, D.B., 2003. "Quantitative Characterization of Spatial Clustering in Three-dimensional Microstructures Using Two-point Correlation Functions.", *Acta Materiala* 52, 307-319.
- Torquato,S, 2002. *Random Heterogeneous Materials: Microstructure and Macroscopic Properties*, Elsevier Verlag Publisher.
- Voigt, W., 1889. "Uber die Beziehung Zwischen Den Beiden Elastizitatskonstanten Isotroper Kroper", *Wied. Ann.* 38, 573-587.
- Willis, J.R., 1965. "The Elastic Interaction Energy of Dislocation Loops in Anisotropic Media.", *Quart. Journal of mechanics and applied math* XVIII, pt 4.